Staged Concrete Bridge Deck Pours Adjacent to Live Traffic

Peter J. Weatherer
Brock Hedegaard
Gustavo J. Parra-Montesinos

University of Wisconsin-Madison

WisDOT ID no. 0092-16-04

November 2018

RESEARCH & LIBRARY UNIT

WISCONSIN HIGHWAY RESEARCH PROGRAM

WISCONSIN DOT
PUTTING RESEARCH TO WORK

TECHNICAL REPORT DOCUMENTATION PAGE

1. Report No. 0092-16-04	**2. Government Accession No.**	**3. Recipient's Catalog No.**
4. Title and Subtitle Staged Concrete Bridge Deck Pours Adjacent to Live Traffic		**5. Report Date** November 2018 **6. Performing Organization Code**
7. Author(s) Peter J. Weatherer, Brock Hedegaard, Gustavo J. Parra-Montesinos		**8. Performing Organization Report No**
9. Performing Organization Name and Address University of Wisconsin-Madison Department of Civil and Environmental Engineering 2205 Engineering Drive Madison, WI 53706		**10. Work Unit No.** **11. Contract or Grant No.** WHRP 0092-16-04
12. Sponsoring Agency Name and Address Wisconsin Department of Transportation Research & Library Unit 4822 Madison Yards Way Madison, WI 53707		**13. Type of Report and Period Covered** Final Report November 2015 - November 2018 **14. Sponsoring Agency Code**

15. Supplementary Notes

16. Abstract

An evaluation of the behavior of longitudinal joints in staged-constructed bridge decks subjected to traffic-induced displacements during curing of concrete was conducted through field inspections and monitoring, numerical analyses, and laboratory tests. Field inspection of deck-on-girder bridges showed no indication of adverse effects from traffic loading during staged construction. Concrete underconsolidation related to construction practices, however, was observed in several bridges. Haunched slab bridges constructed in stages, on the other hand, were found to be significantly more susceptible to deterioration along the longitudinal joint over time. The construction of haunched slab bridges in stages is thus not recommended.

Results from field monitoring and numerical analyses of two bridges showed that differential deflections in short-to-medium-span prestressed concrete girder bridges are extremely small and are highly unlikely to adversely affect the integrity of the deck. Results from laboratory tests of two longitudinal joint specimens subjected to traffic-inducted displacements during concrete curing indicated that differential deflections up to 0.125 in. downward or 0.175 in. total movement did not appreciably impact the integrity of the concrete-bar bond in spliced reinforcement. A lap-splice length of 48 bar diameters was found to be adequate to develop the yield strength of the reinforcement after being subjected to traffic-induced displacements during concrete curing.

17. Key Words Longitudinal joints, finite element analysis, field tests, laboratory tests, deterioration, concrete curing.	**18. Distribution Statement** No restrictions. This document is available through the National Technical Information Service. 5285 Port Royal Road Springfield, VA 22161

19. Security Classif. (of this report) Unclassified	**20. Security Classif. (of this page)** Unclassified	**21. No. of Pages** 197	**22. Price**

Form DOT F 1700.7 (8-72) Reproduction of completed page authorized

DISCLAIMER

This research was funded through the Wisconsin Highway Research Program by the Wisconsin Department of Transportation and the Federal Highway Administration under Project 0092-16-04. The contents of this report reflect the views of the authors who are responsible for the facts and accuracy of the data presented herein. The contents do not necessarily reflect the official views of the Wisconsin Department of Transportation or the Federal Highway Administration at the time of publication.

This document is disseminated under the sponsorship of the Department of Transportation in the interest of information exchange. The United States Government assumes no liability for its contents or use thereof. This report does not constitute a standard, specification or regulation.

The United States Government does not endorse products or manufacturers. Trade and manufacturers' names appear in this report only because they are considered essential to the object of the document.

Executive Summary

Highway bridges are some of the most common and frequently used structures in today's built environment, but they are also some of the most heavily demanded. Decades of heavy traffic loading and harsh environmental conditions cause concrete bridge decks to degrade over time, requiring them to be repaired or replaced. Additionally, ever increasing traffic demands mean that aging infrastructure needs to be updated and expanded, all while minimizing the disruption to road users. For this reason, staged construction, where traffic is maintained on the bridge while it is constructed in phases, is often turned to for bridge replacements, rehabilitations, and widenings.

Certain concerns exist, however, with the use of staged construction. When cast-in-place concrete decks are used with staged construction, the concrete deck must cure while subjected to loads and displacements caused by the adjacent traffic using the same structure. There is concern that as the concrete hardens and turns from a fluid to a solid, traffic-induced displacements and vibrations may affect its bond with the embedded reinforcement and the durability of the longitudinal joint. This research focused on evaluating the integrity and performance of longitudinal construction joints in highway bridge decks that are subjected to traffic-induced differential deflections during curing.

This research included a survey of regional transportation officials, in which common practices, procedures, and concerns were examined. The survey showed that staged construction is often preferred by various stakeholders, but no consistent measures are taken to limit damage to curing bridge decks and longitudinal construction joints often do not perform adequately. Visual inspections of several Wisconsin highway bridges were also performed, with a majority showing only minor signs of distress, which may or may not be attributed to the staged construction process. Some minor defects were seen, such as underconsolidated concrete in the construction joint region

and leakage through the joint itself. Eight structurally “identical” haunched slab bridges showed severe deterioration at the construction joints, but it was not possible to determine the cause of the damage through visual inspection.

Differential displacements due to live traffic were measured in two prestressed concrete girder bridges during staged construction. The resulting maximum differential deflections were almost always less than 0.030 in. and, on average, between 0.015 in. and 0.020 in. These two bridges were structurally similar and of comparable main span lengths, so it was reasonable that the magnitudes of differential deflections were also similar.

Finite element analyses were performed for the same two bridges that were instrumented during construction to see if differential deflections could be accurately estimated. A truck loading was selected that would produce an upper-bound estimate of differential deflections, which was approximately 0.065 in. for both bridges. For comparison, a third model was created for a longer-span steel plate girder bridge that carried more traffic lanes during construction. In this case, larger differential deflections were predicted, up to 0.35 in., but it was shown that reducing the number of loaded traffic lanes would reduce this considerably.

Laboratory tests were also conducted to evaluate the effect of traffic-induced vibrations on the performance of longitudinal joints of bridge decks constructed in stages. Two concrete bridge deck test specimens were constructed using a simulated staged bridge construction process. The two specimens were subjected to different magnitudes of differential deflections during curing, after which they were subjected to an ultimate flexural strength test. Strain data from the reinforcing bars spliced at the construction joint showed that the concrete-bar bond was adequate to develop the yield strength of the reinforcement, even when the specimen was subjected to exceptionally large differential displacements during curing. Testing also showed that under

bending there was a tendency for rotations to be localized at the ends of the lap splice, which could potentially cause long-term durability issues.

Finally, tests were conducted to evaluate the effect on joint leakage of treating the side surface of the first-stage deck with a concrete retarder. Four pairs of joints were tested, two with and two without surface treatment. After application of the concrete retarder to the first-stage concrete, high-pressure water was applied to the joint surface to remove surface paste and expose the course aggregate. Under the application of a water head over a 6-in. diameter area, joint leakage was evaluated and compared through the change in water head over time. The results from these tests were inconclusive with regard to the ability of joint surface treatment to reduce leakage through the joint. However, only one out of four specimens without joint treatment could hold the water head (i.e., water in other three specimens ran through the joint in a matter of seconds), while three out of four specimens with joint treatment held the water over time, suggesting that the applied surface treatment does have potential to reduce water leakage or, at least, it would not be detrimental to the performance of the joint.

Acknowledgements

The research reported herein was sponsored by the Wisconsin Department of Transportation through the Wisconsin Highway Research Program. Additional support was provided by the National Center for Freight and Infrastructure Research and Education (CFIRE). The opinions presented in this report are those of the writers and do not necessarily represent the views of the sponsor.

The writers also wish to acknowledge the contributions of Dr. Luis Fargier-Gabaldón, Mohamed El-Tameemi, Angel Pérez-Irizarry, and Jacob Zeuske to the laboratory and field testing phases of this research.

Table of Contents

Chapter 1: Introduction

1.1 Background

Highway bridge decks, due to the nature of their function and environment, often experience considerable degradation over time. Substantial cracking and in some cases spalling of deck concrete is expected after several years of repeated dynamic impact loading from large vehicles and heavy traffic. Further, bridges in cold climates are exposed to freeze-thaw cycles, road salts and deicing chemicals, which often leads to corrosion of steel reinforcement and deterioration of expansion joints, among other issues. This means that concrete bridge decks will often need to be repaired or replaced during the lifetime of the bridge, resulting in severe disruption to traffic in the area.

When substantial repairs to a bridge must be made, there are few options for accommodating the bridge traffic. Detours that take the traffic away from the bridge route are costly to commuters in the form of longer travel times, and undesirable to residents who would experience large traffic volumes being diverted through their communities. When an adjacent bridge exists or a temporary one can be constructed, another option is to detour traffic within the right-of-way, such as with a temporary median crossover. This is also sometimes undesirable as number of lanes and lane widths may have to be reduced on the adjacent bridge, which may cause backups in both traffic directions as well as additional safety concerns. Median crossovers are also expensive due to the extra pavement and lane markings that must be made through the median and additional concrete barriers that are required to separate traffic directions, which can significantly increase the project cost (Manning 1981). A third option is to use staged construction, where a portion of the existing bridge is left open to traffic while the closed portion is repaired or replaced. This eliminates the need to detour the traffic off the bridge, and only requires a reduction in the

number and/or width of traffic lanes. In addition to a bridge or deck replacement, staged construction can also be utilized for a bridge widening, where traffic remains on the existing bridge while the widened portion is constructed, or in new construction where there is a need to open the route to traffic as soon as possible. By eliminating the need for expensive and dangerous detours, staged construction is the most advantageous solution in certain situations.

A primary concern that has been raised in using staged construction is how traffic-induced deflections and vibrations can affect the integrity of the longitudinal construction joints between the portions of the bridge deck. In this scenario, the side of the bridge deck that is open to traffic experiences deflections due to the traffic live and dead loads. When the adjacent side of the concrete bridge deck has been cast and is curing, it is primarily subjected only to dead loads. Therefore, the curing portion of the deck must harden in place and join up to the existing deck while it is experiencing these traffic-induced differential deflections. Another method of construction involves casting each portion of the deck in stages and leaving a gap in between to isolate the curing deck from traffic-induced deflections, and then once the deck concrete has gained sufficient strength, joining them together using a closure pour or closure strip. Concern over whether traffic-induced deflections will affect the bond between the steel reinforcing bars and concrete or the concrete itself in the deck side constructed last has warranted several research studies on the subject in the past few decades. In Wisconsin and other regions with harsh environments, minimizing cracking, longitudinal joint deterioration, and spalling of concrete in bridge decks that may occur due to staged construction is of the utmost importance in improving the durability and long-term performance of highway bridges.

1.2 Scope of Project

This research concerns the integrity and performance of longitudinal joints in bridge decks constructed in stages, where deflections induced by traffic on the first stage deck occur during curing of the concrete on the second stage. Specific topics include evaluating current design and construction practices, assessing the condition of existing staged construction bridge decks, field measuring and estimating magnitudes of differential deflections in the region adjacent to the longitudinal joint, and evaluating the effect of traffic-induced deflections on longitudinal joint behavior through large-scale laboratory tests.

Many bridge construction projects discussed throughout this report were completed in several stages. These stages can include lane closures in preparation for bridge reconstruction, removal of a portion of the existing bridge, and construction of a portion of the new bridge. These stage numbers do not always correspond across projects, so discussions included herein are simplified to just include Stage 1 and Stage 2 construction. Throughout this report, Stage 1 refers to the construction of the first portion of the new bridge deck, including all secondary processes that are necessary to complete this task (i.e. closing traffic lanes, removal of existing bridge segments, placing new girders, etc.). Stage 2 refers to the construction of the second portion of the new bridge deck, including all the secondary processes require to complete this task. While it is possible to construct a bridge in more than two stages, this was not the case for any projects examined as part of this research.

1.3 Research Objectives

The primary objectives of this study are:

I. To evaluate the current state of bridge decks in the State of Wisconsin that were either constructed or repaired using a staged construction process

II. To evaluate the performance of various longitudinal joint designs applicable to bridge decks constructed in stages

III. To evaluate the bond between steel reinforcing bars and surrounding concrete when cured under traffic-induced deflections

IV. To evaluate changes in joint leakage with the application of a concrete retarder on the longitudinal joint

V. To develop recommendations for the design and construction of staged concrete bridge decks

1.4 Research Approach

To complete the research objectives, investigative, analytical, and experimental studies were conducted to evaluate the performance of longitudinal joints in concrete bridge decks constructed in stages. Five main tasks were identified to enable the comprehensive evaluation of staged bridge construction practices.

Task 1: Review of Regional Practices Regarding Staged Deck Construction

Staged bridge construction practices of Wisconsin and other regional state departments of transportation (DOT) were surveyed in the form of an online questionnaire. The survey was also extended to bridge inspectors and engineers at private firms that have experience designing bridges using staged construction. Consideration was given to imposed traffic limitations and detailing of longitudinal construction joints. A review of specifications and policies from the respective DOTs was also performed.

Task 2: Evaluation of Existing Staged Bridge Decks

Construction and design practices of staged bridge decks were further evaluated by investigating the condition of existing bridges that were constructed in stages. By working with

the Project Oversight Committee and utilizing the Wisconsin Highway Structures Information System (HIS), several staged bridge decks were identified for field inspection. Particular interest was given to bridges where previous inspections had noted issues in the longitudinal construction joint regions. The condition of the existing bridge decks was evaluated based on crack distribution and severity, concrete spalling, and delamination. Trends relating deck condition to design and construction practices were discerned, identifying the practices that resulted in the best deck performance.

Task 3: Field Monitoring of New Longitudinal Joint Construction

To quantify the magnitudes of displacements imposed by traffic during staged bridge construction in the area adjacent to the longitudinal joint, an instrumentation setup was designed to be placed on bridges under construction, immediately after casting of the Stage 2 concrete deck. Working with the Project Oversight Committee, two highway bridges were identified as candidates for field monitoring of displacements during their construction in the summer of 2016. The main parameter of interest was the differential deflection between adjacent girders on either side of the longitudinal staged construction joint. The magnitude of the differential deflections across the construction joint were calculated for each traffic event and used to validate the finite element models in Task 4 and the displacement protocol for the laboratory testing in Task 5.

Task 4: Determination of Loading History Using Numerical Analysis

Three-dimensional finite element models of entire bridge superstructures were created to further investigate the live load deflections in bridges during staged construction. ABAQUS was used for all finite element modeling. Models were created for the two bridges that were instrumented in Task 3, and finite element results were compared with the field measurements to validate the accuracy of the model. After verifying that the modeling techniques used for these two

bridges were appropriate, a model was created for another existing bridge constructed in stages with a different main span length and girder configuration. The models were created with separate parts for each constructed stage of the concrete deck. This allowed the modulus of elasticity of the newer deck segment to be varied to represent the increase in stiffness as the concrete cures and the associated change in deflections to be calculated. The results from these analyses served as an estimation of the expected magnitudes of differential deflections, and along with results from Task 3, were used to determine the displacement history for the laboratory tests.

Task 5: Experimental Study of Longitudinal Joints

Lastly, large-scale laboratory specimens were fabricated and tested in the University of Wisconsin Structures and Materials Testing Laboratory. The specimens were constructed using a simulated staged construction process to investigate the effect live traffic deflections applied during concrete curing have on the integrity of the longitudinal construction joint and the bond between concrete and steel reinforcement over the reinforcement splice region adjacent to the longitudinal joint. Each specimen consisted of two segments. The first, Stage 1 segment, was cast and cured without being subjected to any movements. After the concrete had attained the design compressive strength of 4000 psi, the Stage 1 segment was connected to a hydraulic actuator used to later apply the simulated traffic displacements. The formwork was then placed for the Stage 2 segment, the segment was cast, and the test was initiated. Cyclic displacements were applied for 12 hours as Stage 2 cured. All reinforcing and formwork details were chosen to represent as close as possible what was seen in actual staged construction projects. After the Stage 2 segment reached design strength, the formwork was removed and the entire specimen was placed in the loading frame for an ultimate strength test of the longitudinal construction joint. Reinforcing bars in the

construction joint region were instrumented over the splice length to evaluate bond stresses developed during testing.

Tests were also conducted on joint specimens to evaluate the effect on joint leakage of treating the side surface of the first-stage deck with a concrete retarder. Four pairs of joints were tested, two with and two without surface treatment. After application of the concrete retarder to the first-stage concrete, high-pressure water was applied to the joint surface in order to remove surface paste and expose the course aggregate. Under the application of a water head over a 6 in. diameter area, joint leakage was evaluated and compared through the change in water head over time.

Chapter 2: Literature Review

To further understand the complexities and concerns associated with staged construction, a review of previous work relevant to the topic was conducted. Past studies vary in research methods used and conclusions drawn. These studies include literature reviews, agency surveys, field inspections, in-place monitoring, analytical modeling, and small- and large-scale laboratory testing. The research performed for this study incorporated these methods, and the review of previous research has been subdivided into these categories accordingly. Many of the included studies incorporate more than one of these methods, and are therefore discussed in multiple sections.

Conclusions from previous studies vary. In rare cases, defects in bridge decks due to the use of a staged construction process were identified, but the majority of inspected bridges showed no signs of premature deterioration. Some reports stated that traffic-induced vibrations and deflections have little impact on the integrity of the concrete-rebar bond, while others observed considerable reductions in bond strength between steel and concrete if subjected to relative displacements during curing. Additionally, experiments have shown that relative deflections during curing can lead to cracking and loss of integrity of concrete in the construction joint region. Therefore, it is still not fully understood and there is currently no consensus on how staged construction might impact the long-term performance of a concrete bridge deck.

2.1 Surveys of Transportation Officials

A synthesis report conducted by Manning (1981) and published by The National Cooperative Highway Research Program (NCHRP) provided background into the constructability and performance issues associated with staged bridge construction, detailing how it is beneficial in certain aspects and risky in others. As part of the synthesis, a nationwide survey of transportation

officials was conducted to examine the various traffic control policies in place for bridge deck repairs, replacements, and widenings. The survey showed that it was common for traffic to continue using bridge structures during concrete repair operations. Of the 45 respondents, only two (Hawaii and South Dakota) indicated that they did not allow traffic to continue using a bridge during full-depth deck repairs or widenings. A majority of those states that did allow traffic to continue using the bridge, however, indicated that they placed some limitations on the traffic during concrete placement and curing.

Issa (1999) performed a study with the objective of determining the causes of early-age cracking in concrete bridge decks. This research also included a similar nationwide survey. The survey was sent to 59 transportation agencies around the United States and focused on bridge traffic regulations during concrete placement and common defects found in these bridges. Again, nearly all agencies said they allowed traffic to continue to use bridges during full-depth deck replacements and overlays, and about half indicated that they enforced some restrictions on traffic during bridge deck construction. Common defects and their causes were also surveyed. The most common defect was transverse cracking usually attributed to thermal changes, environmental conditions, curing procedures, and traffic-induced vibrations.

From these surveys, bridge designers were concerned that relative deflections during staged construction may impact the integrity of a curing bridge deck, and most believed some basic measures are needed to prevent this. These were most often in the form of reduced speed limits, lane restrictions, and lower weight limits. Interestingly, Manning (1981) concludes that the most effective way to reduce live traffic effects is to maintain a smooth riding surface leading up to and on the bridge to reduce vibration amplitudes, while speed and weight limits only have a secondary

effect. Maintaining a smooth roadway was not mentioned by any respondents from either survey, suggesting that this may be often overlooked as an essential precautionary measure.

2.2 Field Inspections

In the previously mentioned NCHRP synthesis report (Manning 1981), also examined were cases of several staged bridge construction projects in Michigan, Missouri, California, New Jersey, Texas, Georgia, Massachusetts, and Pennsylvania where live traffic was present during concrete bridge deck curing. Of these, only two documented cases of defects due to traffic-induced vibrations were reported (in Michigan and Texas), and are discussed in further detail below. On reviewing the various condition assessments, the vast majority of bridges showed no adverse effects from maintaining traffic, and that certain precautions can be taken that minimize the possibility of any defects while still allowing traffic on the bridge during construction. The recommendations believed to have the largest impact include using high quality, well-proportioned concrete for the bridge deck, moving traffic and/or heavy trucks into lanes away from the fresh concrete when possible, and maintaining a smooth riding surface. Additionally, it was also recommended to always provide moment continuity and securely tie lapped bars between stages to prevent differential movement, as well as using closure pours to isolate bridge widenings from traffic during construction. By adhering to these practices, it was concluded that traffic-induced vibrations and deflections will have no meaningful impact on the long-term performance of staged concrete bridge decks.

Defects, however, were reported on the aforementioned bridges in Michigan in Oehler & Cudney (1966). Various bridges widened while open to traffic during the 1965 construction season showed abnormal defects in the bridge deck. The bridges showed a rippling effect on the deck surface, with troughs directly over transverse reinforcing bars and crests between bars. The

amplitude of these ripples was measured to be as large as 7/32 in., which occurred in the main span of the I-75 bridge over Rouge River. Additionally, surface cracking was observed directly over the transverse reinforcing bars in many bridges with deck ripples. These cracks allowed deicing salts pooling in the troughs to infiltrate the concrete and corrode the steel reinforcement, which eventually led to excessive spalling of the top concrete cover. It was initially hypothesized that the finishing machine or concrete slump was to blame; however, no correlation was determined between the finishing method or concrete slump and the presence of deck ripples. Ultimately, these issues were concluded to be a result of differential movements of the curing deck due to live traffic combined with excessive water in the concrete mix and not enough clear cover between the reinforcing bars and the deck surface. It was recommended to reduce water in the concrete mix and increase cover over steel reinforcing bars, especially in lap splice regions. It was also suggested that traffic control measures be taken to limit the severity of traffic-induced displacements during bridge deck curing (Arnold 1966). No similar defects have been reported since this study, so the recommendations seem to have been effective.

A study sponsored by the Texas Department of Transportation and performed at Texas A&M (Furr and Fouad, 1981) involved the visual inspection of 30 bridges of various ages, span lengths, girder types, and construction joint details. Four different longitudinal construction joint details, shown in Figure 2.1, were observed during these inspections. The detail shown in Figure 2.1(a) was only observed in one bridge and was the only connection type shown to not perform well. Differential deflections between the two sides of the joint caused cracking and spalling of concrete around the joint, and thus this detail was avoided in the future. No bridges using the other three details showed defects that could definitively be attributed to traffic-induced deflections and vibrations during staged construction.

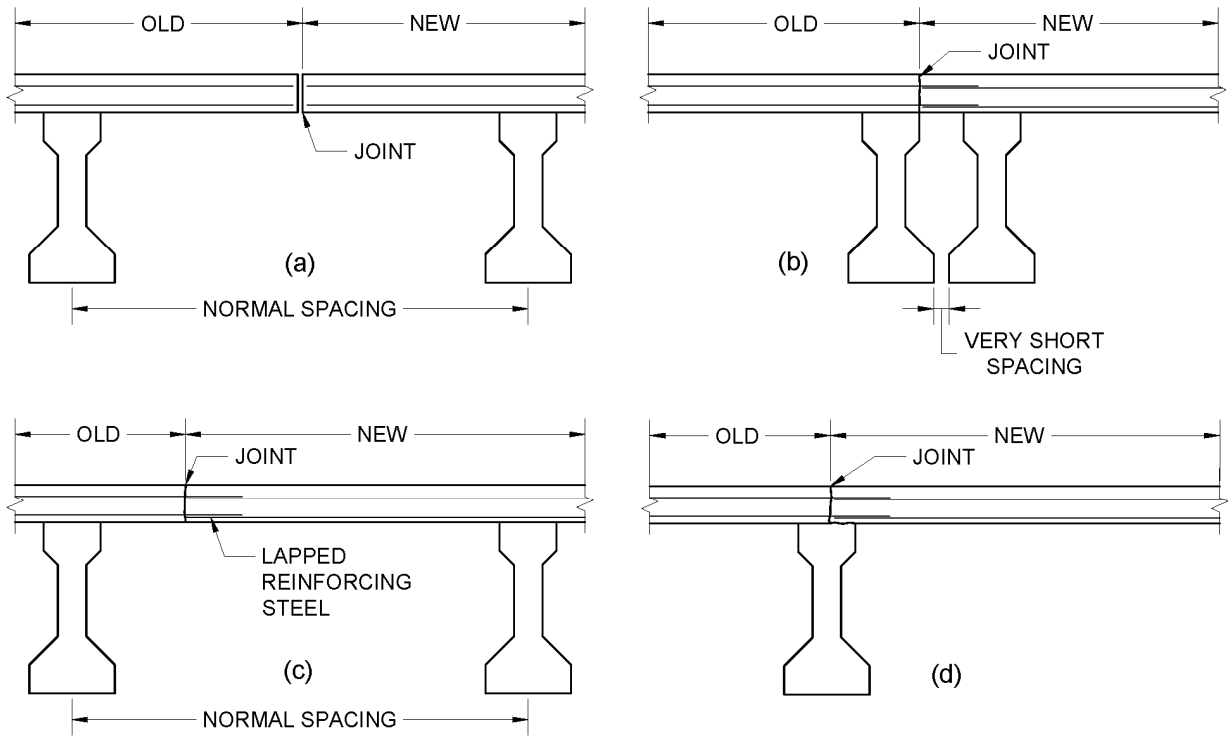

Figure 2.1- Longitudinal construction joint details encountered in Furr and Fouad (1981) (Adapted from Furr and Fouad 1981)

Furr and Fouad (1981) sampled a total of 109 core specimens from nine bridges in areas that were disturbed by traffic vibrations, such as near midspan, and in areas that were undisturbed, such as near the supports. The cores were analyzed for defects using visual inspection, ultrasonic pulse velocity tests, dye tests, and strength tests. Fifty eight percent of the cores from the undisturbed areas and 47% of the cores from the disturbed areas showed random cracking, suggesting that random cracking is not caused by traffic disturbance during concrete curing. Eighteen percent of the cores showed wider cracks, either longitudinal, transverse or diagonal, which were most likely flexural or shrinkage cracks and not attributed to traffic vibrations or displacements during curing. One core did show signs of a deteriorated bond between concrete and steel bars due to a specific reinforcement detail. In this case, transverse bars from the existing deck were bent 90 degrees into the new work, and voids were discovered around this bar in the

core. Details of this type of connection can be seen in Figure 2.2. Based on these findings, the researchers recommended extending reinforcement straight from the existing portion of the deck 24 bar diameters, and lapping them at least 20 bar diameters.

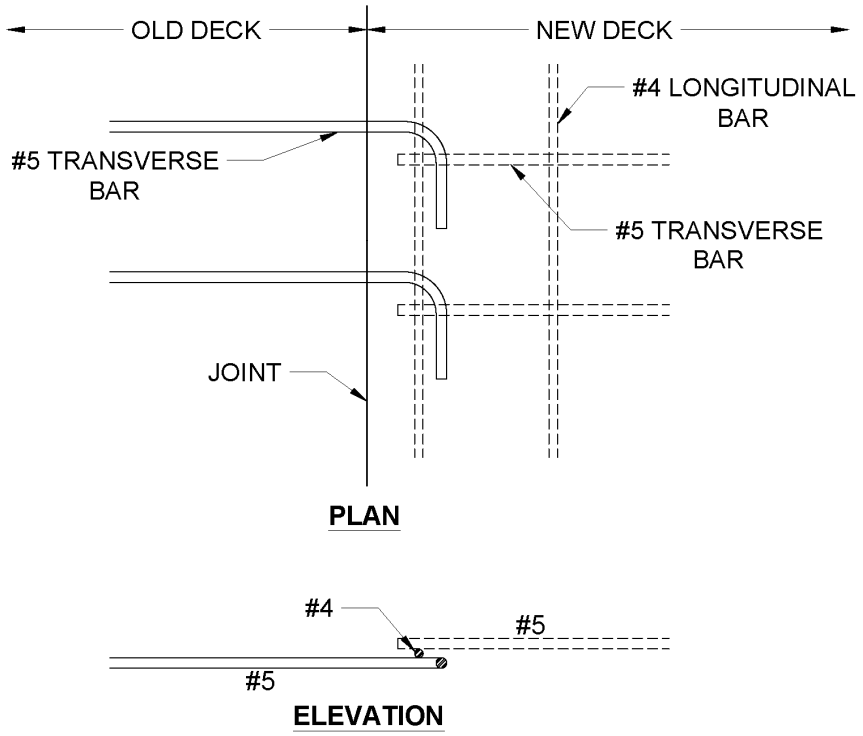

Figure 2.2 - 90-Degree Dowel Bar Reinforcing Detail (Adapted from Furr and Fouad 1981)

A research project conducted by the Georgia Department of Transportation (Deaver 1982) focused on understanding the effects live traffic displacements have on the bond of reinforcement in closure pours. Visual inspections of 23 previously widened bridges in Georgia mainly noted type and severity of cracking or defects. Of these, fourteen bridges showed no significant defects, and seven bridges showed minor, randomly distributed transverse cracking. Only two bridges showed continuous transverse cracking in the closure pour region, but these cracks were all considered minor and did not extend into the adjacent deck pours or vice-versa. From these inspections, it was concluded that no defects could be attributed to maintaining traffic during construction, either with a closure pour or without.

In a case study performed in Ohio (Montero 1980), the widening of the I-71 WB bridge over Morse – Sinclair Road in Columbus, Ohio, was visually inspected and monitored throughout construction. This bridge is a four-span continuous concrete slab superstructure, with two 38-ft end spans and the two 47.5-ft interior spans. The bridge was carrying three traffic lanes and was widened by one more lane. The longitudinal construction joint detail consisted of straight spliced reinforcing bars and a roughened edge of the existing deck. After curing of the widened portion, transverse cracks were noted in the middle of the main spans and longitudinal cracks over the piers and falsework supports. However, none of these cracks were directly attributed to traffic-induced deflections in the curing concrete, and were more likely due to shrinkage and inadequate concrete cover to the steel reinforcement. It was concluded that the major issue with maintaining traffic during bridge widenings is the possible degradation of concrete in the longitudinal joint region. It was also recommended to place shrinkage and temperature steel over the main reinforcement in the deck to help reduce shrinkage and reflective cracking, and thus improve durability of the deck.

Most of the field inspections previously conducted noted no major defects directly attributed to traffic-induced displacements during concrete deck curing. The few defects that were identified (deck rippling in Michigan and voids around 90-degree bent dowel bars in Texas) were determined to be avoidable by making slight changes to the design and construction procedures. Except for the previously mentioned cases, inspections noted no visual signs of a deteriorated bond between reinforcement and concrete, or deterioration of the concrete itself in the longitudinal joint region. This suggests that if any damage does occur from this practice, it is minor and does not affect the overall performance of the bridge.

2.3 Field Monitoring of Staged Construction Deflections

As part of the research performed at Texas A&M University (Furr and Fouad 1981), nine bridges were instrumented during and after concrete placement to quantify any relative deflections between girders adjacent to longitudinal construction joints. Deflections were measured by attaching linear potentiometers to the bridge girders at midspan and measuring the absolute deflections from traffic events. From this, the natural frequency of the structures, transverse deck curvatures and relative deflections were determined. The measurements were taken for random traffic that occurred during the construction of the bridges and vehicle weights were unknown. The findings related to relative deflections are summarized in Table 2.1.

In addition to the visual inspections, the Georgia DOT project (Deaver 1982) also included field monitoring of bridges under construction. Two bridges undergoing widenings were instrumented using linear potentiometers to obtain the absolute and relative deflections of the girders. Both bridges incorporated an isolated widening which was then connected to the existing bridge using a closure pour. The measurements were taken for random traffic events and vehicle weights were not available. These relative deflections are also included in Table 2.1.

According to the results from these two studies, the magnitudes of relative deflections between girders adjacent to longitudinal construction joints are very small, with a maximum recorded differential deflection of 0.12 in. There seems to be no correlation between the bridge girder type, span length or girder spacing and the magnitude of relative deflections. Major contributing factors to relative deflection magnitudes are the transverse stiffness of the bridge provided by diaphragms and braces, and the lane configuration. For example, relative deflections would be expected to decrease as the transverse stiffness increases, and would be expected to

increase as the live traffic load is distributed more to the girder in the existing deck and closest to the construction joint.

Table 2.1 Differential deflections from previous research

Reference	Bridge	Girder Type	Span Length (ft)	Girder Spacing (ft)	Max Differential Deflections (in)
Deaver (1982)	Gordon Rd. / SR 139	Cont. Steel	80	6 ft – 6 in. to 7 ft – 0 in.	0.010
Deaver (1982)	Old Dixie Rd. / SR 3	S.S. Steel	70	5 ft – 3 in to 6 ft – 0 in.	0.012
Furr and Fouad (1981)	I-35 / Ave. D	Cont. Steel	60	8 ft – 1.5 in. to 8 ft – 4 in.	0.032
Furr and Fouad (1981)	I-35 / AT&SF RR	Cont. Steel	70	6 ft – 7.5 in. to 8 ft – 1.5 in.	0.041
Furr and Fouad (1981)	I-45 / FM 517	Cont. Steel	54	6 ft – 0 in. to 8 ft – 6 in.	0.120
Furr and Fouad (1981)	I-10 / Dell Dale Ave.	S.S. PC	87	5 ft – 7 in. to 6 ft – 5 in.	0.060
Furr and Fouad (1981)	US 75 / White Rock Creek SB	S.S. PC and Cont. Steel	50	5 ft – 5 in. to 8 ft – 9 in.	0.032
Furr and Fouad (1981)	US 75 / White Rock Creek NB	S.S. PC and Cont. Steel	90	5 ft – 5 in. to 8 ft – 9 in.	0.058
Furr and Fouad (1981)	US 84 / Leon River	O.H. Steel	67.5	6 ft – 3 in. to 6 ft – 8 in.	0.058
Furr and Fouad (1981)	Texas 183 / Elm Fork Trinity River	Cont. Steel and S.S. PC	50	6 ft – 6 in.	0.040

2.4 Analytical Modeling

An analytical study performed at the University of Maryland (Fu, Zhao, Ye, and Zhang 2015) focused on studying live load deflections in steel girder bridges, particularly those constructed in stages using closure strips. Three different software packages (DASH, CsiBridge

and DESCUS-I) were used to model existing bridges and estimate live loads deflections. One bridge was selected for further study of relative deflections during construction stages. This bridge is a three-span continuous steel girder bridge constructed using a closure pour between stages. CsiBridge was used to estimate the relative deflections between girders adjacent to the closure strip. When diaphragms across the closure strip were connected, the differential deflection was calculated to be 0.07 in. compared with 0.12 in. when not connected.

In this study, it was found that it is possible to accurately calculate deflections of steel girder bridges being constructed in stages using two-dimensional grid models and three-dimensional finite element models. By accurately calculating the magnitudes of relative deflections that can be expected in closure strip regions, it was concluded that measures can be taken to prevent excessive relative deflections. The recommendations made included not connecting diaphragms/cross-frames across a closure strip until right before casting of the closure strip, properly cambering steel beams, and waiting at least 30 days between casting of a new deck and placement of an adjacent closure pour to reduce the effects of concrete creep and shrinkage.

2.5 Laboratory Experiments

For the final research task performed at Texas A&M University (Furr and Fouad 1981), five laboratory test beams representative of a bridge deck were fabricated and subjected to simulated traffic-induced deflections from the time of casting up to an age of 24 hours. Test beams were 10-ft - 8.5-in. long, 12-in. wide, 7-in. deep, and mounted on flexible supports. In these tests, deflection cycles were applied directly to the dowel bars at one end of the specimen using a hydraulic actuator. The magnitude of these deflections was either 0.25 in. or 0.15 in., applied in a half sine wave over one second, with one test superimposing a 0.020-in. amplitude vibration at 6 Hz.

As expected, curvatures were found to depend on the age of the concrete and the magnitude of the displacements. Crack patterns and widths were measured for all specimens, and the most serious cracking was seen in the specimen subjected to 0.25-in. displacements and the superimposed vibration. The superimposed vibration was shown to have no detrimental effect on the bond between reinforcement and concrete, because the forms, concrete, and steel were all vibrating in unison. Furthermore, deflections measured between concrete, forms, and reinforcing bars were undetectably small. Cores were then taken from the specimens to determine severity of cracking and concrete-steel bar bond condition. The cores showed that crack depth was related to curvature, but when comparing this with results from their field monitoring, it was determined that relative deflections between adjacent girders in the field resulted in a transverse deck curvature that was too small to cause cracking of the fresh concrete. The laboratory specimen cores also showed that differential movement did occur between reinforcing bars and concrete. The report suggests that this movement could be detrimental to bond quality, but a quantitative measure of bond performance was not performed.

A later study performed at the University of Kansas (Harsh and Darwin, 1984; Harsh and Darwin, 1986) was conducted to determine the effects of traffic-induced vibrations on concrete compressive strength and reinforcement bond strength for full-depth bridge deck repair applications. Fifteen 4x8 ft. by 12-in. thick test slabs were constructed, with ten being subjected to simulated traffic-induced vibrations and five being control specimens. The slabs were precast with 23-in. by 18-in. blockouts where the full depth repairs would be made. Concrete was placed in these areas and subjected to constant vibrations for 30 hours after concrete placement. Properties such as bar size, concrete slump, and concrete cover were varied to evaluate their effect on bond strength. Cylindrical test specimens were also cast, with some being subjected to the same

simulated vibrations as the slabs, to evaluate the effect of the vibrations on concrete compressive strength. Pullout tests were performed on the reinforcing bars in the repair areas to quantify bond strength.

In this study, it was concluded that vibrations do not affect concrete compressive strength or bond strength between steel bars and concrete if high quality, low-slump (less than 3 in.) concrete is used. Tests showed that compressive strength and bond strength of concrete with a slump of 5 in. or greater would be degraded by vibrations. It was also observed that increasing the concrete cover results in an increase in bond strength. The bond strength with smaller bars seemed to be degraded less than that with larger bars when subjected to vibrations. However, in these experiments the concrete and the steel reinforcement were vibrated together, and thus it is not clear how differential deflections affect the concrete-steel bar bond.

The experimental program reported on by Issa (1999) consisted of testing 3.0-in. wide by 3.0 -in. deep by 19.7-in. long concrete beam specimens to failure in flexure. Tests were performed on concrete five, eight, and twelve hours after casting. From this, a preliminary equation for the modulus of elasticity of concrete between four and twelve hours after casting was presented. Minimum curvatures required to crack the young concrete were also determined to be 2.06×10^{-4} in^{-1}, 3.12×10^{-4} in^{-1}, and 4.50×10^{-4} in^{-1} at five, eight, and twelve hours after casting, respectively. Similar conclusions were drawn as in previous studies, e.g., well-proportioned low slump concretes would not be degraded by traffic-induced vibrations and in some cases the curvature of a freshly placed concrete deck was less than the curvature required to cause cracking. It was further stated that early-age cracking can more often be attributed to faulty construction practices, improper concrete proportions and poor reinforcement detailing than traffic-induced vibrations.

In the Georgia DOT study (Deaver 1982), a testing program was also conducted in addition to field inspections and monitoring. The two bridge widenings that were field monitored as part of this study used closure pours. Test specimens were placed directly on these two bridges over the closure pours to subject them to the same live traffic-induced displacements. Test specimens consisted of two 24-in. x 36-in. by 7-in. deep blocks anchored to the bridge deck on both sides of the closure pour with dowel bars extending into the closure pour region. Formwork was placed between the two blocks, and plastic was placed between the deck closure pour concrete and the test specimen, as shown in Figure 2.3. The specimen was filled with the same concrete, allowed to cure in the same conditions, and subjected to the same displacements as the real closure pour. Control specimens were also cast away from the bridge and not subjected to any movements.

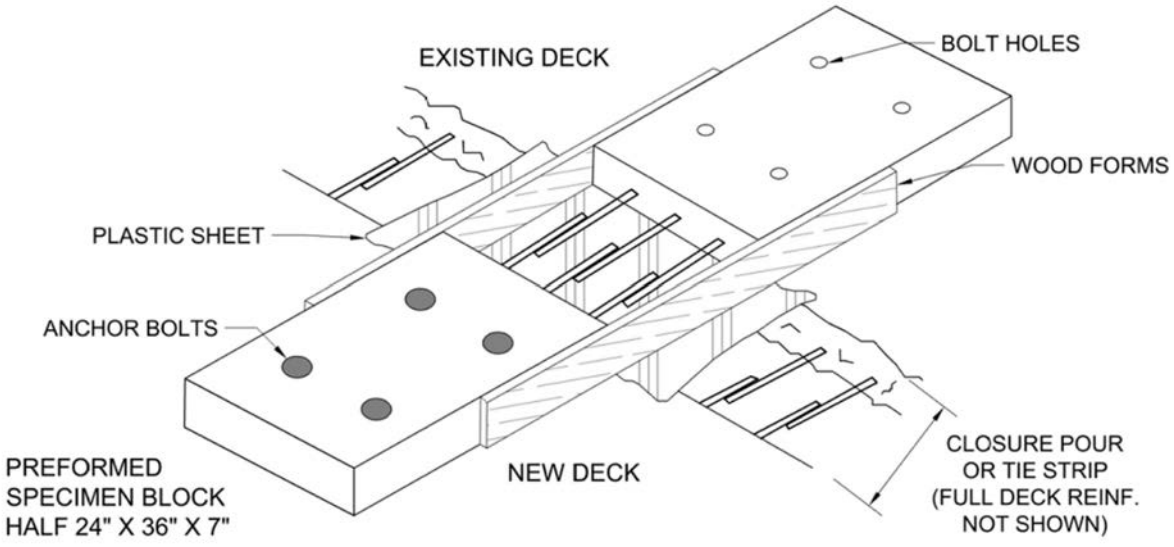

Figure 2.3 – Closure strip field specimens tested in Deaver (1982). (Adapted from Deaver 1982)

After hardening, the specimen was removed from the bridge and the dowel bars were removed from the anchor blocks. The specimens were saw cut to isolate individual reinforcing bars and pull-out tests were performed to quantify the bond between the bars and the concrete in the closure pour region. No significant difference was seen in bar pull-out test results of vibrated

samples versus control specimens. It was concluded that the deflections experienced in the test bridges were extremely small, and thus had no effect on the bond of bars in the closure pour. Furthermore, it was recommended that closure pours may be eliminated in bridges where live load and long-term deflections are expected to be very small.

A laboratory experiment conducted in Hong Kong by Ng and Kwan (2007a, 2007b) employed a more sophisticated testing setup to study the effects of traffic-induced vibrations on closure pours. In this study, the researchers intended to ensure that concrete test specimens were subjected to a double curvature loading scenario, which better represents the flexural behavior of a curing closure strip. Additionally, the displacements applied to the specimens were dependent on the instantaneous stiffness of the specimen to simulate how differential deflections would decrease and the load transferred across the closure strip would increase simultaneously as the closure strip cures and gains strength. Concrete test specimens consisted of two 5.9-in. x 5.9-in. x 15.7-in. precast end blocks, and a 19.7-in. long closure strip of the same cross section joining the two end blocks. One end block was held fixed against rotation and translation, while the other was subjected to vertical displacements without rotation, resulting in double curvature in the closure strip. Specimens were subjected to vibrations ranging in amplitude from 0.02 in. to 0.20 in. for a period of 24 hours. A total of 24 specimens were fabricated, with four being control specimens not subjected to vibrations.

After 28 days, test specimens were subjected to either a double curvature strength test or a rebar pullout test to quantify any degradation in the closure strip as a result of the imparted deflections. This research provided approximate limits for curvatures corresponding to onset of minor, medium and serious cracking in concrete decks. These limits were found to be 4.6×10^{-4} in.$^{-1}$, 6.9×10^{-4} in.$^{-1}$, 9.1×10^{-4} in.$^{-1}$, and 11.4×10^{-4} in.$^{-1}$ respectively. A curvature limit was also

provided at which bond and strength start to degrade, which was reported to be $20.6x10^{-4}$ in^{-1}. In this case, it was concluded that differential deflections can cause a reduction in bar bond and closure strip strength, but the deflections would need to be large enough such as to induce significant cracking of the deck. Thus, since cracking can affect longevity of the deck, measures should be taken to limit these deflections, even if the overall strength of the closure strip is unaffected.

More recently, Swenty and Graybeal (2012) reported on an experimental program of the Federal Highway Administration focused on the effects that relative movements between bars and concrete during curing have on the bond strength in nine different embedment materials, including grouts, ultra-high-performance concretes, and conventional bridge deck concretes. The test specimens and procedures were based on ASTM C234 with some modifications. Standard #4 deformed bars were embedded in 6-in. cube specimens. For each embedment material, six specimens, including three control specimens were fabricated. Control specimens were not subjected to deflections during curing. The embedment material of the test specimens was subjected to a constant displacement every 30 seconds until final set, while the bars remained stationary. These displacements ranged from 0.005 in. to 0.1 in. of linear bar movement perpendicular to the bar axis and were applied at frequencies of 2 Hz and 5 Hz. After the material had fully set, a pullout test was performed and the results compared with those from the undisturbed control specimens. It was concluded that a differential bar movement of 0.01 in. or less did not significantly reduce bond strength in any of the materials. However, relative bar movements of 0.05 in. or greater did significantly reduce bond capacity. These reductions were around 70% for the conventional bridge deck concretes that were tested (both high and low slump).

The frequency at which displacements were applied seemed to have a minimal effect on bond capacity.

Research conducted at Clemson University (Andrews 2013) focused on how magnitude, type, and duration of differential deflections affect the bond strength of reinforcing bars embedded in 8000 psi Quickrete® Non-Shrink Precision Grout. Test specimens consisted of standard #4 deformed bars embedded 6 in. into 6-in. x 12-in. cylinders. Twenty-seven specimens were fabricated, including three control specimens. Immediately after grout placement, cyclic movements of the bars were initiated and lasted for eight hours, but with different time sequences. Bars embedded in the cylinders were subjected to both translational and pivoting movements during curing. The initial applied displacements varied from 0.015 in. to 0.036 in. for the translational movements, and from 0.025 in. to 0.047 in. for the pivoting movements. The three time-sequences that were used consisted of applying the displacements for the entire 8-hour test period, only before the initial set, and only after the initial set of the grout. After ten days of curing, the specimens were subjected to a bar pull-out test.

For both types of movements, larger amplitude displacements resulted in a greater reduction in bond (in some cases more than 20 percent), but all disturbed specimens experienced bond strength reduction when compared to the control specimens. There was a "critical window" for which differential deflections had the greatest impact. This window was observed to be between initial and final set of the grout. Loss of bond is expected to be negligible if the displacements are applied outside of this window. For this specific material, the critical window was determined to be between 30-60 minutes after casting, but these exact limits cannot be applied to other materials. From these experiments, it could not be concluded whether translational or rotational movement

of the bars is more critical due to the displacement amplitudes being different., but both movements affected bond strength.

Conclusions drawn from these laboratory experiments indicated that a certain amount of differential movement between curing concrete and reinforcement can be tolerated before the concrete starts to crack and the bond begins to be degraded, but after some threshold of movement, degradation is expected to occur. Studies also agreed that small amplitude vibrations of the reinforcing bars have a less significant impact on the quality of the bond than large amplitude movements of bars. Larger amplitude translation or pivoting of the bars within the concrete are likely to cause damage. Values for these movements at which the concrete and bond will begin to degrade were reported, but are strictly concerning the movement of the bar with respect to the concrete. Thus, these values are of little practicality to designers, as it would be difficult to calculate them beforehand. Limits on deck curvatures in the joint region or differential displacements of girders adjacent to the longitudinal construction joint are both more practical from a design perspective.

2.6 Summary and Conclusions

Committee 345 of the American Concrete Institute (ACI) published a *Guide for Widening Highway Bridges* (2013) that provided direction regarding practices that reduce the possibility of damage to a concrete bridge deck constructed in stages. Past studies and experiences are reviewed, and an excellent summary of best practices that minimize the chance of defects developing in staged bridge decks is provided. It was reported that longitudinal construction joints should always provide for moment and shear transfer to eliminate problems identified in previously noted studies. It was also recommend that, when possible, the longitudinal construction joint should be located in the median or an untraveled area, in which case a structural connection is not needed, eliminating

the concern of live load damaging curing concrete. However, in most cases this is not an option and the construction joint must be located in the traveled way.

Citing numerous reports and past experience, it was acknowledged that differential deflections during concrete curing have the potential to cause defects in bridge decks, with several recommendations provided for limiting damage. These included using moderate-slump concrete (2 to 3 in.), using only straight dowels in longitudinal joint connections, and securing formwork to both the existing and new structures. Additionally, it was stated that traffic-induced vibrations can be reduced by providing a smooth riding surface, reducing traffic speed and/or traffic weight limit, temporarily closing the traffic lane closest to the longitudinal joint, connecting adjacent diaphragms before deck placement to help equalize girder deflections, and providing temporary shoring underneath the existing bridge.

Lastly, the committee recommended using closure pours in certain situations to help maintain the integrity of the bridge widening. By using closure pours, the widened section of the bridge remains isolated from the live load deflections during curing of the deck concrete, and the widened portion is allowed to experience all the dead load deflections due to weight of the slab, prestressed shortening, creep and shrinkage prior to making the final connection with the existing bridge. In short spans or narrow widenings where these factors are not an issue, the use of closure pours may not be necessary. When using closure pours, it was recommended not to attach reinforcing bars and diaphragms across the joint region until immediately before concrete is placed in the closure pour, thereby eliminating forces being transferred to the widened portion of the bridge. By following these recommended practices, it was believed that differential deflections could be tolerated and would generally not cause defects in concrete decks.

While reports of bridges that have experienced problems directly caused by staged construction are rare, many of these studies have concluded that relative movement between bar and curing concrete can negatively impact concrete-bar bond strength and induce cracking in the longitudinal joint region. While the potential for damage is acknowledged, it is unclear what displacement limits designers should impose to minimize this possibility, or what methods they should use to calculate these displacements. This lack of consensus suggests that the degree to which differential deflections during staged construction affect the overall integrity of bridge decks is not yet fully understood. Additional research is thus required to determine how much the performance of longitudinal construction joints is affected by using a staged construction. To obtain meaningful results and conclusions, an experimental study should incorporate:

1) Evaluation of the condition of existing bridge decks with staged construction joints that have been in service for several years
2) Field measurements of differential displacements during staged construction of bridge decks
3) Numerical analysis using finite element analysis software to estimate the magnitude of differential displacements
4) Large-scale laboratory testing of representative concrete bridge deck specimens with qualitative and quantitative methods to evaluate the integrity of the concrete-bar bond and the concrete itself.

Chapter 3: Review of Regional Practices

To gauge opinions on how much of an issue differential deflections during staged construction are and how to treat them, an online survey was prepared and sent to nearby transportation agencies. Topics included limitations on traffic using the bridge during concrete placement and curing, concrete specifications, longitudinal joint detailing and common defects observed. All the questions and the full summary of responses are in Appendix A.

3.1 Survey of Regional Organizations

The online survey was sent to regional Departments of Transportation (DOT) in Wisconsin, Illinois, Minnesota, Michigan and Missouri, as well as bridge designers and inspectors in the State of Wisconsin. These agencies were chosen mainly because they have similar environmental considerations to the State of Wisconsin, and thus bridges in these states were expected to see similar degradation over time due to freeze-thaw cycles, road salts, and deicing chemicals.

3.2 General Trends Observed

Every state that responded to the survey indicated that they do allow vehicular traffic to use one or more lanes of a bridge while concrete is being placed on the same structure. Nearly every respondent cited less disruption to traffic as the primary reason for doing so, but economy was also a factor. One-third of respondents indicated that they impose some restriction on bridge traffic during concrete placement. These limitations included reducing speed of traffic, either by enforcing lower speed limits or by narrowing travel lanes, closing lanes adjacent to the concrete pour, and reducing truck loads.

The specifications used for bridge deck concrete were generally similar for all respondents. Each organization specified concrete with a minimum compressive strength at 28 days of 4000 psi, a maximum slump of 4 in., maximum aggregate size of 1.0-1.5 in., and approximately 6% air

entrainment. One respondent also noted that they have specific requirements for evaporation rate, placement temperatures, humidity, and wind speed during concrete curing. Two responding agencies indicated that they have weight restrictions in place until the concrete fully cures and reaches or nearly reaches its design strength.

Respondents generally did not specify that a typical reinforcement detail is required by their agency, as they will usually vary from plan to plan, but they did note some specific requirements. One respondent said they provide a rebar splice if space permits, and if not, they use mechanical connections. Another noted that they always require threaded bar splicers based on space and safety considerations. Another response noted that the reinforcement in the joint region should be checked for the overhang case during construction, and additional steel should be added if needed. One agency specified that a longitudinal construction joint must be provided if the bridge deck exceeds a certain width. It was also said that common practice is to place sealant in the construction joint before fully opening the bridge to traffic.

There was more agreement on where the longitudinal joints should be located. Most respondents specified for the construction joints to be between girders, and not in the final wheel path (i.e. between lanes, middle of lane or on the shoulder). One respondent specified that longitudinal construction joints should not be located over girders because they are more likely to retain water, which will create performance issues from freeze-thaw cycles and corrosion, but another agency specified that they prefer to place construction joints over girders when geometry allows. A detail where the construction joint is within the top flange of the girder was encountered in Texas by Furr & Fouad (see Figure 2.1d) and no defects were noted in bridges with this type of joint. However, the climate in the Midwest is much less forgiving, and it seems reasonable to

expect that any entrapped water in the joint region would be more likely to cause problems in a colder climate.

The most common premature defect reported by those surveyed was unsatisfactory joint performance (58% of respondents) followed by longitudinal and transverse cracks (both 50%) and random cracks (42%). Less common defects experienced are concrete spalling (33%), joint leakage (8%), poor ride quality (8%) and reduction in transverse rebar bond (8%).

3.3 Conclusions

This survey provided unique insight into the perception of this issue. Some topics were agreed upon unanimously, and others had very little consensus. The respondents were consistent in that they allow vehicles to continue using bridges during concrete placement and curing because the impact to traffic by not doing so would be too great. The specifications for the concrete used in bridge decks was also very consistent across all agencies, and conforms to the recommendations provided by previous researchers for a high-quality, low-slump, well-compacted concrete. There is near unanimous agreement that longitudinal construction joints should be located between girders and out of final wheel paths whenever possible, which is consistent with observations seen in Chapter 4. Nearly every respondent also noted that defects were often present and occurring prematurely in longitudinal joint regions, so there was some consensus that construction joints were not performing satisfactorily.

There was however, no consensus as to how to handle traffic using the bridge during concrete placement and curing. Speed limits, weight limits, and lane closures were all mentioned as ways to reduce live load deflections during concrete curing, but none have been widely adopted. Previous research suggests that moving traffic as far away from the concrete pour as possible and

providing a smooth road surface are the two most effective ways of limiting traffic-induced deflections and vibrations, but it seems that few agencies have adapted these policies.

Chapter 4: Evaluation of Existing Staged Construction Bridges

To further understand the types of defects that could possibly be created in concrete bridge decks due to traffic displacements during construction, several existing bridge decks constructed under these conditions were inspected. These bridges were primarily located in Southern Wisconsin, and were identified with the help of the Project Oversight Committee and the Wisconsin Department of Transportation's Highway Structures Information System (HSI).

4.1 Selection of Bridges

This research was chiefly concerned with problems arising from differential deflections of girders adjacent to longitudinal construction joints, a phenomenon that is mainly relevant to concrete deck-on-girder bridges. As such, the field investigations were performed almost exclusively on this type of bridge, either with prestressed concrete or steel girders. Using the HSI online database, bridges with longitudinal construction joints were identified by applying criteria filters to the nearly 12,000 bridge structures in the WisDOT inventory. There exist no criteria denoting staged construction within HSI, so possible staged construction bridges had to first be filtered using other criteria, and then their plans checked for staged construction. Examples of these filtering criteria are location, bridge type, year built, and work performed. Bridges located near Madison, Wisconsin were given priority to reduce the amount of travel required to reach the bridge sites. The number of years the concrete deck had been in service was also considered, as the investigations were concerned primarily with premature defects, and it would be difficult to make any conclusions about decks that were nearing the end of their useful life.

Reviewing the construction history was critical in finding bridges that had been constructed in stages. Previously widened bridges almost always incorporate staged construction and a longitudinal construction joint. It is also relatively common for bridges undergoing deck

replacement to be constructed in stages. A smaller percentage of new construction bridges utilized staged construction, but this was sometimes the case when the new structure was replacing an existing one. Several bridges were identified that had concrete decks constructed in stages, but in many cases a concrete or bituminous overlay had previously been placed on the wearing surface. These bridges were not inspected, as any damage that had occurred to the wearing surface during the construction process would be unidentifiable underneath the overlay.

Recent inspection reports are also available for most bridges within HSI. Once a staged construction bridge was identified, the notes from inspectors were reviewed. If there was any mention of defects in the longitudinal joint region from a previous inspection, this bridge was given priority as one to inspect further.

In total, 83 bridges were identified as being constructed in stages and possible candidates for inspection. Of these, 41 bridges were visually inspected by the research team, including 23 steel girder bridges, 10 prestressed concrete girder bridges, and eight haunched concrete slab bridges. No information was available regarding traffic conditions at the time the concrete deck was poured, so it was assumed in all cases the traffic was maintained on the bridge during and after concrete placement. However, this eliminates the possibility of correlating bridge deck condition with traffic control measures in this task. A comprehensive list of these bridges, along with their details and inspection notes, is in Appendix B.

4.2 Methods of Inspection

Visual inspections were performed for each of the 41 bridges mentioned previously. These included taking still photographs from underneath and on top of the bridges. No lane closures were used during the inspections, and traffic control measures were limited to a parked vehicle with flashing lights. These inspections focused on the presence of any cracks, spalls, corroded

reinforcement, leakage, etc. in the bridge decks. Consideration was given to the distribution of visible defects in the different deck stages. If staged construction practices cause defects, then the stage poured adjacent to live traffic should exhibit more damage than the stage constructed while isolated from traffic.

Due to traffic considerations and the fact that many of the bridges were on or over major highways, it was often not possible to get next to the longitudinal construction joints, which were often located in a travel lane. To overcome this, a GoPro HERO4 Black Action Camera was mounted to a vehicle and used to photograph the condition of the deck while traversing the bridge. This camera was chosen for this task because it is rugged, easily mounts to a variety of surfaces, can be operated remotely, and can record video using up to 240 frames per second. This relatively high frame rate is crucial when trying to photograph fast moving objects (or in this case a stationary object from a fast-moving vehicle).

By mounting the GoPro Camera to a vehicle, pointing it at the roadway, and then driving over the bridge's longitudinal joint, a recording made up of thousands of still images of the bridge deck was created. These were analyzed frame-by-frame and any defects were noted. However, there were limitations to this method. If the vehicle was traveling at normal highway speeds (50 miles per hour or more) the images could become blurry and any details unidentifiable. To solve this, it was necessary to either use a higher frame rate or drive slower. Unfortunately, higher frame rate also means higher price, and traveling much slower on a major highway is extremely dangerous. Consequently, this method of photographing the wearing surface of the bridge was most effective on quieter roads and ones with a lower speed limit.

4.3 Condition of Bridges and Defects Noted

Overall, the condition of the decks inspected as part of this task were good, with few defects noted that could be directly attributed to the live load deflections during construction. During each inspection, notes were taken regarding any defects seen in the bridge. Common types of defects seen in longitudinal joint regions include cracking (longitudinal, transverse and random), efflorescence, leakage through the construction joint, insufficient concrete consolidation, and spots of corrosion. Less commonly seen defects were delaminated concrete, spalled concrete, and exposed corroded rebar.

4.3.1 Deck-on-Girder Bridges

Each deck-on-girder bridge inspected had one of three common reinforcement details at the longitudinal construction joint, which was always located between normally spaced girders. These three details can be seen in Figure 4.1. Detail A uses a simple lap splice of transverse reinforcement and was by far the most common in the pool of bridges inspected as part of this study. In this detail, the transverse reinforcing bars from the existing deck extend through the joint, and are lapped with transverse bars for the new deck. Splice lengths ranged from 37 to 51 bar diameters. Detail B uses a dowel bar splicer, where dowel bars are lapped with the transverse reinforcement on both sides of the joint, and connected by a bar coupler embedded in the existing deck side of the joint. All dowel bar splices encountered had a length of 52 bar diameters. Detail C uses one-piece bar couplers, where the transverse steel from both stages are simply connected using a coupler embedded in the existing deck side of the joint, with no lap splices on either side. Each detail was observed with and without the shear key formed into the existing edge of the deck. No inspected bridge had a longitudinal construction joint directly over a girder.

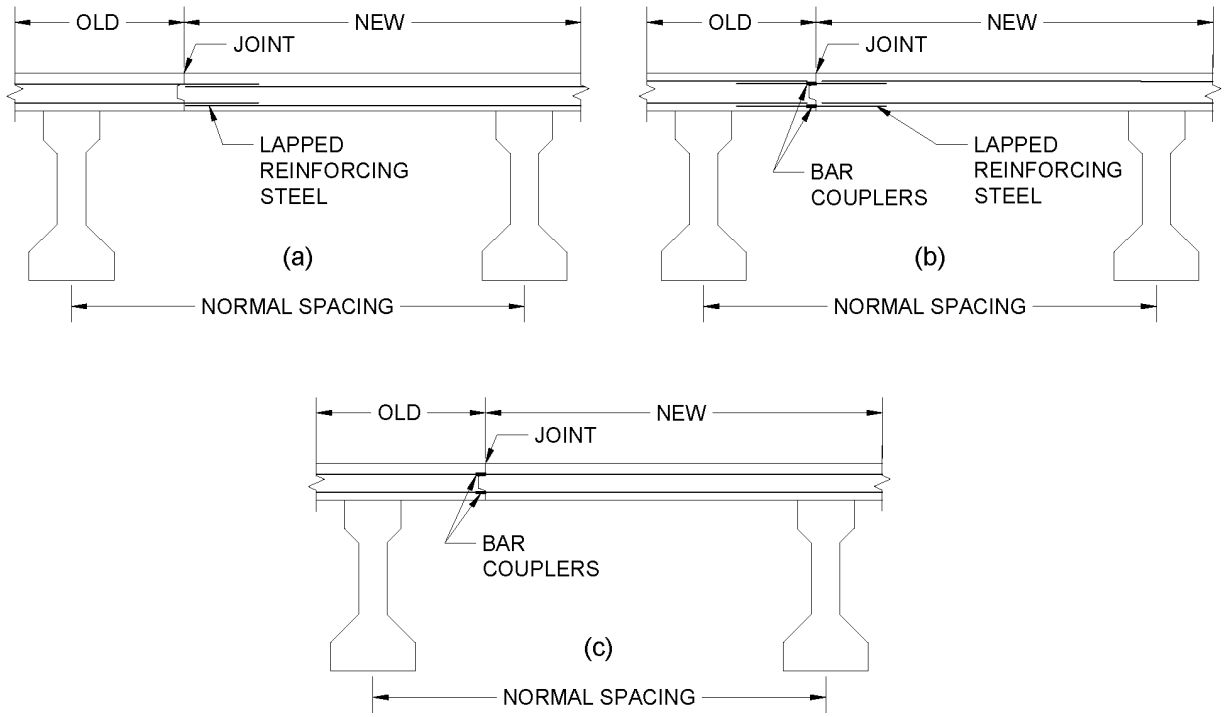

Figure 4.1- Longitudinal construction joint reinforcement details seen in Wisconsin.

Visual inspections did not prove one detail to be preferable over the others. Bridge decks with each detail were seen that were free of defects and performing well. One issue often encountered was under-consolidated concrete in the longitudinal joint region. The presence of spliced bars and shear keys in this region results in more congestion, which often makes it more difficult to properly consolidate concrete into these tight areas. Couple this with the medium slump concrete that is required for bridge decks and underconsolidation in this area becomes common. An example of inadequate consolidation can be seen in Figure 4.2. To prevent this, workers should use extra effort to ensure the concrete in the longitudinal joint region is properly consolidated by internal vibration. Alternatively, using one-piece bar couplers (Figure 4.1– Detail C) will result in the least amount of congestion and should improve this issue.

Figure 4.2- Inadequate concrete consolidation exposing reinforcement in the longitudinal joint region. (B-40-216 – Dowel bar splicer, detail B per Figure 4.1)

Nearly every bridge exhibited transverse cracking with efflorescence to some extent. These cracks were typically widely spaced in the midspan region, and were most likely flexural cracks. In some cases, these transverse cracks were concentrated more in one side of the deck (i.e. Stage 1 or Stage 2) but there was no evidence to suggest they were related to differential deflections during construction. If differential movement between concrete and reinforcement were to cause transverse cracking, it would be expected to be more closely spaced, at approximately the same spacing as the transverse reinforcement. Typical transverse flexural cracks with efflorescence can be seen in Figure 4.3.

Figure 4.3- Typical regularly spaced transverse cracks with efflorescence (B-70-176)

Per structural analysis, differential deflection of adjacent girders will cause negative moment in the concrete deck over the girder that is deflected downward less. In the case of staged construction, this negative bending will occur over the girder adjacent to the longitudinal construction joint on the side of the new deck. When the concrete has just been placed and is curing, it has very little if any tensile strength and will be prone to cracking. If differential deflections are large enough, one would expect a longitudinal crack to form in the top surface of the deck above this girder near midspan.

A small number of the bridges inspected contained longitudinal cracks over girders adjacent to the staged construction joint. However, these cracks were not limited to just the Stage 2 section of the deck. In some cases, the longitudinal cracks were also present in the deck segment

that was poured while isolated to traffic, and thus were not caused by live traffic loads during the staged construction process. Therefore, no conclusions were reached whether these cracks developed because of displacements during curing of the concrete or after the bridge had remained in service for years.

Signs of leakage through the longitudinal construction joint were also commonly observed. This should be avoided; if water, deicing chemicals, road salt and other corrosive agents can seep through the construction joint and reach the reinforcement, the steel crossing the construction joint will be vulnerable to premature degradation. A typical leaking construction joint can be seen in Figure 4.4. This was typical for many of the inspected bridges. The Wisconsin DOT has a standard detail (Figure 4.5) to prevent this type of leakage, in which the top of the construction joint is saw-cut and sealed after construction of both adjoining decks. It is possible that this was not performed on the bridges that showed leakage through the joint. Bridges that utilized this sealant showed minimal signs of leakage through the joint, suggesting that this detail is adequate when used.

Figure 4.4 - Typical leakage through a longitudinal construction joint (B-53-083)

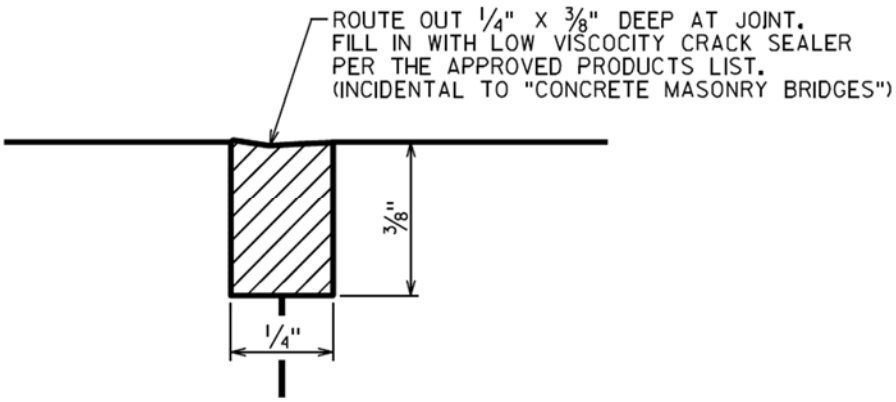

Figure 4.5- WisDOT longitudinal construction joint standard detail (WisDOT 2017)

Related to the longitudinal joint leakage problem, in some cases spots of corrosion were noticed underneath the deck at the joint location, indicating that the embedded steel has already begun to corrode. This was also occasionally seen at cracks in the bottom surface of the deck. These cases were not considered to be serious, as the spots of corrosion were small and isolated, but were nonetheless evidence of corrosion of the embedded reinforcement. A typical case of this can be seen in Figure 4.6.

One specific bridge deck constructed in stages that was determined to be in poor condition was on bridge B-13-593. This Dane County bridge was on State Highway 19 over Halfway Prairie Creek. This single-span, 58.9 ft simply-supported steel girder bridge was built in 1939, and then had a deck replacement in stages in 1989. Extensive transverse cracking at approximately the same spacing as the transverse reinforcement was seen in this bridge, extending from both sides of the construction joint. There were also delaminations in the longitudinal joint region, and two locations with spalled concrete exposing corroded reinforcing bars (Figure 4.7). The integrated wearing surface was in decent condition, with a few transverse cracks that had been recently sealed. The staged construction joint also appeared to have been sealed recently.

Figure 4.6 - Typical spots of corrosion on the underside of the longitudinal construction joint (B-56-022)

The only known design details for this bridge that may have contributed to this degradation were that the concrete deck was thin (only 7 in.), and the bottom layer of reinforcement in the slab was not epoxy coated. The plain steel bars are more susceptible to corrosion, which would then lead to the spalled patches of concrete seen in the underside of the deck. Although the deterioration in this bridge seems compelling, it is difficult to definitively attribute it to staged construction practices. At the time of the inspection, this bridge deck was 27 years old and approaching the end of its service life. It is therefore difficult to classify this damage as premature, which is the main concern of this research.

Figure 4.7- Spalled concrete and corroded reinforcement. Transverse cracking at approx. same spacing as transverse reinforcement (B-13-593)

Another bridge of interest was B-70-176 in Winnebago County. This bridge was on the southbound lane of Interstate Highway 41 over State Highway 76. This continuous steel girder bridge consisted of two 115.5-ft spans and was initially constructed in 1995 and widened in 2011. Extensive patching of the longitudinal construction joint was present along the entire length of the bridge. Upon closer inspection, the patches appeared to be concentrated toward the existing side of the construction joint. There were also no patches in the identical adjacent bridge (B-70-177) which received a full deck replacement in stages. It is possible that in preparation for the widening, the existing deck was damaged during demolition of the existing parapet. The patches were likely used repair this, and not damage to the deck caused by differential deflections during curing of the

widened deck portion. However, the widened portion of the deck had regularly spaced transverse cracks with light efflorescence throughout the length of the bridge, where the existing deck only had similar cracks in the midspan regions (see Figure 4.8). The transverse cracks in the widened portion of the bridge deck are likely shrinkage cracks. The two deck portions were constructed 16 years apart, so they were likely subjected to different environmental conditions during curing and would therefore have varying distributions of shrinkage cracks. Additionally, these transverse cracks were mainly observed in the widened portion of the deck directly adjacent to the longitudinal construction joint. Shrinkage cracks would be more prevalent in this area because the hardened deck adjacent to the curing concrete provided some restraint against shrinkage. The adjacent bridge (B-70-177), which was identical, was chosen to be a subject for the analytical modeling portion of this research as discussed in Section 6.4.

Figure 4.8- Transverse cracks extending to abutment in Stage 2 deck (right side). Transverse cracks in Stage 1 deck (left side) only near midspan region. (B-70-176)

4.3.2 Haunched Slab Bridges

Eight concrete haunched slab bridges along a stretch of Interstate Highway 41/94 were also investigated as part of this task. These bridge structures were in pairs, with each bridge carrying one direction of traffic. Each of these bridges were almost identical structurally. All had three spans of 33, 43, and 33 ft and varied in total thickness from 10 in. to 27.5 in. They were initially constructed in stages in 1959, and then widened again using staged construction in 1970. All eight bridges received a concrete overlay in either 1980 or 1987, and then a bituminous overlay in 1998 or 2001. One bridge, B-30-015, was identified by the Project Oversight Committee as having unique longitudinal construction joint issues, which sparked the investigation of these eight similar bridges.

The condition of the longitudinal joints in these haunched slab brides was determined to be very poor. Many of the defects described previously for deck-on-girder bridges were also seen here, except at a more serious level. Many of these bridges had extensive patching of concrete in the longitudinal joint region, indicating concrete had previously spalled off (Figure 4.9). Some bridges had not been patched yet, and very large spalled areas exposing corroded rebar were visible (Figure 4.10). Other common defects in these bridges were longitudinal cracks and delaminations adjacent to the longitudinal construction joints (Figure 4.11 and Figure 4.12).

In 1970, when these bridges were widened, epoxy coated steel reinforcement was not being used in Wisconsin, which explains why such severe corrosion of the reinforcement was seen. Due to the overlays in place, the original wearing surface could not be inspected, but based on the condition of the underside of the slab, it may be inferred that cracks and other defects in the longitudinal construction joint region allowed for the corrosion of the underlying steel reinforcement, resulting in the eventual defects seen in this region.

Figure 4.9- Patching of previously spalled concrete at longitudinal construction joint in haunched slab bridge. (B-30-026)

Moisture between adjacent bridge structures (Figure 4.13) was observed for all the inspected haunched slab bridges. There was no structural connection between the adjacent bridges, just an embedded 6” rubber waterstop. This connection appeared to be retaining moisture in this region and not allowing the concrete to dry. Thus, extensive corrosion and efflorescence was observed at each connection. Although not related to live load deflections in curing concrete, this detail does appear to have compromised the long-term integrity of the bridges.

Of these eight bridges, B-30-015 which was identified by the Project Oversight Committee, appeared to be in the worst condition. In addition to all the defects mentioned previously, one startling observation was visible movement between bridge deck stages during the passage of large trucks. In both approach spans, large longitudinal cracks in the construction joint region visibly

opened under traffic loading. This differential movement at the construction joint was measured to be approximately ¼ in., and occurred in the construction joint from the original 1959 construction (Figure 4.14). This repeated opening and closing of large cracks was slowly wearing away the concrete, which was piling up on the embankment underneath. Visible differential movement at the longitudinal construction joint verified that the continuity across the joint had been severely degraded. This likely meant the concrete-rebar bond across the joint had been compromised, possibly due to corrosion of the steel, damage to the surrounding concrete, or other factors.

Figure 4.10- Spalled concrete at longitudinal construction joint exposing corroded reinforcement. (B-30-014)

The different construction procedures for deck-on-girder bridges and haunched slab bridges results in different live load deflection problems during staged construction. In deck-on-girder bridges, the formwork is often supported by the precast concrete or steel girders, so the

curing concrete and reinforcement deflect together with the girders under traffic loads. Diaphragms and cross braces also help to distribute forces transversely and equalize deflections. In concrete slab bridges, the formwork is often supported by the ground below so the curing concrete does not deflect at all. If there is no shoring in place for the existing portion of the bridge, all the live load deflection will be transferred to the reinforcement embedded in the curing portion of the slab. These conditions, if not accounted for, could result in staged construction concrete slab bridges experiencing larger displacements between adjacent stages than deck-on-girder bridges.

Figure 4.11- Large longitudinal crack adjacent to construction joint. (B-51-017)

Figure 4.12 - Delaminated area adjacent to longitudinal construction joint in widened portion of deck. (B-30-014)

Minimal details were available concerning the shoring and falsework for these eight haunched slab bridges, so it was impossible to say if a lack of shoring under the existing bridge resulted in large differential deflections and the subsequent deterioration of the construction joints over time. These bridges also had a short lap splice provided between construction stages, which may also have contributed to the observed degradation. In both 1959 and 1970, the construction stages were connected with a 24-bar diameter lap splice. This is considerably shorter than the lap splices seen in any of the deck-on-girder bridges that were investigated, which had a minimum splice length of 37 bar diameters, but utilized epoxy coated bars which require more development length. Today, AASHTO LRFD (2012) would require these uncoated bars to be spliced 26 to 34 bar diameters, depending on the class of lap splice. A shorter splice would increase the possibility for the bond to become deteriorated by differential deflections during curing. However, it is unclear exactly what materials were used in the construction of these bridges, and this splice length may have been appropriate for developing reinforcement with a yield strength less than 60 ksi.

Figure 4.13 - Efflorescence and corrosion due to retained moisture at waterstop joint between adjacent bridges. (B-30-025/026)

Figure 4.14 - Large longitudinal crack opening approximately 1/4"during the passage of large trucks. (B-30-015)

4.4 Conclusions

Field inspections of 41 bridges across Wisconsin did not provide conclusive evidence that *live traffic* during staged bridge construction causes deterioration of concrete bridge decks, but did indicate that some defects and degradation may arise from the *construction practices* for longitudinal joints. For concrete deck-on-girder bridges, no cases were found where traffic-induced differential deflections during curing of the concrete deck definitively caused damage or a loss of integrity in the concrete. A small number of these bridges did show signs of deterioration and damage in the longitudinal joint region, but due to their age, these defects could not be definitively attributed to the staged construction process. The one defect that was frequently noted in deck-on-girder bridges was areas of underconsolidation in the longitudinal joint region. This was definitively attributable to the construction practice, because this can only occur during concrete placement. Longitudinal construction joints often incorporate spliced reinforcement and shear keys, which can cause congestion and make it more difficult to properly consolidate the moderate slump concrete that is used in bridge decks. Extra attention should be given to consolidating the concrete in this region to ensure that the concrete does not have any large voids under the reinforcement or in the shear key. Using one-piece bar couplers will reduce the amount of reinforcement in the construction joint region and should allow the concrete to be more easily consolidated.

One objective of this task was to determine if there exists any connection between longitudinal construction joint design details and long-term performance. The details of each slab-on-girder bridge were examined in terms of span length, girder configuration, girder spacing, deck thickness, location of joint between girders and joint connection details. No trends were observed between these variables and the defects seen. The only factor noted to influence the presence of

defects was the age of the bridge deck. Leakage through the joint may be controlled by the Wisconsin DOT standard detail in which the top of the construction joint is saw-cut and sealed after construction of both adjoining decks. Another option that may control leakage through the joint is the use of a concrete retarder on the side surface of the first stage concrete, as discussed in Section 7.4.

Based on inspections of eight identical haunched slab bridges, bridges of this type may be more susceptible to damage from the staged construction process. Each of these bridges had longitudinal construction joints that were in poor condition. The shoring system used during construction of slab bridges could result in larger differential movements between hardened and curing stages. Differential deflections between stages could be an issue if the new stage is shored while the existing stage is not. No information was available regarding the type of shoring that was used and how long it was in place for, so no definite conclusions can be made on how this factored in to the poor performance of the construction joint. However, providing shoring for both construction stages throughout the construction of the bridge will eliminate any possibility of differential deflections occurring.

Another possible explanation for this degradation is that the construction joint was not well detailed, and many years of increasing traffic demands has taken its toll on the deck. Defects in the wearing surface would have allowed corrosive agents to attack the uncoated steel reinforcement beneath, which would begin to lose its bond with the surrounding concrete, and make the construction joint even more susceptible to damage. Additionally, at the time of inspection, these bridges, which are on one of the busiest highways in Wisconsin, were 58 years old with a 47-year-old widening. Years of heavy traffic loads and harsh environmental conditions are likely to be the main reasons why the construction joints were in such poor condition. In this

case, it was not possible to determine the key factor for the deterioration of these joints, but it is highly likely that the use of staged construction and the resulting presence of longitudinal construction joints has led to the rapid deterioration of this slab structure. These eight bridges were all part of the same construction project and were almost identical structurally, making it difficult to establish conclusions for concrete slab bridges in general.

If maintaining traffic during staged construction does cause deterioration of bridge decks, then these defects would become present shortly after construction and then compromise the durability of the structure over its service life. To make more definitive conclusions on defects directly caused by staged construction, inspections should be performed immediately and routinely after completion of construction.

Chapter 5: Field Monitoring of Displacements During Staged Construction

The next objective of this research was to identify bridges being built using staged construction, and then install instrumentation to measure differential deflections of the construction stages during the concrete curing period. Two Wisconsin highway bridges constructed in stages during the Summer of 2016, B-16-136 and B-64-123, were chosen to be subjects of the field monitoring. Once these bridges had been identified, the setup for the instrumentation was designed and fabricated before being deployed at the bridge sites.

The first bridge that was field monitored, B-16-136, is a single-span prestressed concrete girder bridge located in Dairyland, WI. This bridge was constructed in stages during the spring and summer of 2016 with one of two traffic lanes open throughout the construction process. The instrumentation setup discussed in Sections 5.1 and 5.2.1 was used to measure differential displacements immediately after casting of the Stage 2 concrete deck. Throughout this chapter, the monitoring of deflections during curing of the Stage 2 deck is referred to as “staged-construction monitoring”.

The second bridge that was field monitored, B-64-123, is a three-span prestressed concrete girder bridge located in Darien, WI. This bridge was also constructed in stages during the spring and summer of 2016 with one of two traffic lanes open throughout the construction process. The instrumentation setup discussed in Sections 5.1 and 5.3.1 was used for the staged-construction monitoring of this bridge. For this bridge, the instrumentation was also used to monitor displacements after the Stage 2 deck had fully hardened and the formwork had been removed. Throughout this chapter, the monitoring of deflections after the Stage 2 deck has fully cured is referred to as “post-construction monitoring”.

After collecting the data, the magnitudes of differential deflections caused by regular traffic conditions were computed for both bridges. Two different methods of calculating the differential displacements were used, as discussed in Sections 5.1.3 and 5.1.4. The distributions of differential deflections from both methods were then analyzed to provide probable magnitudes of differential deflections. In the case of bridge B-64-123, the magnitudes of differential deflections during staged-construction monitoring and post-construction monitoring were also compared.

5.1 Instrumentation and Setup

To measure differential deflections during staged construction, an instrumentation setup was designed to be placed on the hardened concrete deck of the first stage, where it would extend over the freshly placed concrete and measure distances to points on the deck surface. The instrumentation that was utilized for this task consisted of string potentiometers (SPs), linear variable differential transformers (LVDTs), accelerometers and tiltmeters. These instruments were all manufactured by Bridge Diagnostics, Inc. (BDI) and data collection was performed using their STS Live software.

All the sensors used for the field monitoring were attached to a custom-made structure that could be quickly set-up and deployed on site. In previous studies where field monitoring was performed (see Section 2.3), the differential deflections were calculated using linear potentiometers to measure absolute displacement of the bridge girders, and then taking the difference. Unlike those studies, the instrumentation setup used here essentially measures differential displacements of the concrete deck directly with linear potentiometers. Absolute deflections of the girders can also be calculated using accelerometer data.

5.1.1 Instrumentation Arm Structure

The BDI sensors were mounted to a braced cantilever structure referred to as the "instrumentation arm". The instrumentation arm was fabricated with a mild steel base and slotted steel angle sections for the cantilever portion. The base was made from an 18-in. long 6x4x3/8 in. hollow steel section welded to a 0.75-in. thick steel base plate. Two slotted angle sections were bolted together to create a T-section, and were then clamped rigidly to the top of the hollow steel section. The brace was also made from a single slotted angle bolted at one end to the base plate and to the web of the horizontal T-section at the other. Slotted steel angle sections were chosen because of their light weight and versatility in attaching the instrumentation. Figure 5.1 shows a sketch of the instrumentation arm structure. Once all the instruments were attached and the arm was moved into position on the bridge decks, counterweights were placed on the base plate to stabilize the structure.

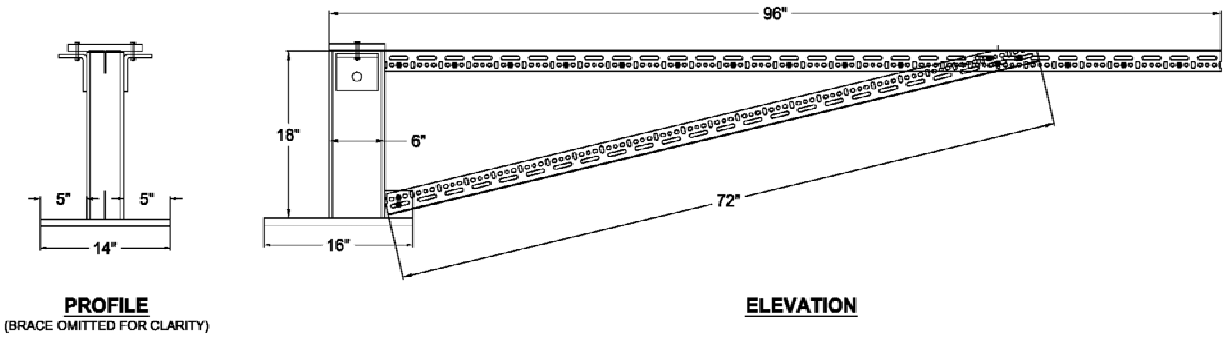

Figure 5.1- Instrumentation arm structure

The arm was designed to be long enough to extend between the two girders adjacent to the longitudinal construction joint. Ideally, the instrumentation arm base would be placed directly over the girder nearest the construction joint on the hardened side of the deck to allow for direct measurement of deflections between the adjacent girders. In the case of bridge B-64-123, the

geometry of the construction staging did not allow for the instrumentation arm base to be placed in this location, so it was set up as close as possible.

5.1.2 Instrumentation and Sensors

The instrumentation used to monitor displacements consisted of two LVDTs, four or five string potentiometers, four or five accelerometers and four tiltmeters. For complete details of the instrumentation used for each field monitoring test, refer to Figure 5.8 in Section 5.2.1 for bridge B-16-136 and Figure 5.13 in Section 5.3.1 for bridge B-64-123. LVDTs were placed at the tip of the cantilever and close to the base and measured relative distance between the arm and the curing concrete deck. String potentiometers were also placed in these locations, as well as points in between. Accelerometers and tiltmeters were located at the tip of the cantilever, the base of the arm, and on small steel plates resting on the fresh concrete surface. These plates were also used as surfaces to connect the string potentiometers and LVDTs to, as it was assumed that these plates displaced the same as the concrete surface they were resting on. A photograph of the complete instrumentation setup in place on a test bridge can be seen in Figure 5.2.

These sensors measured displacements at points on the fresh concrete surface as well as on the instrumentation arm itself, which then allowed for the calculation of differential deflections between the two adjacent girders. Two different methods were used to compute differential deflections. They are discussed further in Sections 5.1.3 and 5.1.4. A collection frequency of 100 Hz was used for all field monitoring.

Figure 5.2- Field monitoring instrumentation setup after casting of Stage 2 deck (B-16-136)

5.1.3 Corrected LVDT/SP Measurement Method

The first method for measuring differential deflections, referred to as the "Corrected LVDT" or "Corrected SP" method, utilized the LVDT or string potentiometer at the tip of the cantilever measuring relative displacement between the arm and the concrete deck. This measurement was then corrected to account for any rotation of the arm. A diagram of how differential deflections are measured using this method is shown in Figure 5.3. Equation 1 was used to calculate differential deflections with this method. With this equation, a negative value of ΔH corresponds to a differential deflection where the girder on the hardened side of the joint displaces downward more than the girder on the recently poured side.

$$\Delta H = \theta * L - D_2 \quad (1)$$

where:

ΔH = Differential deflection of adjacent girders
D_2 = Displacement measured by LVDT or SP at tip of instrumentation arm
θ = Rotation of arm
L = Length of arm

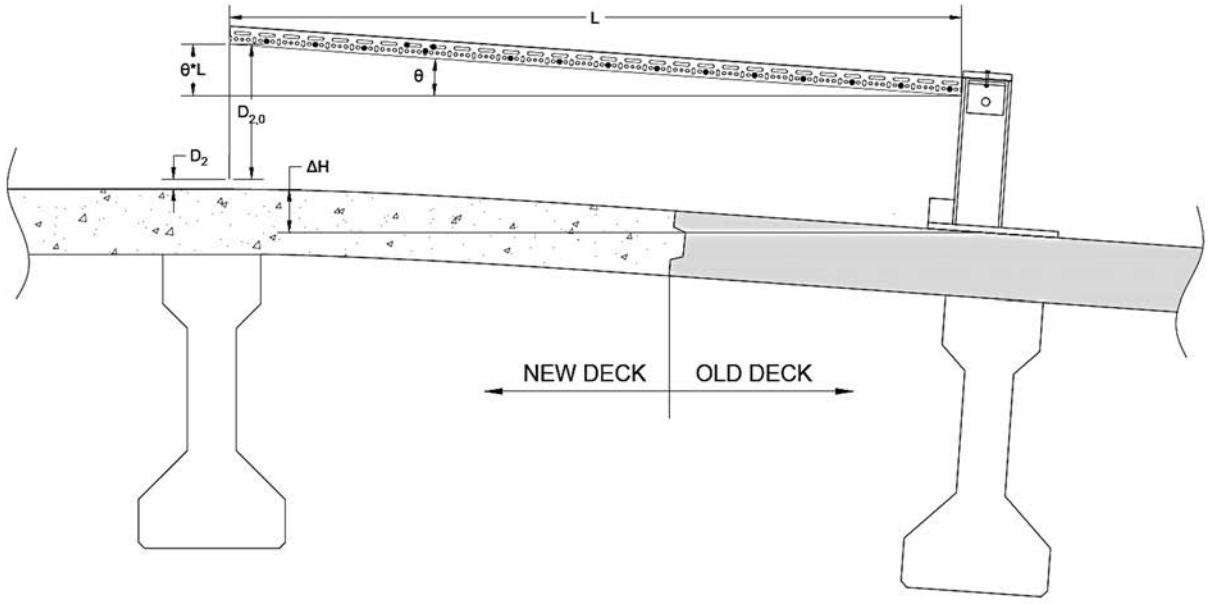

Figure 5.3 - Measured and calculated distances used in the corrected LVDT method. $D_{2,0}$ is the initial reading from the LVDT/SP at the tip of the arm. (Diagonal brace and sensors not shown for clarity).

This method for calculating differential deflections is only valid if the instrumentation arm remains rigid and does not deform during traffic event excitations. Comparing the rotation of the tiltmeters mounted at the base and tip of the instrumentation arm showed whether the arm remained rigid during a traffic event. Figure 5.4 shows that the arm does indeed remain almost perfectly rigid, because both tiltmeters show almost the exact same rotation over the course of a traffic event. However, it was later determined through testing that the tiltmeters could not respond quickly

enough to accurately measure the magnitude of the rotation of the arm during a dynamic event. Nevertheless, the tiltmeters responded together, indicating that the structure to which they were attached remained rigid.

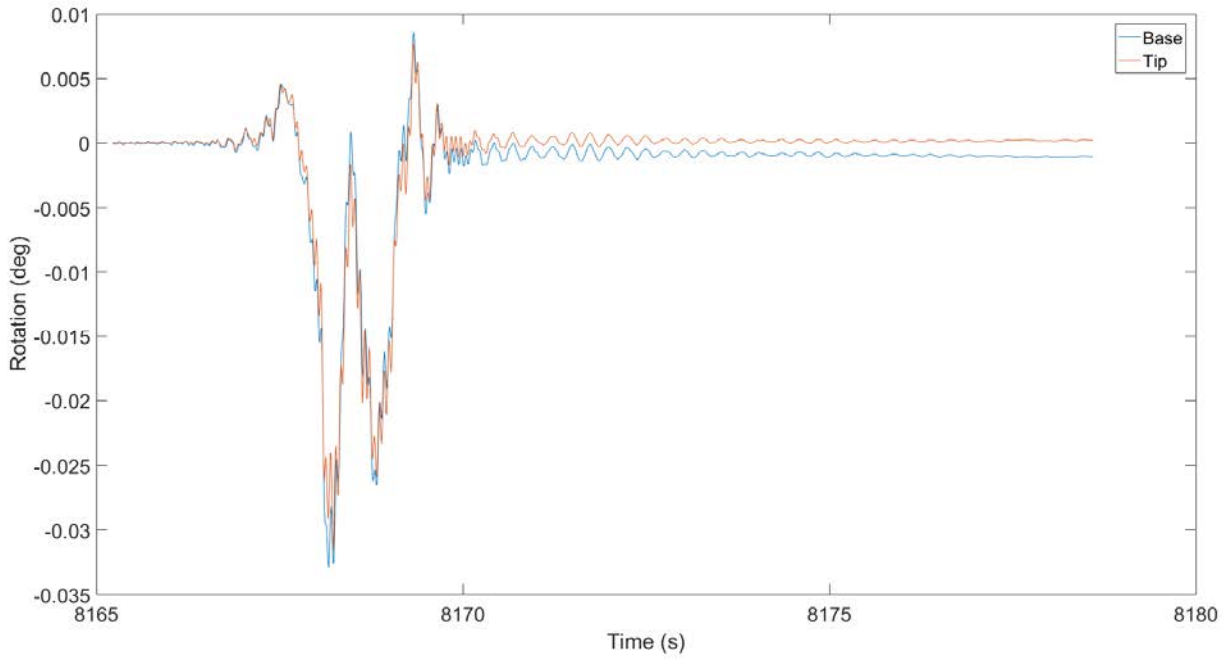

Figure 5.4 - Response of arm tiltmeters to typical traffic event

When calculating the deflection at the tip of the instrumentation arm due to rotation, it was suspected that the tiltmeters were producing inaccurate data. To verify this, a test of the instrumentation arm was performed in the laboratory. The arm and the instruments were set up just as they had been in the field, and then the base was rotated slightly and allowed to drop to the floor. As before, rotations from tiltmeters attached to the base and tip of the arm were studied to determine if the arm remained rigid. Figure 5.5 shows that this is the case, because the responses of the tiltmeters to the excitation are nearly identical.

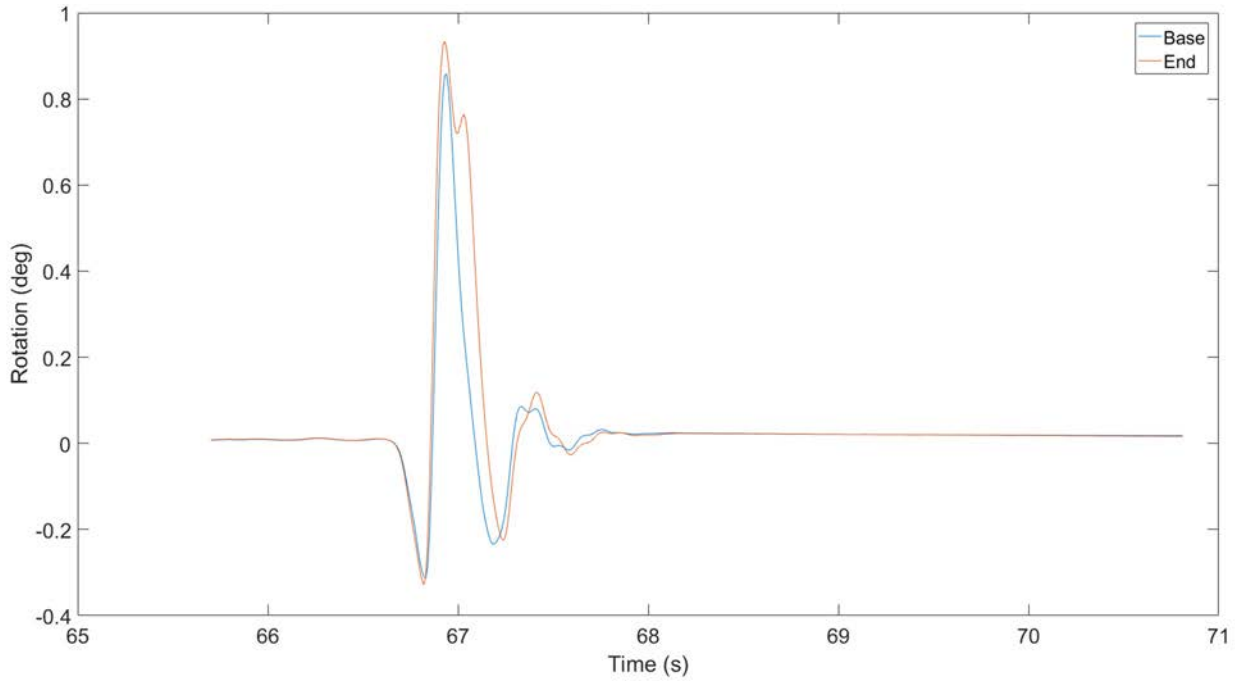

Figure 5.5 - Arm rotation versus time for laboratory test of instrumentation arm

During this test, the displacement at the tip of the arm was measured by an LVDT which was taken to be the true tip displacement. The displacement was then also calculated by multiplying the rotation from the tiltmeter at the base of the arm by the arm length. For comparison, the tip displacement was also calculated by twice integrating the acceleration from an accelerometer at the tip of the arm. These calculated displacement curves are plotted in Figure 5.6.

This test of the instrumentation showed that the tiltmeters do not provide an accurate measurement of the arm rotations for this type of excitation. It was believed that the response time of the tiltmeter was too slow to accurately measure rotations occurring at higher frequencies. The true tip displacement measured from the LVDT had an approximate response frequency of 7.5 Hz. The response of the tiltmeter had a frequency of approximately 2.4 Hz., showing that it cannot respond fast enough to measure displacements at higher frequencies than this. It appeared that after the initial excitation, the tiltmeter overshot slightly and then overcorrected considerably when the displacement reversed. Data recorded during the bridge tests showed frequencies that were

considerably higher than this, and thus it was determined that the tiltmeters would not provide accurate measurements for rotations during the test.

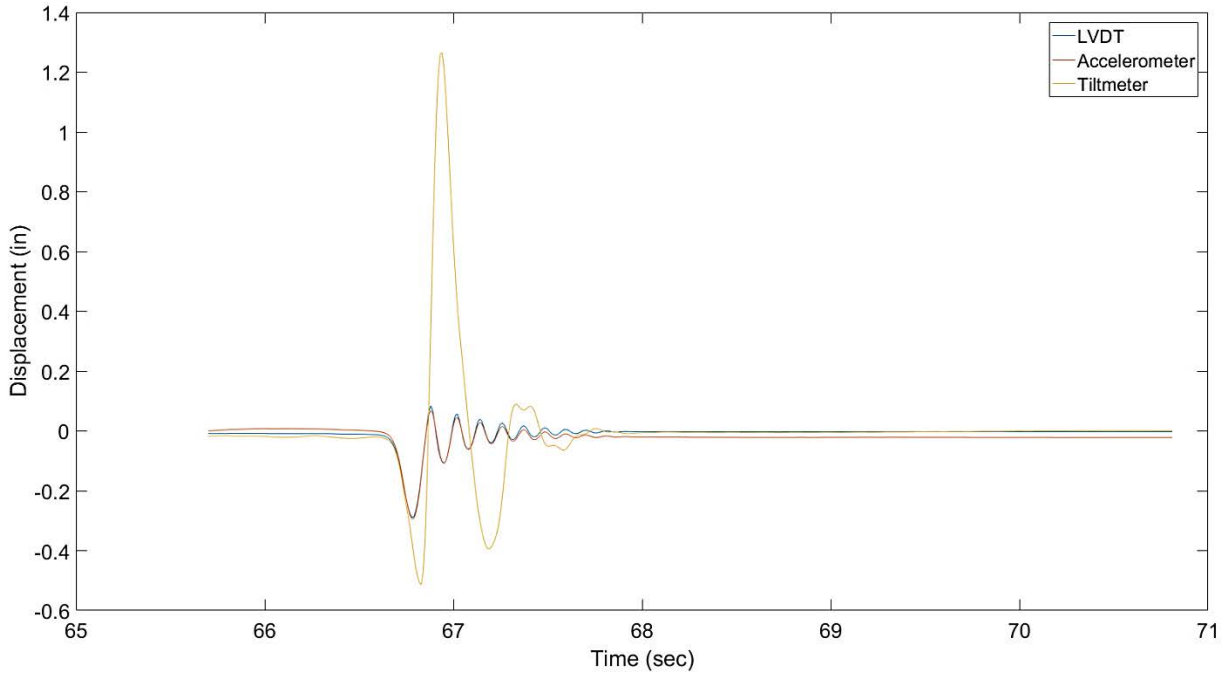

Figure 5.6 - End displacement versus time for laboratory test of instrumentation arm

Fortunately, the plot of these displacement curves also showed that displacements can be calculated accurately by double integration of the accelerations. Integration of the acceleration data results in the velocity of the accelerometer, and then integrating again provides the absolute displacement of the accelerometer. One issue with using numerical integration is the possibility for compounding integration errors to accumulate and provide false results. By minimizing the length of the trace that is being integrated and using a combination of high and low pass filters, the integration errors can be reduced, resulting in an acceptable way to calculate displacements.

The trace lengths were minimized by using the base accelerometer to isolate individual traffic events. When a disturbance detected by the accelerometer was above the level of ambient movement, only that segment of data was kept and anything before or after the disturbance was trimmed. By doing this, errors resulting from integrating accelerations due to ambient movement

of the arm could be minimized. The accelerometer data were also run through a series of high and low pass filters to minimize these errors. Accelerations with a frequency above 30 Hz and below 0.1 Hz were initially filtered out before performing the first integration. The resulting velocities with a frequency above 30 Hz and below 0.25 Hz were filtered out before performing the second integration that produced displacement of the accelerometer.

By performing this filtering and integration to the data sets from the accelerometers used in the bridge field monitoring, absolute displacements were calculated for the base of the arm, the tip of the arm, and points on the bridge deck above the adjacent girders. Arm rotation can then be calculated by taking the difference of the tip and base displacement of the instrumentation arm and dividing by the length between the two.

5.1.4 Deck Accelerometer Measurement Method

The second method, referred to as the "Deck Accelerometer" method, utilized the accelerometers attached to the steel plates resting on the concrete deck above the adjacent girders. By performing the same process of filtering and integrating the acceleration data discussed in Section 5.1.3, displacements of each accelerometer were calculated; the difference between these two deflections was the differential deflection, as presented in Equation 2.

$$\Delta H = D_{A3} - D_{A4} \qquad (2)$$

where:

$\Delta H =$ Differential deflection of adjacent girders
$D_{A3} =$ Displacement calculated by double integration of the accelerometer marked A-3 in Figure 5.8 and Figure 5.13
$D_{A4} =$ Displacement calculated by double integration of the accelerometer marked A-4 in Figure 5.8 and Figure 5.13

5.2 Bridge B-16-136

5.2.1 Description

Bridge B-16-136 was a simply-supported prestressed concrete girder bridge in Dairyland, Wisconsin. This two-lane bridge was on State Highway 35 and crossed over Chase Creek in Douglas County. The bridge had a 60-foot span, and the five 36-in. deep prestressed concrete girders had a constant spacing of 8 ft. The cast-in-place concrete deck was 8-in. thick. Transverse reinforcement of #5 bars were spaced at 6.5 in. on top and bottom of the deck. Longitudinal reinforcement of #4 bars were spaced at 8.0 in. on top and bottom of the deck. At the longitudinal construction joint, the construction plans called for transverse reinforcing bars to be lapped 31 in., which is equivalent to 50 bar diameters. Actual field measurements of the splice length varied between 34.5 in. and 36 in. (55–58 bar diameters). There was no shear key formed into the edge of the Stage 1 deck.

This entirely new structure replaced an existing bridge and was constructed in stages. The first stage involved construction of the northbound lane, and extended 12 in. past the centerline of the bridge. The concrete deck for the first stage was poured 43 days before the second stage was poured. The remaining portion of the deck, including the southbound lane, was constructed during the second stage (see Figure 5.7). Immediately after casting of the Stage 2 portion of the deck, it was covered in moist burlap and plastic to begin moist curing. The instrumentation arm setup was then moved into place at midspan of the center girder, where the largest differential deflections were expected. Because the instrumentation could not be moved into place until after the deck had been poured and finished, the data collection began approximately 4 hrs. after the concrete pour started, and about 2 hrs. after all the concrete had been placed. Data were collected for approximately 4 hrs. 15 mins., a limitation primarily based on the safety of the research team in

collecting data through the evening and night without other supervisory personnel. Thus, the data collected correspond to a time frame from 4 hrs. to 8 hrs. 15 mins. after concrete placement commenced.

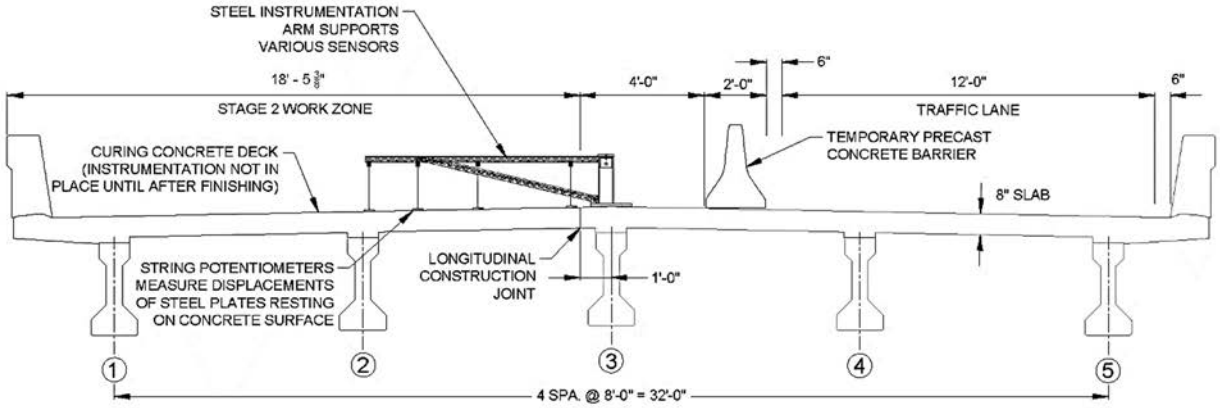

Figure 5.7 – Cross section of bridge B-16-136 during stage 2 construction (looking north)

The instrumentation used for the staged-construction monitoring of B-16-136 consisted of two LVDTs, five string potentiometers, four accelerometers and four tiltmeters. Exact locations of these sensors are shown in Figure 5.8. Sensors marked A-1 through A-4 are accelerometers, T-1 through T-4 are tiltmeters, SP-1 through SP-5 are string potentiometers, and LVDT-1 and LVDT-2 are LVDTs.

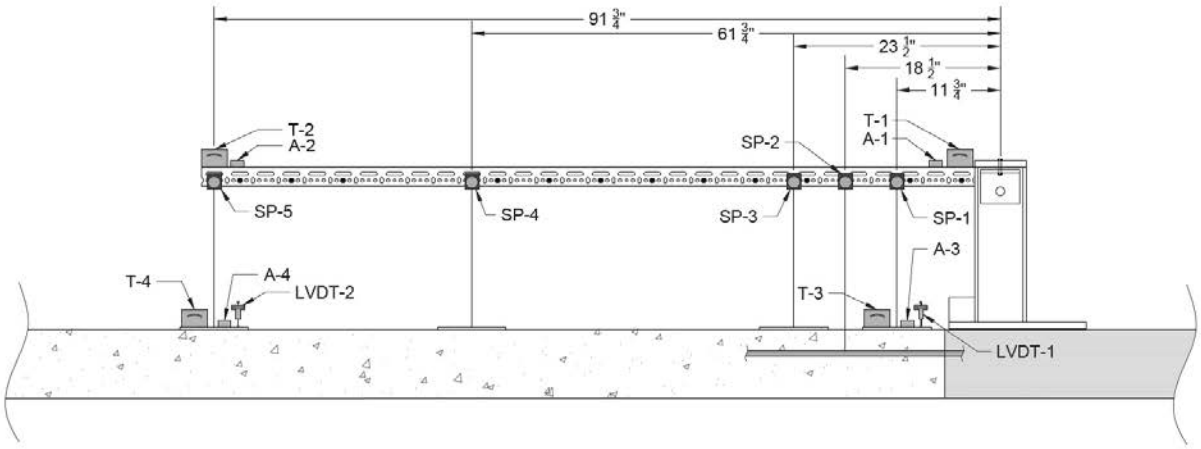

Figure 5.8 - Instrumentation setup for the staged-construction monitoring of bridge B-16-136.

During the monitoring of bridge B-16-136, SP-2 was connected to the top layer of the embedded reinforcement, with the goal of measuring any relative displacement between reinforcement in the longitudinal joint region and the surrounding concrete. This did not prove to be successful, so it was eliminated for the following test.

5.2.2 Results

During the data collection period, 228 traffic events were detected and measured by the instrumentation setup, which corresponds to approximately one traffic event every 67 seconds. Traffic events were determined by excitation measured by the accelerometer at the base of the instrumentation arm. The beginning of an event was triggered when a threshold acceleration was reached, and the event ended once the acceleration dropped below the threshold value for a period of four seconds. For this test, the acceleration threshold was set to be a range of 0.002 g (i.e. when the range of acceleration exceeded 0.002 g, the start of the event was triggered). Each traffic event does not necessarily correspond to a single vehicle, and could be the response of several vehicles one after another. It was not possible to isolate the bridge's response to each vehicle passing as sometimes vehicles were on the bridge at the same time and their influence on the bridge would therefore be combined.

The calculated differential deflection between adjacent girders for a typical traffic event can be seen in Figure 5.9. Both methods of calculating the differential deflections discussed previously are shown and there is reasonable agreement between the peak displacement values. In this case, a negative value for differential deflection means that the girder on the hardened side of the construction joint deflected downwards more than the girder on the freshly poured side. The total differential deflection for each event is taken to be the total range of deflection (i.e. difference between maximum and minimum). The total differential deflection measured for this specific

event was 0.0193 in. as measured by the Corrected LVDT method, and 0.0156 in. as measured by the Deck Accelerometer method.

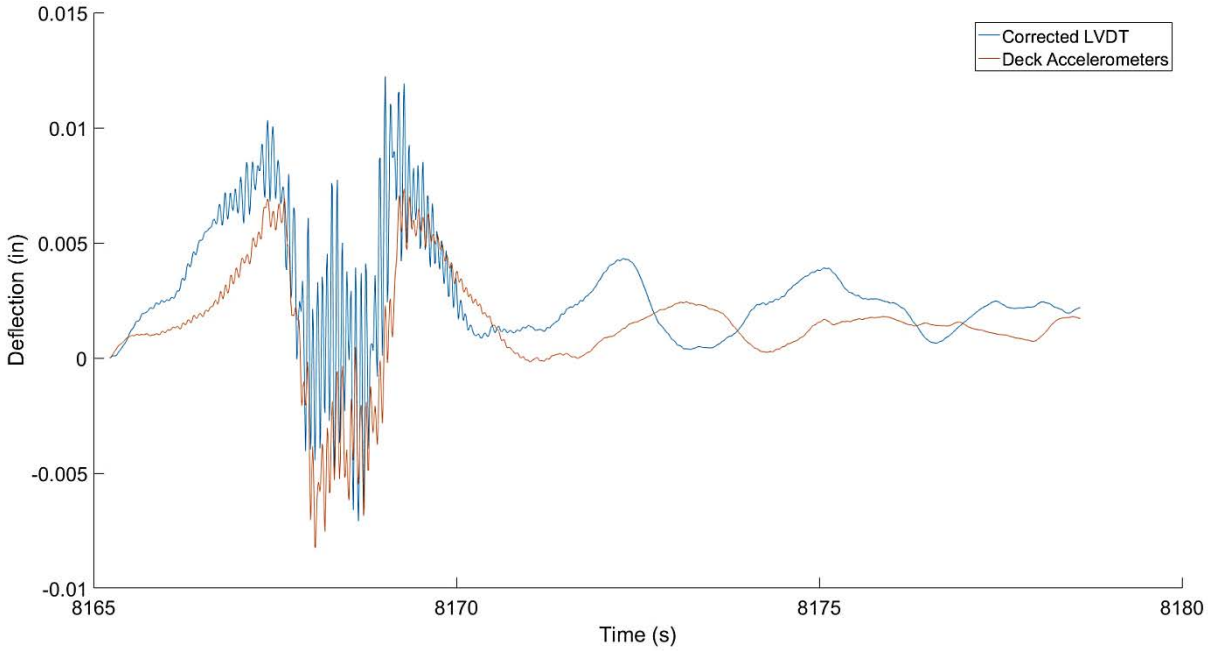

Figure 5.9- Typical trace of differential deflection versus time for bridge B-16-136

Differential deflections were calculated in this way for each of the 228 traffic events. To determine the probability of experiencing a certain differential deflection, the collection period was divided into five-minute windows and the maximum differential deflection in each five-minute period was recorded. These maximum differential deflections were then plotted using a histogram and fit to a type-I extreme value distribution, also known as a Gumbel distribution. An extreme value distribution was used because extremely large differential deflections cause the most concern. During this monitoring, there were many small vehicles that crossed the bridge, but they had no significant effect on the bridge. The vehicles to be concerned about are the less common, large trucks. For this type of scenario where the extreme events are the main interest, the Gumbel distribution is useful because it only considers the maximum event in a given period of time, and the more frequent, smaller, and less important events are not included and therefore do not skew

the distribution. The Gumbel distributions for the Corrected LVDT and Deck Accelerometer methods of calculating differential deflections are shown in Figure 5.10 and Figure 5.11, respectively.

Figure 5.10 shows that the maximum differential deflection measured by the Corrected LVDT method during this curing period was 0.0379 in. From the fitted Gumbel distribution, it can be said that for a given 5-minute window, there was a 95% probability that the maximum differential deflection experienced would be less than 0.0263 in. The average expected maximum differential deflection during this window was 0.0143 in. Figure 5.11 shows that the maximum differential deflection measured by the Deck Accelerometer method during this curing period was 0.0338 in. With this method, for a given 5-minute window there was a 95% probability that the maximum differential deflection experienced would be less than 0.0253 in. The average expected maximum differential deflection during this window was 0.0124 in.

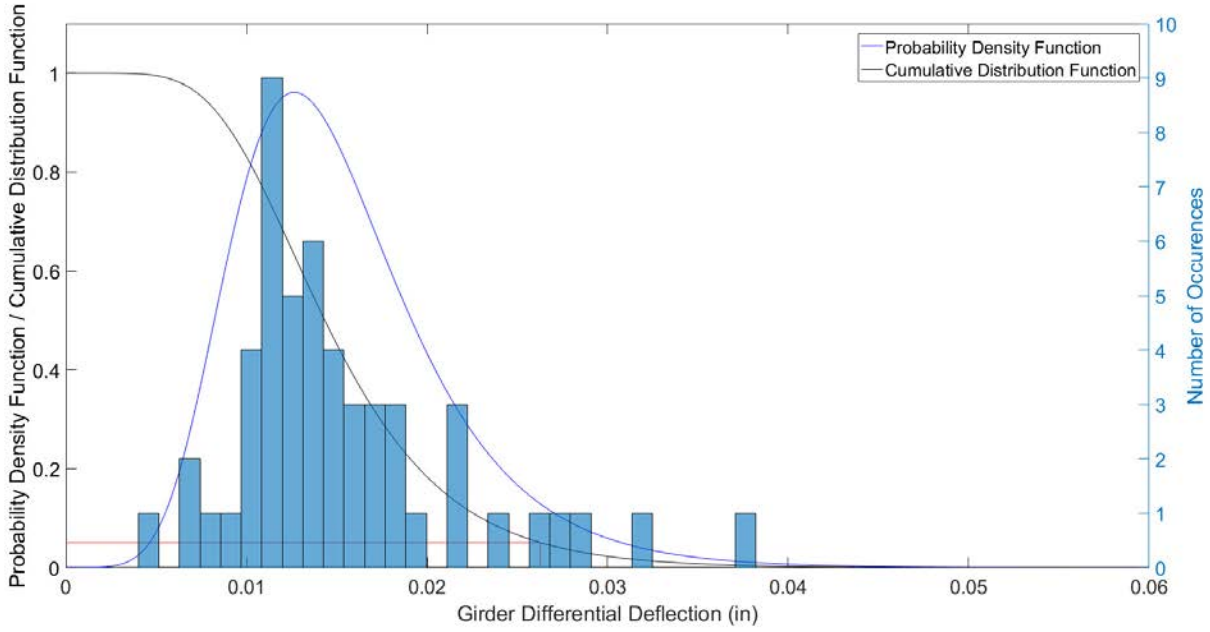

Figure 5.10 - Distribution of maximum differential deflections of bridge B-16-136 calculated using the Corrected LVDT method. Note: PDF scaled by a factor of 50.

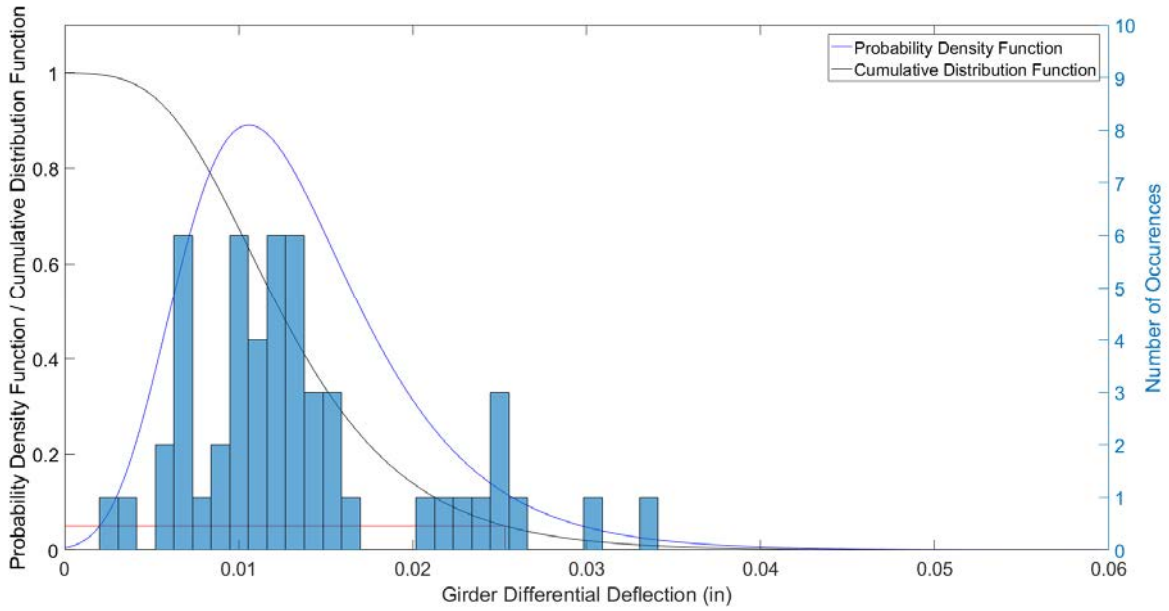

Figure 5.11 - Distribution of maximum differential deflections of bridge B-16-136 calculated using the Deck Accelerometer method. Note: PDF scaled by a factor of 50.

During the 4 hrs. 15 min. that data were collected, a reduction in the magnitude of differential deflections was expected. As the concrete hardens and gains strength and stiffness, the deck should transfer more load and work to equalize girder deflections. This trend was not apparent from the staged-construction monitoring data. The small deflection magnitudes and randomness of traffic made any change in differential deflection over time indistinguishable. To accurately measure this reduction in the field, a vehicle with known weight would need to be placed on the bridge in the same location at different times after the onset of concrete curing.

5.3 Bridge B-64-123

5.3.1 Description

Bridge B-64-123 was a three-span prestressed concrete girder bridge in Darien, Wisconsin. This two-lane bridge was on the southbound lane of Interstate Highway 43 and crossed over Elm Ridge Road in Walworth County. The three span lengths were 44.5, 64.0, and 33.5 ft, respectively. The four 45-in. deep prestressed concrete girders had a constant spacing of 12 ft - 3.5 in. The cast-

in-place concrete deck was 10-in. thick, with transverse reinforcement of #6 bars top and bottom at 7.0-in. spacing and longitudinal reinforcement of #4 bars top and bottom at 8.0-in. spacing. At the longitudinal construction joint, transverse reinforcing bars were lapped 37 inches, which is equivalent to 49 bar diameters. A shear key was provided in the edge of the Stage 1 deck.

This project consisted of a bridge deck replacement constructed in stages. The first stage involved replacement of the south lane, and extended 4 ft – 1.75 in. past the centerline of Girder 3 as shown in Figure 5.12. The remaining portion of the deck, including the north lane, was constructed during the second stage. The Stage 1 portion of the deck was cast 64 days before the Stage 2 portion. Immediately after casting of the Stage 2 portion of the deck, it was covered in burlap and soaker hoses to begin wet curing. The instrumentation arm setup was then placed in the main span at midspan of the construction joint line, where the largest differential deflections were expected. Because of the geometry of the construction staging, the base of the instrumentation arm could not be placed directly over Girder 3. The base was instead placed on the hardened Stage 1 deck between the traffic barrier and the longitudinal construction joint, offset approximately 46 in. It was assumed that the deck overhang would experience minimal deflection relative to Girder 3, so differential deflections could still be measured with the instrumentation arm in this location.

Again, because the instrumentation could not be moved into place until after the deck had been poured and finished, the data collection began approximately 4 hrs. 15 mins. after the concrete pour started, and about 2 hrs. after all the concrete had been placed. Data were collected for approximately 4 hrs. 30 mins. Thus, the data collected correspond to a timeframe from 4 hr. 15 mins. to 8 hrs. 45 mins. after concrete placement commenced.

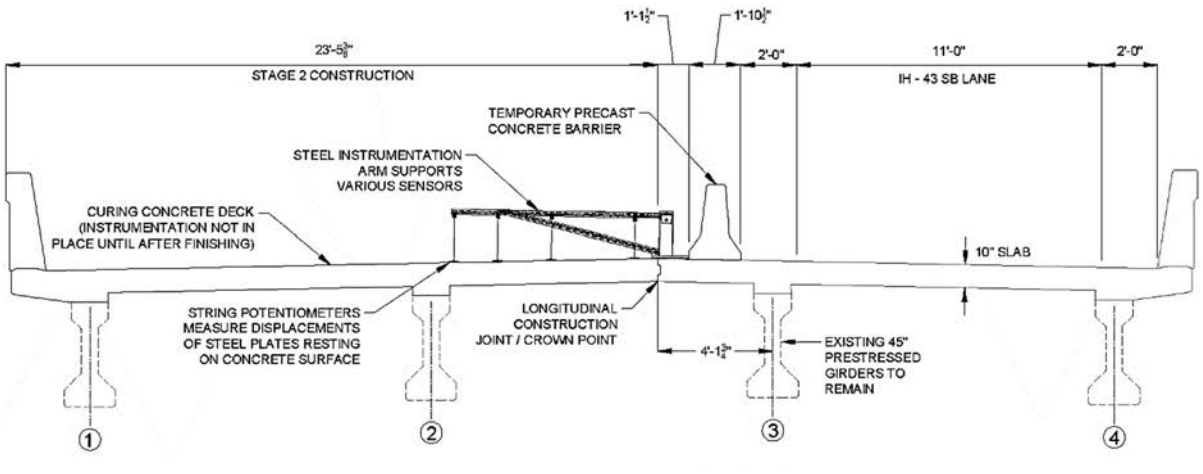

Figure 5.12 - B-64-123 Cross section of bridge B-64-123 during stage 2 construction (looking

The instrumentation was later reinstalled for the post-construction monitoring after the deck had fully hardened and the formwork had been removed, but before the bridge was fully opened to traffic. This occurred 20 days after casting of the Stage 2 deck. Data collection for the post-construction monitoring lasted for approximately one hour.

The same instrumentation setup was used for both the staged-construction monitoring and the post-construction monitoring. This consisted of two LVDTs, four string potentiometers, five accelerometers and four tiltmeters. Exact locations of these sensors are shown in Figure 5.13. Sensors marked A-1 through A-5 are accelerometers, T-1 through T-4 are tiltmeters, SP-1 through SP-4 are string potentiometers, and LVDT-1 and LVDT-2 are linear variable differential transformers. During the staged-construction monitoring, the LVDT-2 was malfunctioning, so instead, the string potentiometer (SP) in this location was used to calculate the differential deflections for the Corrected LVDT/SP method discussed in Section 5.1.3. LVDT-2 was functioning for the post-construction monitoring, and was therefore used for the calculation of differential deflections during this test.

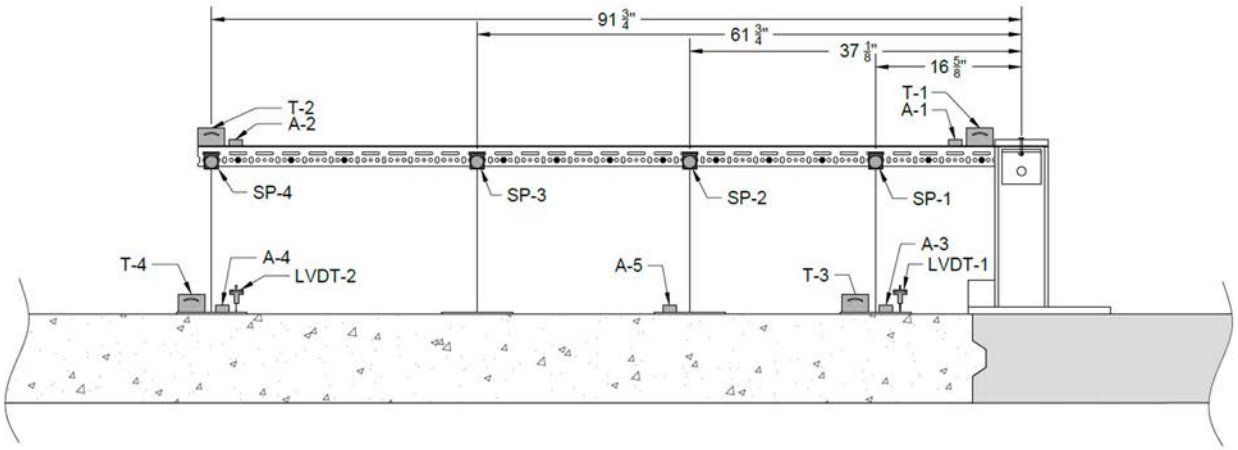

Figure 5.13 - Instrumentation setup for staged-construction monitoring and post-construction monitoring of bridge B-64-123.

5.3.2 Results

5.3.2.1 Staged Construction Monitoring

During the staged-construction monitoring, 1039 traffic events were detected and measured by the instrumentation setup, which corresponds to approximately one traffic event every 15 seconds. The calculated differential deflection between adjacent girders for a typical traffic event can be seen in Figure 5.14. Again, both methods of calculating the differential deflections produced similar results. The total differential deflection measured for this specific event was 0.0206 in. as measured by the corrected SP, and 0.0153 in. as measured by the accelerometers on the bridge deck.

Differential deflections were calculated using both methods for each of the 1039 traffic events. As with the field monitoring of Bridge B-16-136, the collection period was divided into five-minute windows and the maximum differential deflection in each five-minute period was recorded. The maximum differential deflection in each period was then plotted using a histogram and fit to a Gumbel distribution. The Gumbel distributions for the Corrected SP and Deck

Accelerometer methods of calculating differential deflections are shown in Figure 5.15 and Figure 5.16, respectively.

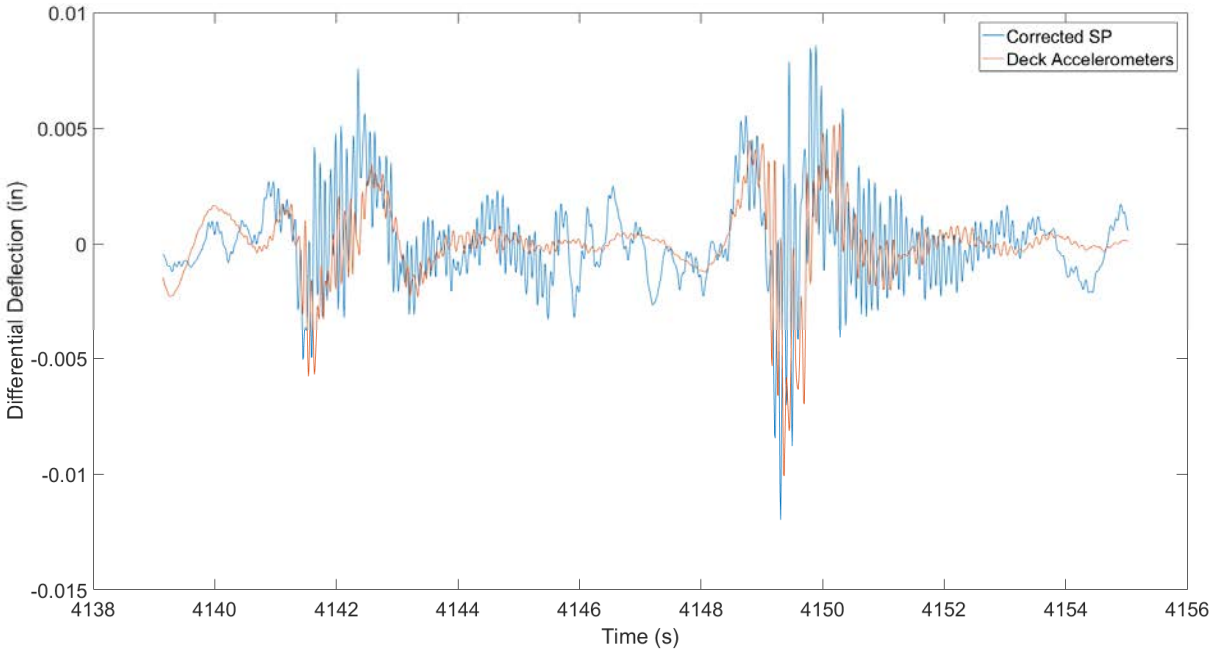

Figure 5.14 - Typical trace of differential deflection versus time for bridge B-64-123

Figure 5.15 shows that the maximum differential deflection measured by the Corrected SP method during this curing period was 0.0399 in. From the fitted Gumbel distribution, it can be said that for a given 5-minute window, there was a 95% probability that the maximum differential deflection would be less than 0.0264 in. The average expected maximum differential deflection during this window was 0.0152 in. Figure 5.16 shows that the maximum differential deflection measured by the Deck Accelerometer method during this curing period was 0.0365 in. With this method, for a given 5-minute window there was a 95% probability that the maximum differential deflection experienced would be less than 0.0278 in. The average expected maximum differential deflection during this window was 0.0178 in.

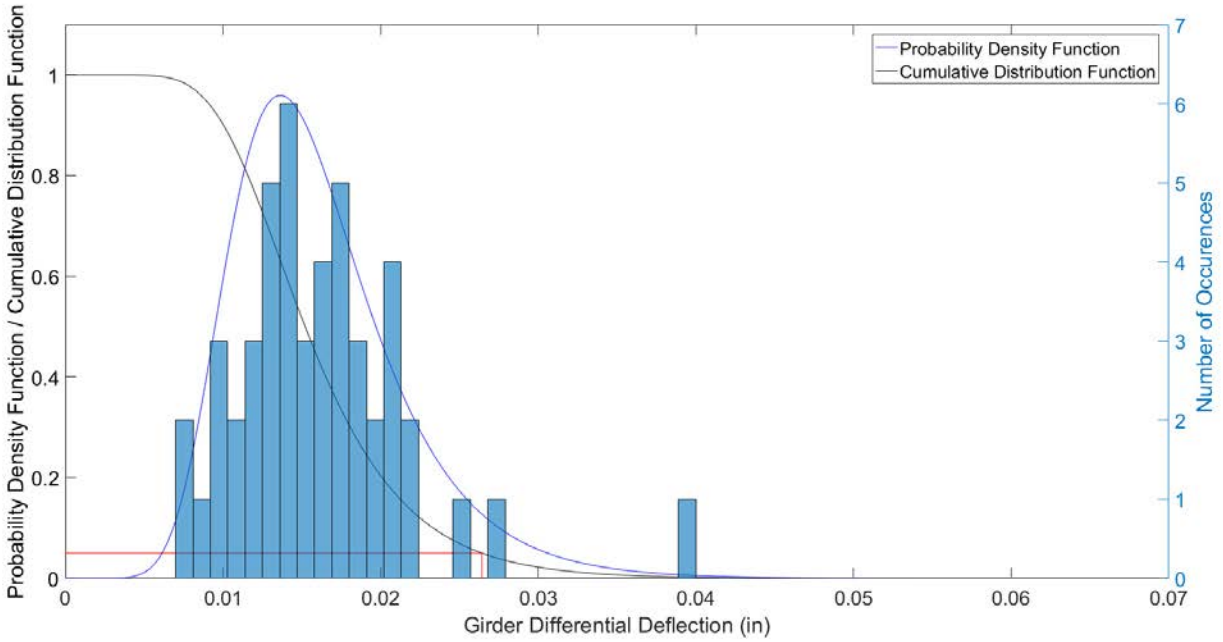

Figure 5.15 - Distribution of maximum differential deflections of bridge B-64-123 calculated using the corrected SP method. Note: PDF scaled by a factor of 40.

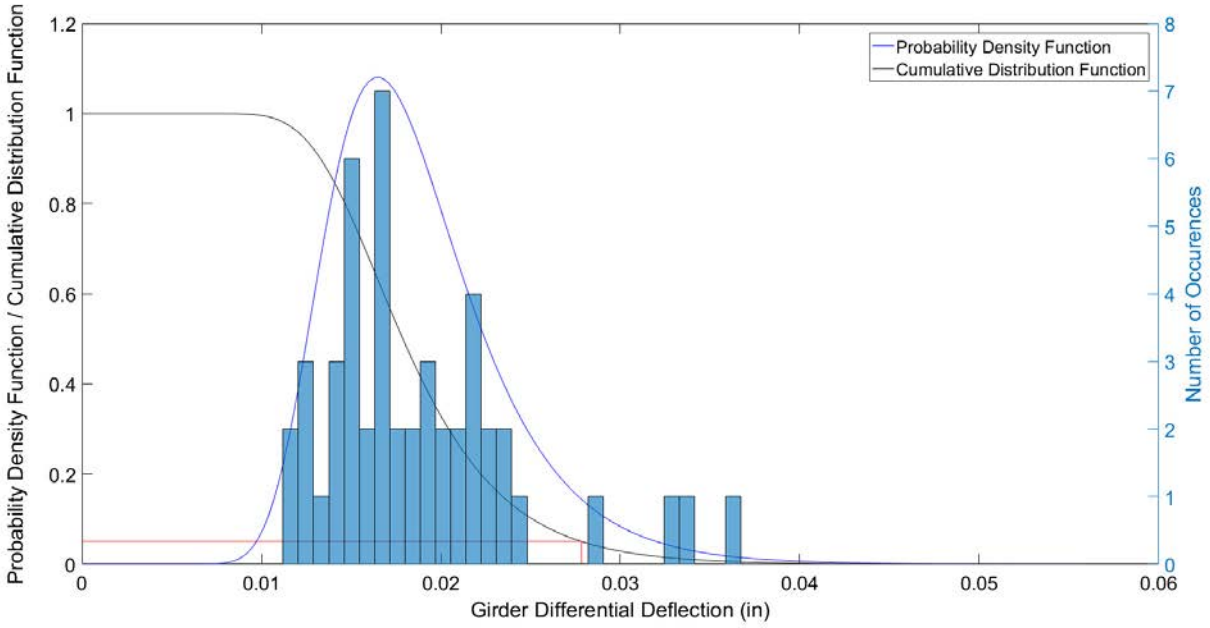

Figure 5.16 - Distribution of maximum differential deflections of bridge B-64-123 calculated using the deck accelerometer method. Note: PDF scaled by a factor of 40.

During the 4 hrs. 30 min. that data were collected, a reduction in the magnitude of differential deflections was expected as the concrete hardened. For the same reasons as bridge B-16-136, this trend was not apparent from the staged-construction monitoring data. Again, no actual vehicle weights were known so differential deflections of the bridge at different times cannot be directly compared.

5.3.2.2 Post-Construction Monitoring

Twenty days after casting of the Stage 2 deck, the concrete had gained sufficient strength for the formwork to be removed. At this time, the instrumentation shown in Figure 5.13 was reinstalled and displacement data were collected for approximately one hour. During this time, 319 traffic events were recorded, which is equivalent to about one event every 13 seconds. As before, the collection period was divided into five-minute windows and the maximum differential deflection in each five-minute period was recorded. The maximum differential deflection in each period was plotted using a histogram and fit to a Gumbel distribution. The Gumbel distributions for the Corrected LVDT and Deck Accelerometer methods of calculating differential deflections are shown in Figure 5.17 and Figure 5.18, respectively.

Figure 5.17 shows that the maximum differential deflection measured by the Corrected LVDT method during this collection period was 0.0363 in. From the fitted Gumbel distribution, it can be said that for a given 5-minute window, there was a 95% probability that the maximum differential deflection experienced would be less than 0.0284 in. The average expected maximum differential deflection during this window was 0.0157 in. Figure 5.18 shows that the maximum differential deflection measured by the Deck Accelerometer method during this collection period was 0.0432 in. With this method, for a given 5-minute window there was a 95% probability that

the maximum differential deflection experienced would be less than 0.0241 in. The average expected maximum differential deflection during this window was 0.0138 in.

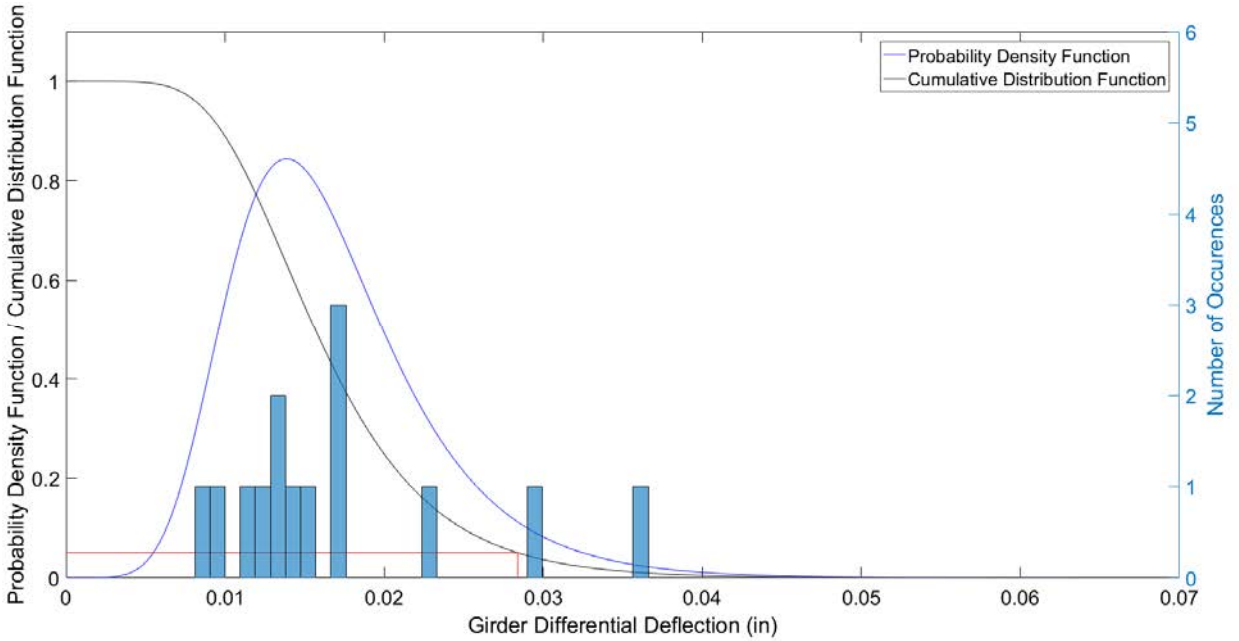

Figure 5.17 - Distribution of maximum differential deflections of bridge B-64-123 calculated using the corrected LVDT method. Note: PDF scaled by a factor of 40.

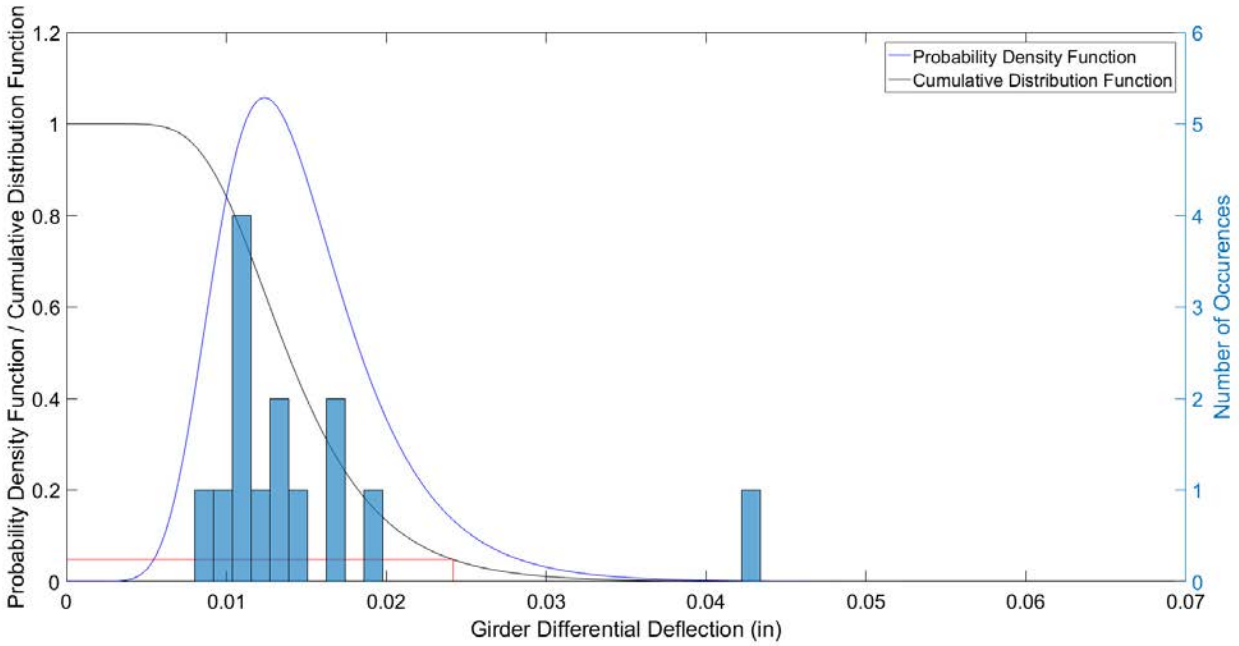

Figure 5.18 - Distribution of maximum differential deflections of bridge B-64-123 calculated using the corrected LVDT method. Note: PDF scaled by a factor of 40.

When comparing the results from the post-construction monitoring with those from the staged-construction monitoring, a reduction in differential deflection was expected as the concrete reaches the design strength. As the concrete hardens and gains strength and stiffness, the deck should transfer more load and work to equalize girder deflections. This trend was not apparent from the staged-construction and post-construction monitoring data. Using the Corrected SP/LVDT method, 95% of the time the expected differential deflection was less than 0.0264 in. during curing and 0.284 in. after the deck had hardened. Using the Deck Accelerometer method, 95% of the time the expected differential deflection was less than 0.0278 in. during curing and 0.241 in. after the deck had hardened. These variations in expected magnitudes are likely not significant and could be due to the randomness of the traffic being recorded. To more accurately measure reductions in differential deflections over time, a vehicle of known weight should be placed on the bridge at different times after the onset of curing.

5.4 Conclusions

The results from the field monitoring of bridges B-16-136 and B-64-123 show that the differential deflections experienced during staged bridge construction, at least in these two cases, were very small. In the nearly ten hours of data collection, the largest measured differential deflection was 0.0432 in. The magnitudes of these differential deflections seem to be reasonable, and agree with those recorded in previous studies (see Table 2.1). These previous studies used linear potentiometers that directly measured absolute deflections of bridge girders, whereas this research used a setup that measured girder differential deflections directly. This suggests that even though the field monitoring methodology used in this study was different to those previous, it is still a viable way to measure bridge girder differential deflections.

Because the differential movements were extremely small, it was sometimes not possible to accurately measure them with this instrumentation setup. For many smaller vehicles, the differential movements were not larger than the ambient movement of the bridge, which dominated the displacement plots. Any movement less than approximately ±0.01 in. was virtually indistinguishable from the ambient movement of the bridge. This issue, however, was avoided using an extreme value distribution to analyze the magnitudes of differential displacements because only the largest displacement measured during a specific time window was used to form the distribution.

Comparing results from the staged-construction monitoring and post-construction monitoring of bridge B-64-123 showed very little difference in the magnitude and distribution of differential deflections. The difference in 95^{th} percentile of maximum differential deflection between the staged-construction monitoring and the post-construction monitoring was not significant. This suggests that reductions in differential deflections from hardening of the Stage 2 deck are not well pronounced. Exact reductions in deflection could not be computed because vehicle weights were not known.

Results from both field monitored bridges proved to be very similar. Both the magnitudes and distributions of differential deflections were nearly identical, which was expected as they are structurally similar. Both bridges used prestressed concrete girders and had similar main span lengths of 60 and 64 ft. The bridges did however have different girder spacings and deck thicknesses which suggests that these details may have a less significant effect on the magnitude of differential deflections during staged construction.

Chapter 6: Numerical Analysis of Staged Construction Bridges

Finite element models were created using ABAQUS for three existing staged construction bridges to further investigate differential deflections during staged construction. These bridges have all been discussed earlier, two of which, B-16-136 and B-64-123, are the bridges where differential deflections were field monitored during staged construction. Modeling these two bridges allowed for the comparison and verification of results between the field monitoring task and the numerical analysis task. The third bridge, B-70-177, is an existing staged construction bridge that was inspected and discussed in Chapter 4. This bridge was selected to provide some variety to the bridges being modeled. Whereas the two field monitored bridges were both prestressed concrete girder bridges with similar main span lengths, B-70-177 was a steel plate girder bridge with span lengths almost twice as long and twice as many traffic lanes during staged construction.

6.1 Assumptions

To construct these finite element models, certain assumptions were made. One such assumption was that all materials and components exhibit linear elastic behavior. This applies to the girders, hardened and curing concrete decks, diaphragms, cross-bracing and parapets. This assumption was determined to be suitable because deflections during construction are part of a service limit state, and thus no yielding or inelastic deformations are expected during regular use of the bridge.

To define a linear elastic material in ABAQUS, only two properties are required: modulus of elasticity and Poisson's ratio. Steel components, such as girders, cross-braces, diaphragms, and reinforcing bars were given a modulus of elasticity of 29,000 ksi and a Poisson's ratio of 0.30. Concrete components, such as prestressed girders, decks, and parapets were given a modulus of

elasticity of $1820\sqrt{f'_c}$, as suggested by AASHTO (AASHTO 2012). Values for the in-place concrete compressive strengths, f'_c, were assumed to be equal to the design compressive strength specified on the bridge plans. This was 4,000 psi for all hardened concrete decks, 3,500 psi for parapets, and either 6,000 psi or 8,000 psi for prestressed concrete girders. Though actual concrete strengths of the monitored bridges were higher than the design strengths, modeling lower strength and lower stiffness concrete was presumed to be conservative in estimating the differential deflections caused by traffic loading. All concrete materials used a Poisson's ratio of 0.20.

To account for the increase in stiffness as the Stage 2 concrete deck hardens, the modulus of elasticity was increased from a minimal value which represents plastic (fresh) concrete, to the final value which represents fully hardened concrete. Results were computed for several intermediate values of the modulus of elasticity to determine how the differential deflections change as the concrete gains strength. The values used for the modulus of elasticity correspond to that of a concrete that has been curing for 0, 0.5, 1, 3, 7 and 28 days. To determine these approximate values of elastic modulus, the compressive strength of the concrete was first estimated at the corresponding time using Equation 3, suggested by ACI 209 for Type I cement (ACI Committee 209 1992). The modulus of elasticity was then estimated as before using $1820\sqrt{f'_c}$.

$$f_c(t) = f_{c28}\left(\frac{t}{4+0.85t}\right) \qquad (3)$$

Where:

$f_c(t) =$ concrete strength as a function of time
$f_{c28} =$ concrete strength at 28 days
$t =$ curing time (days)

All components were modeled as homogenous materials except for the concrete decks. The decks were modeled using shell elements with embedded layers of reinforcement. ABAQUS has a built-in feature for adding layers of reinforcement to shells. Rather than modeling individual reinforcing bars, this feature adds an internal layer of different stiffness to the shell element formulation. The stiffness of the layers is calculated based on the reinforcing material, area of individual reinforcing bars, bar spacing, and reinforcement orientation and position. Four total layers were included, one each for the top and bottom longitudinal bars and top and bottom transverse bars. Additional steel reinforcement placed in the deck overhangs was ignored. When the concrete deck was modeled using plastic (fresh) concrete, the steel reinforcement was not included. Before hardening, the steel reinforcement does not work compositely with the concrete deck and provides very little stiffness to the section, if any.

Prestressed concrete girders were modeled as homogeneous materials. Prestressing strands were not modeled because the steel itself does not contribute significantly to the stiffness of the section. The prestressing force applied by the steel strands counters the applied gravity loads and causes the girder to remain uncracked under normal operating loads. Considering this, as long as the prestressing force was maintained, a homogenous, linear-elastic material was assumed to be appropriate to model prestressed concrete girders.

Further decisions were taken regarding the vehicle loading applied in the finite element models. The geometry for the loading truck was chosen to be similar to the AASHTO LRFD design truck, with three axles at a constant 14-ft spacing and a 6-ft width between wheels. The total vehicle weight was selected to be the maximum allowed by WisDOT on Class A highways. For a truck with three axles and a total length between axles of 28 ft., this was equal to 57,100 lbs (WisDOT 2007). The load was distributed to the three axles in the same proportion as the AASHTO design

truck, with 11.11% of the total vehicle weight going to the front axle, and 44.44% going to the each of the two rear axles. A 24-in. square contact patch was used for each wheel, and the load was applied as a uniform pressure over this area. A 33% dynamic load allowance was included for all vehicle loads. Details of the truck loading used in the finite element models are shown in Figure 6.1. This loading truck was selected to provide an upper-bound estimate of differential deflections experienced during staged bridge construction. Larger, overweight vehicles that would require a special permit were assumed to be prohibited from using a route when a staged construction bridge pour is taking place.

Dead loads were not included in this numerical analysis. Differential deflections are primarily due to vehicular live loading, which is thus the only load considered in this analysis.

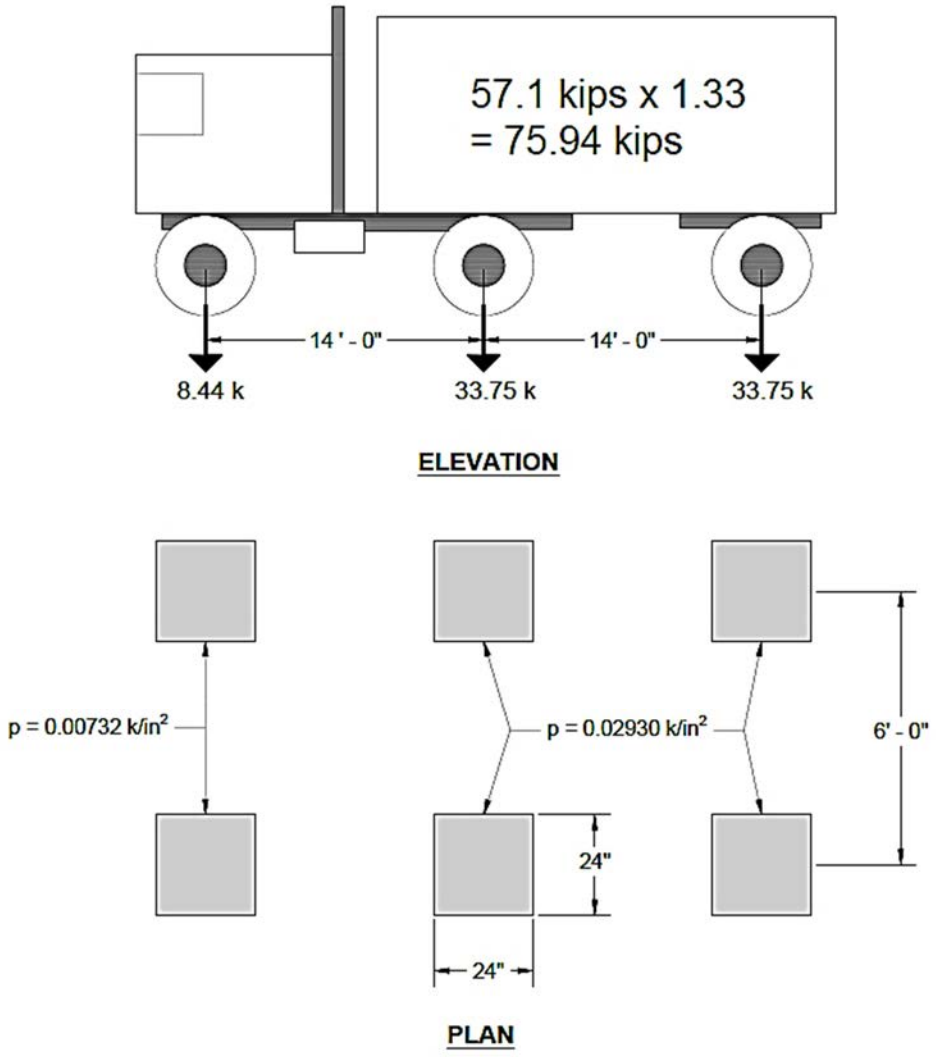

Figure 6.1 - Details of truck loading used in all finite element models

6.2 Bridge B-16-136 Model

6.2.1 Description

The structure of bridge B-16-136 has previously been described in detail in Section 5.2.1. The 36” deep prestressed concrete girders were modeled using linear-elastic, homogeneous solid elements. These girders were all simply supported and were therefore restrained in the vertical direction at the ends where the bearing pads were located. To prevent rigid body motions, each girder was also restrained at a single point against translations in the horizontal directions.

Both the Stage 1 and Stage 2 concrete decks were modeled using composite shell elements. As stated previously, four layers of steel reinforcement were modeled into the concrete decks. The decks and girders were connected using a tie constraint to prevent any relative displacement between the elements. The longitudinal construction joint between the two deck stages was also constrained in this way. Steel diaphragms were modeled using shell elements. All diaphragms were hot-rolled channel shapes with their webs bolted to the webs of the concrete girders. Thus, the diaphragms were connected to the girders by constraining the webs only, and not the flanges. The parapet on the existing Stage 1 side of the deck was modeled using solid elements and was tied in place to the hardened deck. The parapet on the other side of the bridge was not included in the model as it was not present during pouring of the Stage 2 deck. An image of the finite element model is shown in Figure 6.2.

One lane of the bridge remained open during curing of the concrete deck, with a signal alternating the direction of traffic. In the model, the truck was moved along the bridge in both directions to determine what location would produce the maximum differential deflection between girders on either side of the longitudinal construction joint. The differential deflection was measured at midspan where it was assumed to be largest. Once the critical loading position was determined, the model was run multiple times while increasing the modulus of elasticity for the curing deck to analyze how differential deflections change as the concrete hardens.

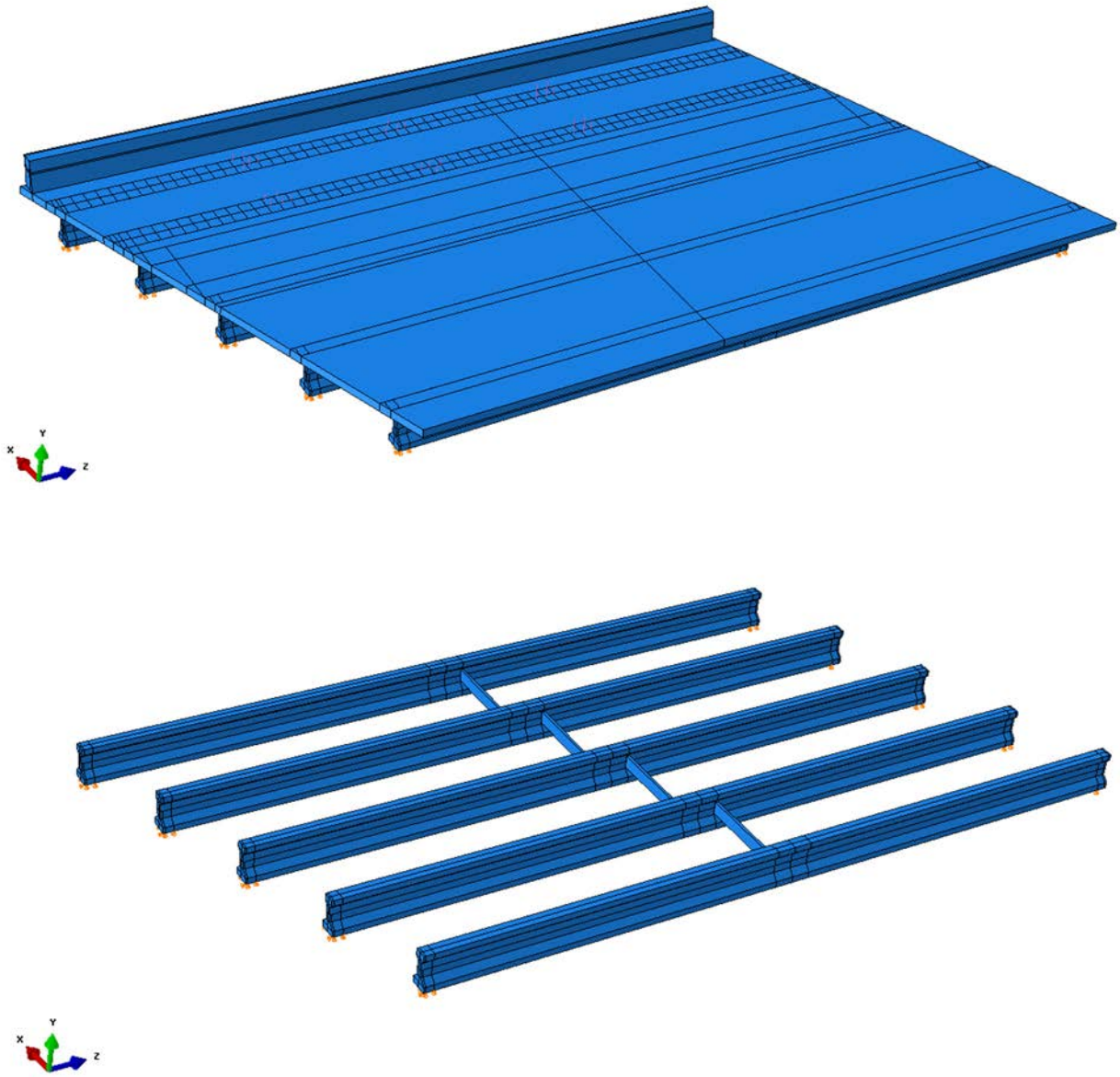

Figure 6.2 - Top: Isometric view of finite element model for B-16-136. Bottom: Concrete deck hidden to show bridge framing and boundary conditions.

6.2.2 Results

The primary purpose of this task was to compute deflections of specific points on the bridge. The finite element models were not used to compute forces or stresses in the deck, girders or steel

reinforcement due to the staged construction traffic. A typical deflection field for this bridge is shown by the contour plot in Figure 6.3.

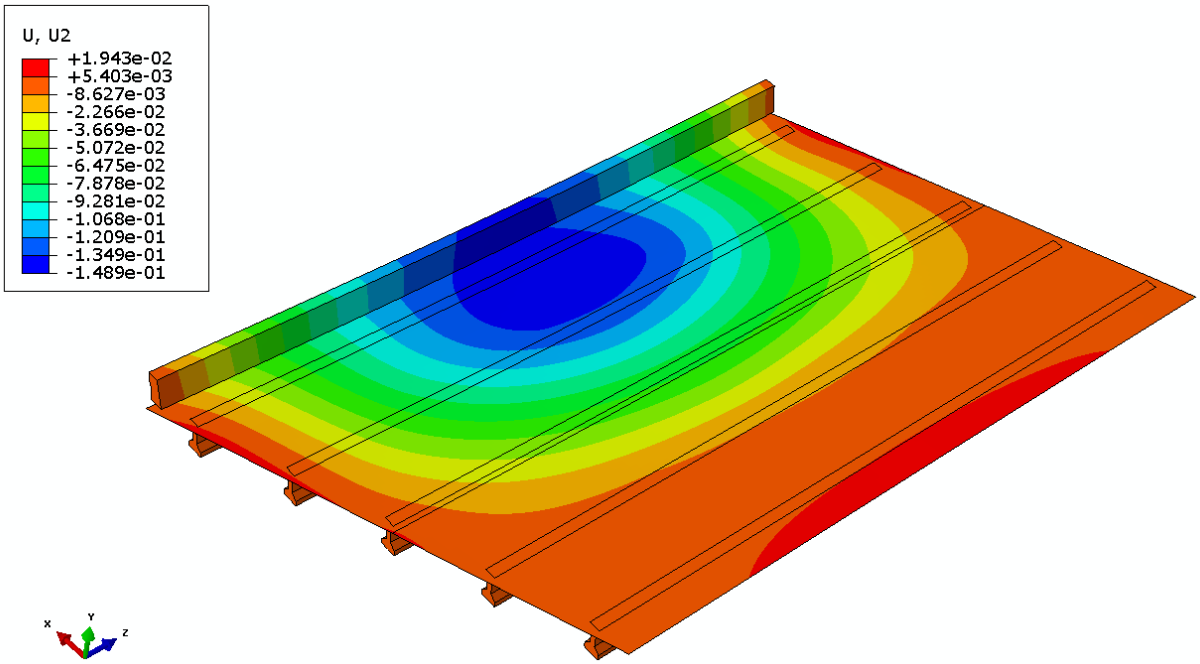

Figure 6.3 - Typical contour plot of vertical displacement for B-16-136

The maximum differential deflection calculated from this model was 0.0637 in. This occurred when the curing deck was still plastic and had essentially no stiffness. As expected, the differential deflection decreased as the Stage 2 deck hardened and was capable of transferring more load between girders. Figure 6.4 shows the deflected shape at midspan computed by the finite element model for the loading case that produces maximum differential deflections. The figure shows how the deflected shape changes as the modulus of elasticity for the curing concrete deck is increased. Solid vertical lines represent locations of girders and the dashed vertical line shows the location of the longitudinal construction joint. The arrows represent where the truck wheel loads were acting. The location of the truck that produced maximum differential deflection was the same for each moduli of elasticity used.

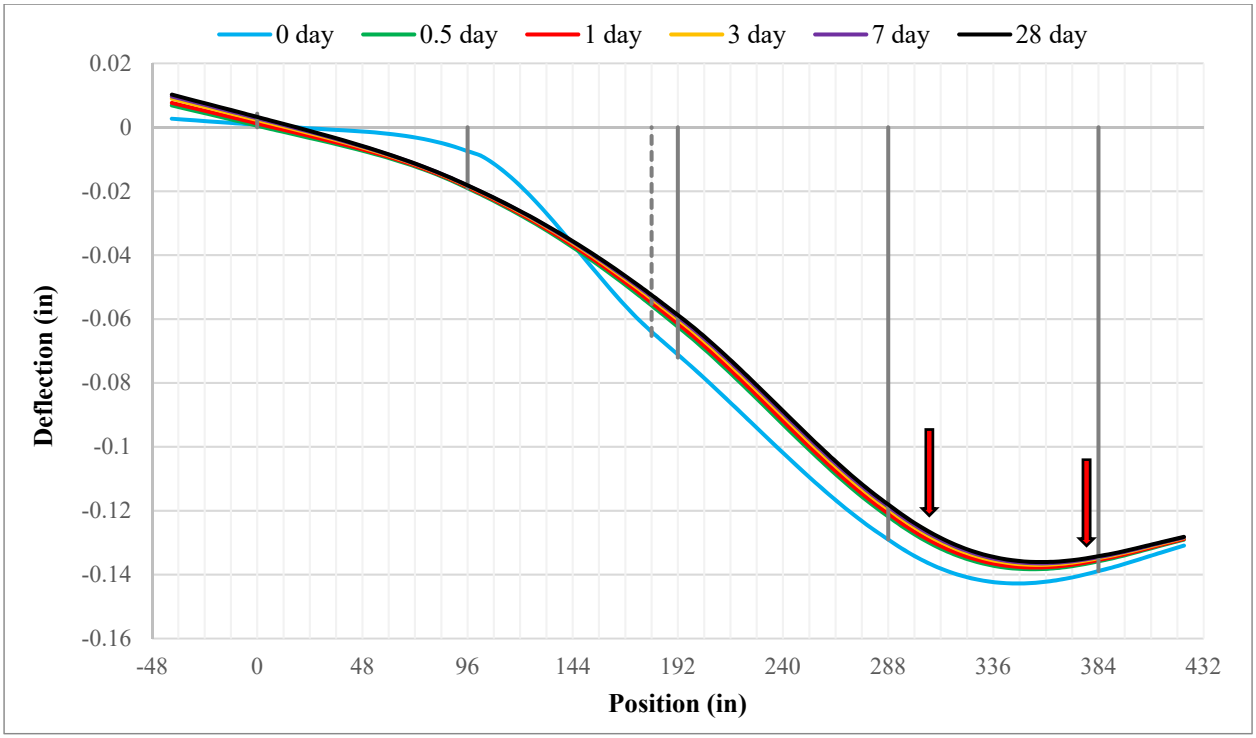

Figure 6.4 - B-16-136 deflected cross section at different ages of Stage 2 deck

Table 6.1 highlights the changing magnitude of maximum differential deflections between girders adjacent to the staged construction joint as the Stage 2 deck hardens. The different elastic moduli used in the finite element model correspond to the approximate stiffness of concrete that has cured for 0, 0.5, 1, 3, 7, and 28 days. The maximum differential deflection reduced slightly, about 0.0231 in. total, as the concrete deck hardened from casting to 28 days.

Table 6.1 - Differential deflections from B-16-136 finite element model

Concrete Curing Time (days)	Concrete Compressive Strength (ksi)	Concrete Modulus of Elasticity Strength (ksi)	Maximum Differential Deflection (in)
0	0.00	1	0.0637
0.5	0.45	1223	0.0434
1	0.82	1652	0.0427
3	1.83	2459	0.0417
7	2.80	3046	0.0411
28	4.00	3640	0.0406

6.3 Bridge B-64-123 Model

6.3.1 Description

The structure of bridge B-64-123 has previously been described in detail in Section 5.3.1. The modeling procedures and techniques for this bridge were mostly identical to those used for B-16-136. The elements used for the prestressed concrete girders, concrete decks, diaphragms and parapets were also the same. The main difference with this bridge was that it had three spans as opposed to just one. All three spans were modeled and special consideration was given to how the ends of the girders were restrained. The girders in each span were simply supported but the deck was continuous over all three spans. At the piers, the ends of the girders were encased in a concrete diaphragm. To account for this, the outside surfaces at the girder ends that were encased by the diaphragm were restrained against translation in the vertical and horizontal directions. The surface at the end of the girder was unrestrained to allow rotation in the primary bending direction (See Figure 6.5). An image of the entire finite element model can be seen in Figure 6.6.

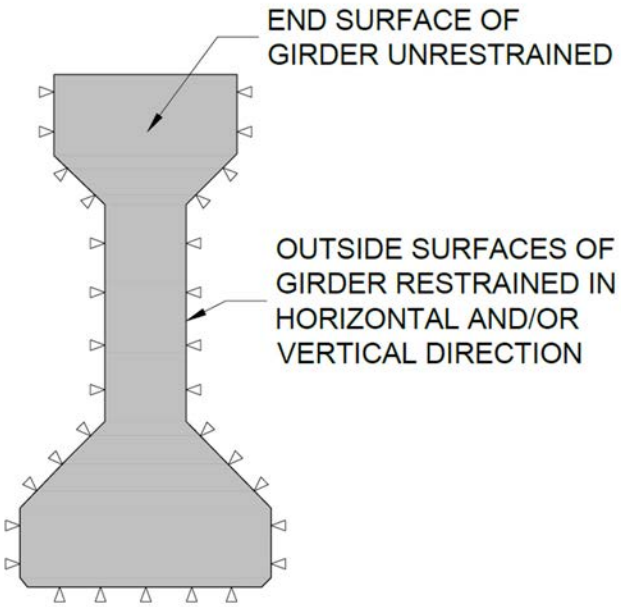

Figure 6.5 - Details of restraints provided at girder ends with concrete diaphragms.

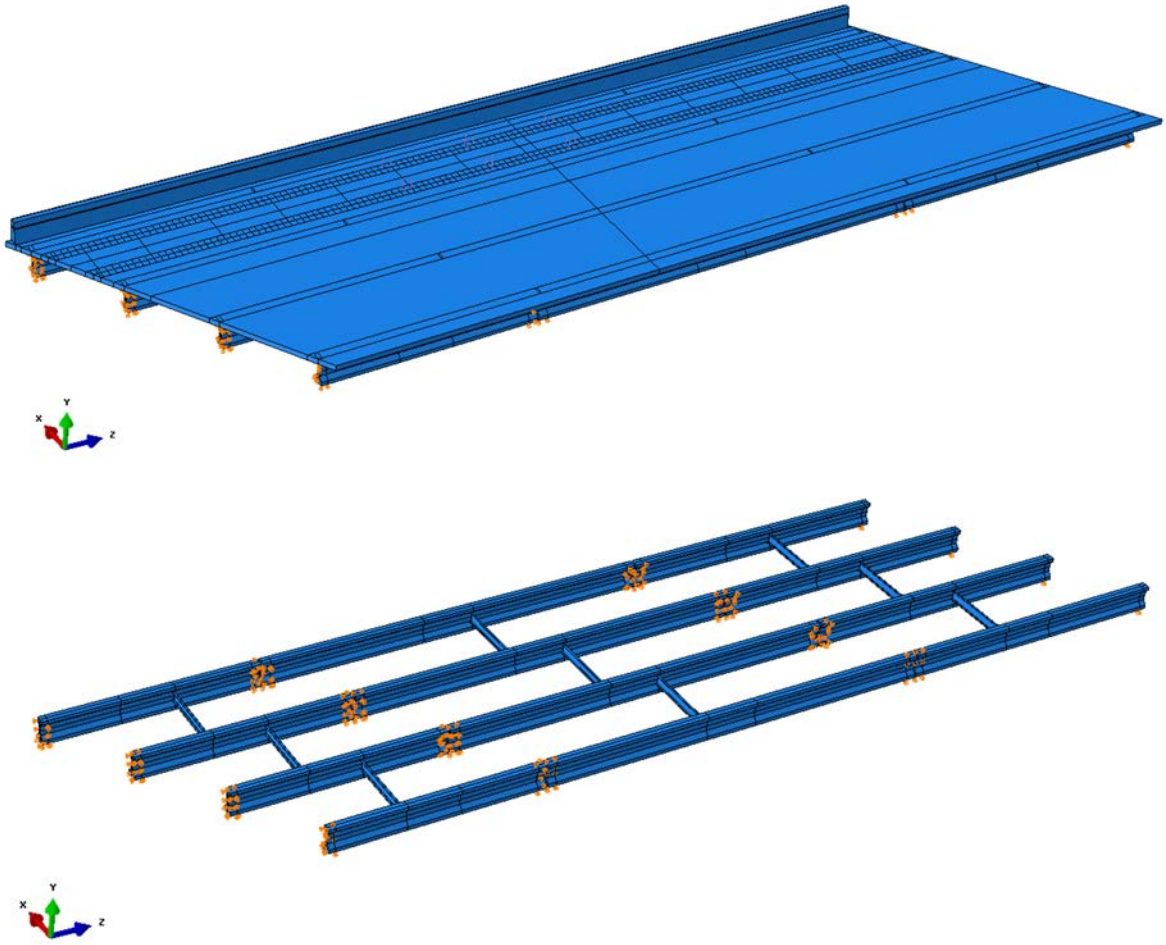

Figure 6.6 - Top: Isometric view of finite element model for B-64-123. Bottom: Concrete deck hidden to show bridge framing and boundary conditions.

One lane of the bridge remained open during curing of the concrete deck, with traffic traveling in one direction. In the model, the truck from Figure 6.1 was again moved across the bridge to determine the location that would produce maximum differential deflections. The deflections were calculated at midspan of the main, longest span because it was assumed that this location will experience the largest deflections of anywhere in the bridge. Once the critical loading position was determined, the model was run multiple times while increasing the modulus of elasticity for the curing deck to analyze how differential deflections change as the concrete hardens.

6.3.2 Results

Displacements were calculated for all nodes in the bridge model. A typical deflection field for this bridge is shown by the contour plot in Figure 6.7.

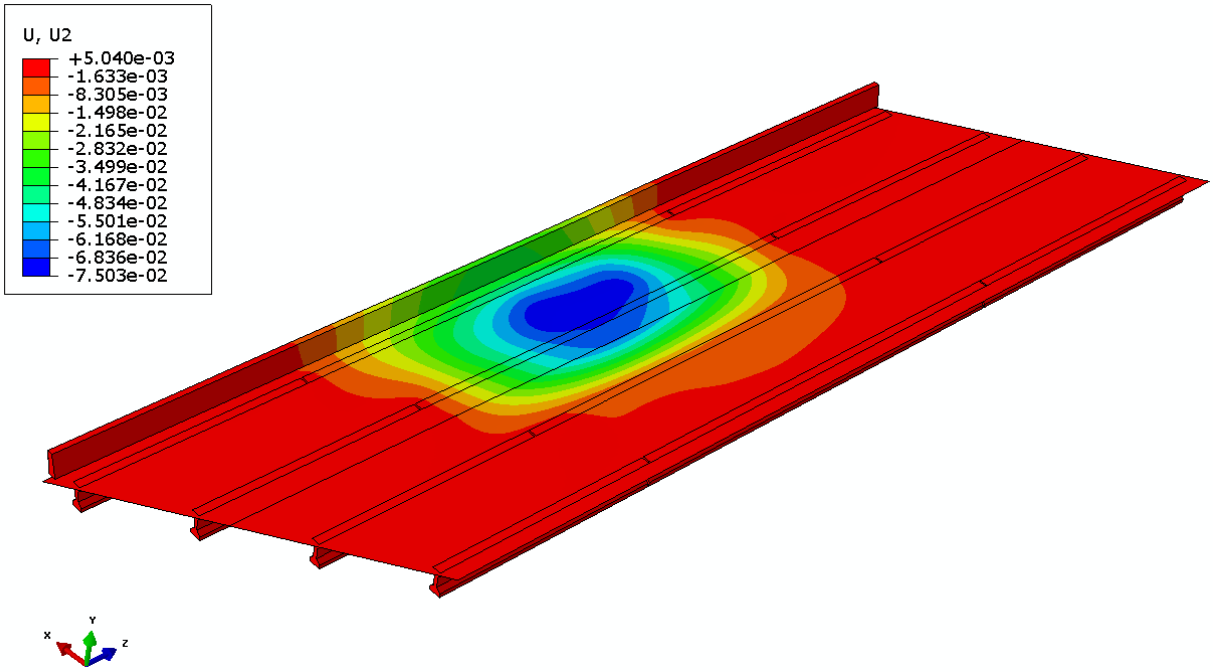

Figure 6.7 - Typical contour plot of vertical displacement for B-64-123

The maximum differential deflection calculated from this model was 0.0673 in. Again, this occurred when the curing deck had minimum stiffness. As before, the differential deflections decreased as the Stage 2 deck hardened and transferred more load between girders. Figure 6.8 shows the deflected shape at midspan computed by the finite element model for the loading case that produces maximum differential deflections. The figure shows how the deflected shape changes as the modulus of elasticity for the curing concrete deck is increased. Solid vertical lines represent locations of girders and the dashed vertical line shows the location of the longitudinal construction joint. The arrows represent where the truck wheel loads were acting. The location of the truck that produced maximum differential deflection was the same for each moduli of elasticity used.

Table 6.2 highlights the changing magnitude of differential deflections between girders adjacent to the longitudinal construction joint as the Stage 2 deck hardens. Again, the reduction in differential deflection during curing is slight, about 0.0258 in. total, with very little change occurring after 12 hours of curing.

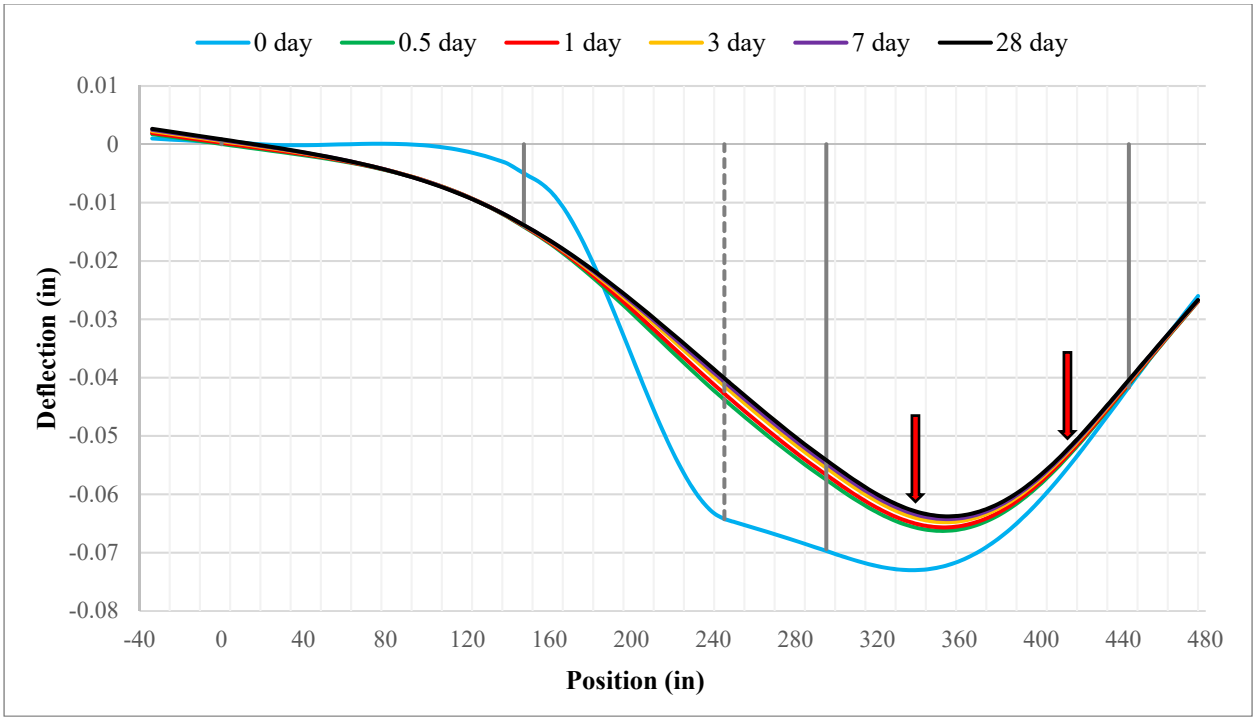

Figure 6.8 - B-64-123 deflected cross section with different elastic moduli

Table 6.2 - Differential deflections from B-64-123 finite element model

Concrete Curing Time (days)	Concrete Compressive Strength (ksi)	Concrete Modulus of Elasticity Strength (ksi)	Differential Deflection (in)
0	0.00	1	0.0673
0.5	0.45	1223	0.0446
1	0.82	1652	0.0439
3	1.83	2459	0.0428
7	2.80	3046	0.0421
28	4.00	3640	0.0415

6.4 Bridge B-70-177 Model

6.4.1 Description

Bridge B-70-177 was a two-span steel plate girder bridge in Oshkosh, Wisconsin. This three-lane bridge was on the northbound lane of Interstate Highway 41 and crossed over US Route 76 in Winnebago County. The two continuous spans had equal lengths of 115.5 ft. In 2010, this bridge underwent a deck replacement and widening in stages. There were six 54-in. steel plate girders, four of which were from the original structure and were spaced at 12 ft – 0 in. Two more identical girders were added during the widening and were spaced at 10 ft – 6 in. The cast-in-place concrete deck was 11-in. thick, with transverse reinforcement of #6 bars top and bottom at 7.0-in. spacing and longitudinal reinforcement of #4 bars top and bottom at 6.5-in. spacing. At the longitudinal construction joint, transverse reinforcing bars were lapped 37 in., which is equivalent to 49 bar diameters. No shear key was provided at the construction joint.

The first stage involved demolishing the inside 15 ft – 3 in. of the existing deck and parapet, then placing the two new girders to support the widening. While traffic continued to use the remaining portion of the existing bridge, the widening was constructed. Traffic was then switched over to the newly constructed widening while the remaining portion of the original deck was removed and replaced. See Figure 6.9 for more details on the construction sequencing. The plans show that two traffic lanes were open during Stage 2 construction. No information was available regarding whether both lanes remained open during casting and curing of the Stage 2 deck.

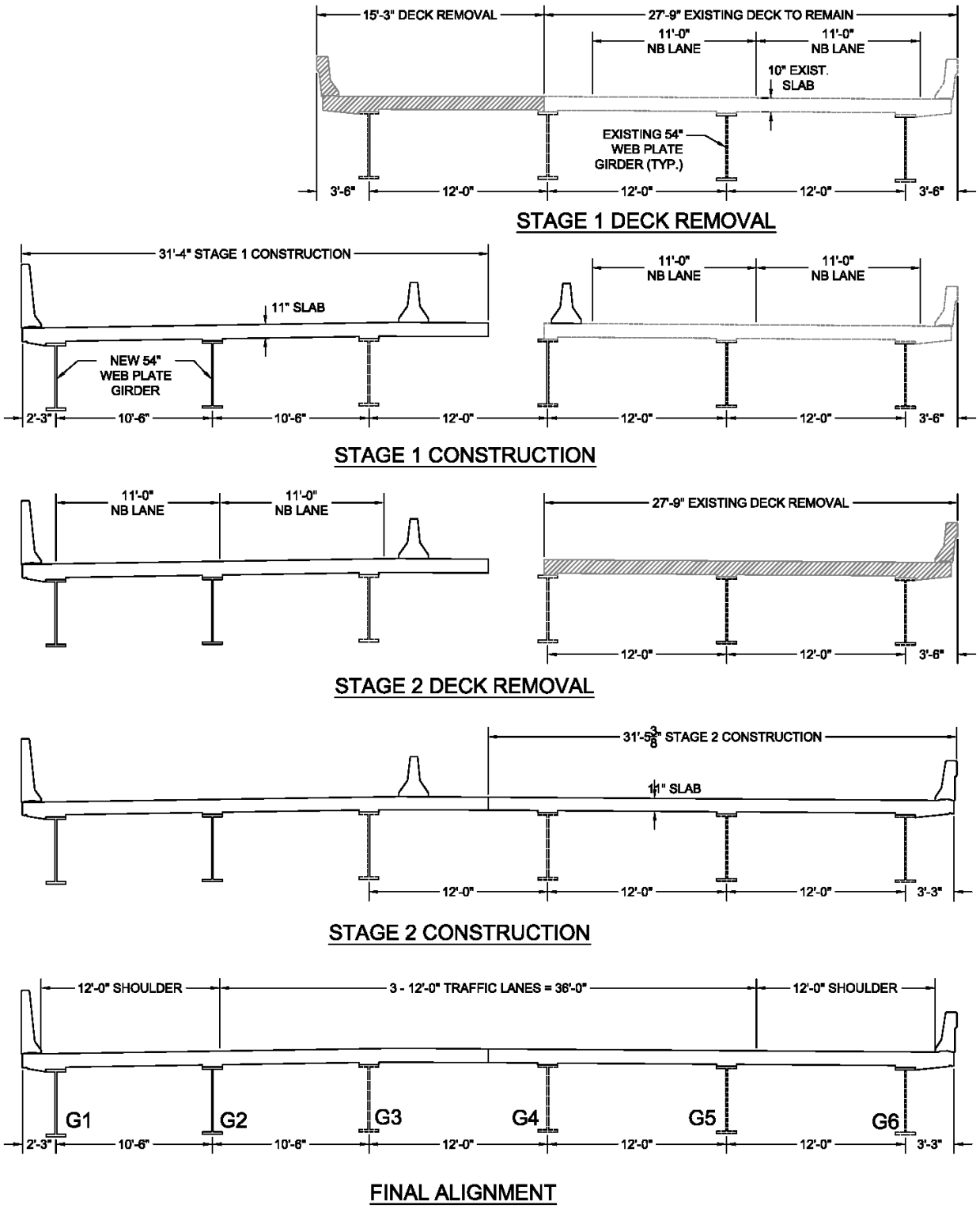

Figure 6.9 - Bridge B-70-177 Deck Replacement and Widening Sequence (looking north)

The 54” steel plate girders were modeled using linear-elastic, homogeneous shell elements. These continuous girders use four different cross-sections along their length, and this was reflected in the model. The girders were restrained in the vertical direction at both ends as well as at the central pier. To prevent rigid body motions, each girder was also restrained at a single point against translations in the horizontal directions.

Both the Stage 1 and Stage 2 decks were modeled using composite shell elements, which included four layers of steel reinforcement. The decks and girders were connected together using a tie constraint to prevent any relative displacement between the elements. The longitudinal construction joint between the two deck stages was also constrained in this way. Steel cross braces were modeled using link elements. The cross braces were connected to the girders using pinned connections ensuring that they only experience axial forces. The parapet was modeled using solid elements and was tied in place to the hardened deck. An image of the finite element model can be seen in Figure 6.10.

Both lanes of the bridge were assumed to remain open during curing of the concrete deck, with traffic traveling in the northbound direction. In the model, the truck from Figure 6.1 was again moved across the bridge to determine the location that would produce maximum differential deflections. This was performed for each of the two lanes and then the trucks were placed in both lanes at the critical locations. The location of maximum differential deflection along the length of the bridge was also noted. The AASHTO Bridge Design Specification (AASHTO 2012) specifies a multiple presence factor of 1.00 for two loaded lanes, so no modification to the truck loading was made. Once the critical loading position was determined, the model was run multiple times while increasing the modulus of elasticity for the curing deck to analyze how differential deflections change as the concrete hardens.

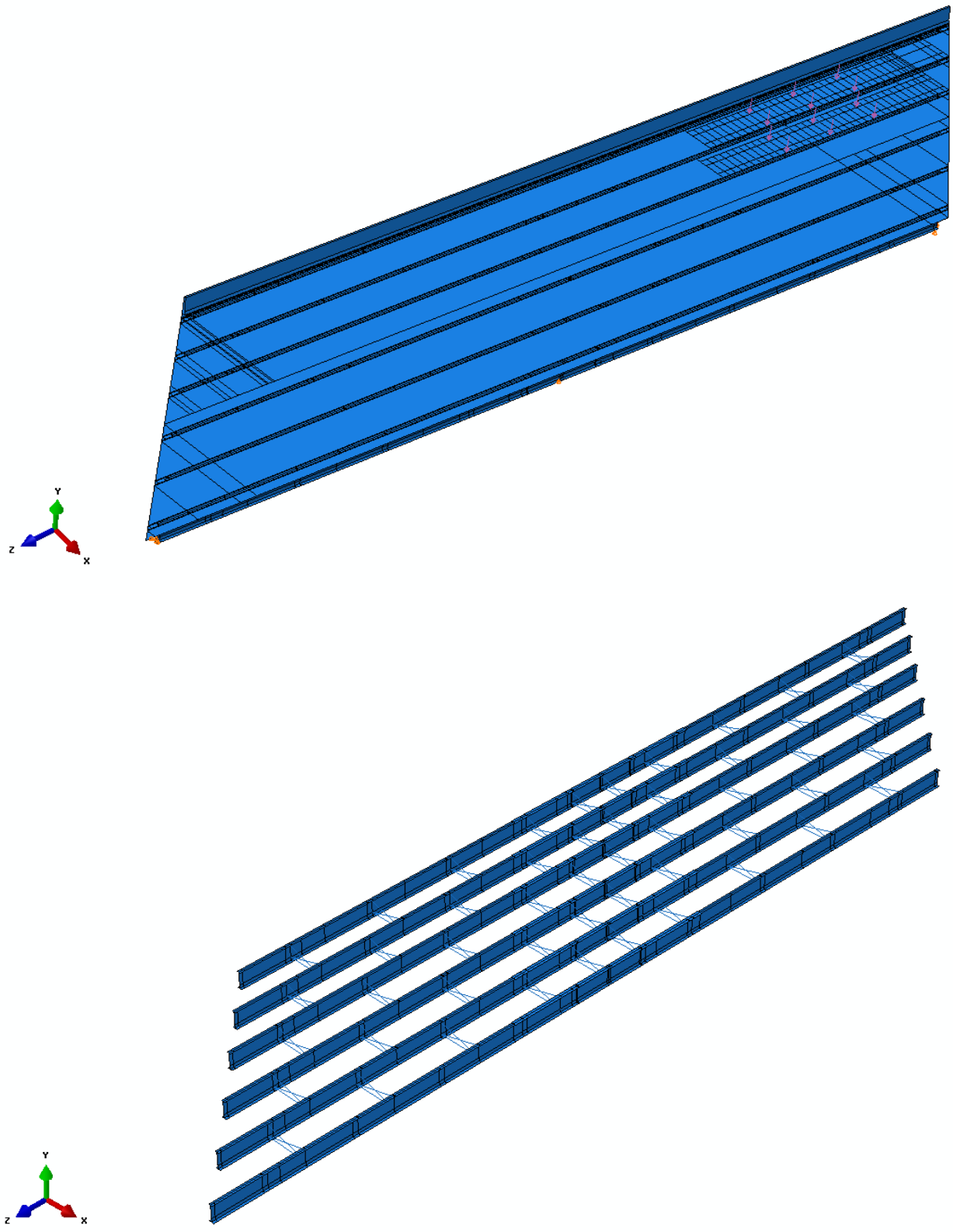

Figure 6.10 - Top: isometric view of B-70-177 model. Bottom: concrete deck hidden to show bridge framing

6.4.2 Results

Displacements were calculated for all nodes in the finite element model. A typical deflection field for this bridge is shown by the contour plot in Figure 6.11.

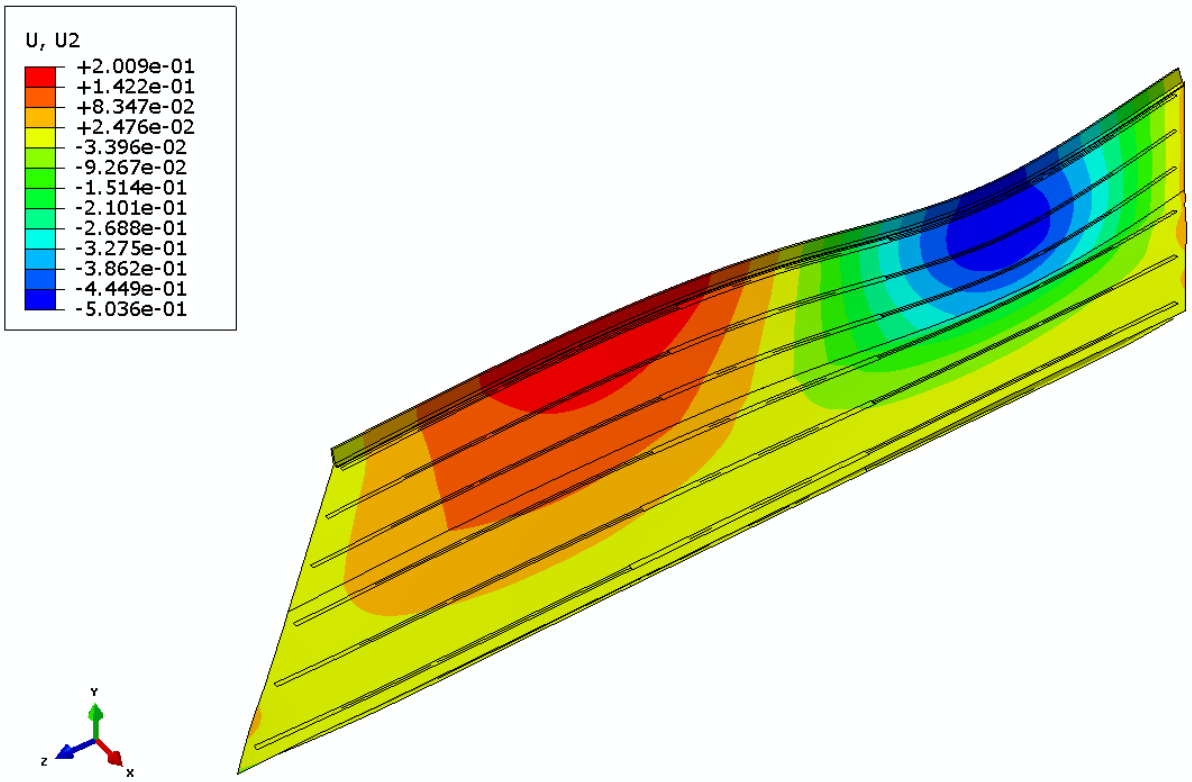

Figure 6.11 - Typical Contour plot of vertical displacement with both lanes loaded for B-70-177

The maximum differential deflection calculated from this model was 0.348 in. This occurred when the curing deck has essentially no stiffness and both traffic lanes were loaded. As before, the differential deflections decreased as the Stage 2 deck hardened and transferred more load between girders. Figure 6.12 shows the deflected shape at the location of maximum differential deflection computed by the finite element model using different moduli of elasticity for the curing concrete deck. Solid vertical lines represent locations of girders and the dashed vertical line shows the location of the longitudinal construction joint. The arrows represent where the truck wheel loads are acting.

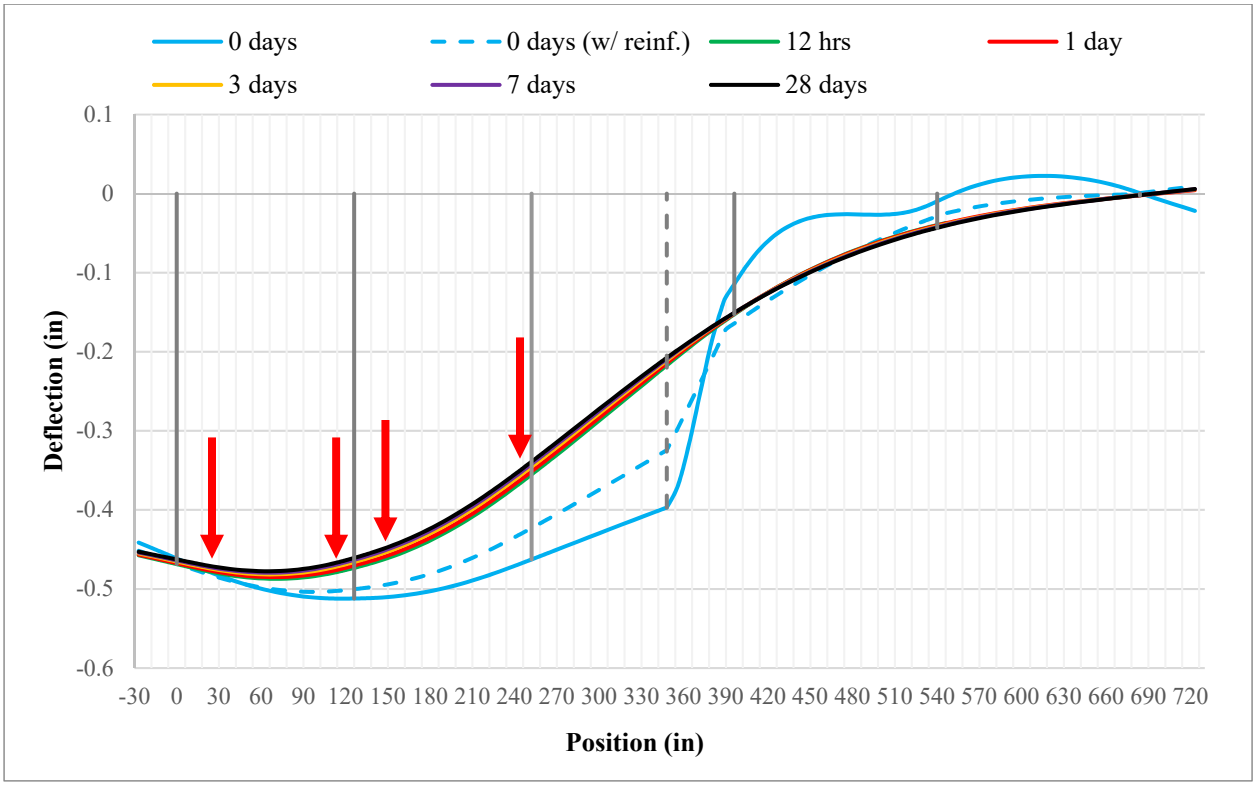

Figure 6.12 – B-70-177 deflected cross section at different ages of the Stage 2 deck and both lanes loaded.

The deflected shape of the bridge deck at the onset of curing, (solid blue line in Figure 6.12) is abnormal. In this case, the cross braces were the only mechanism transferring forces between the girders. Thus, the deflected shape of the curing deck was mainly influenced by the displacements and rotations of the girders to which it was attached. Additionally, the right end of the cross section plotted in Figure 6.12 is in the region of the obtuse angle of the skewed bridge deck, which adds to the complexity of the load distribution in this area of the deck. This deflected shape was considered to be extreme because in practice the Stage 2 deck would have some stiffness provided by the concrete formwork. To account for this, the model was rerun with additional stiffness added to the Stage 2 deck in the form of shell reinforcement layers. This curve (dashed blue line in Figure 6.12) is perhaps a more realistic representation of the deflected shape at the onset of concrete curing. With this added stiffness, the maximum calculated differential deflection

reduced considerably from 0.348 in. to 0.259 in. The dramatic difference between the two analyses highlights how sensitive the relative girder deflections are to small changes in stiffness of the early-age concrete deck.

Furthermore, Table 6.3 highlights the changing magnitude of differential deflections between girders adjacent to the longitudinal construction joint as the Stage 2 deck hardens. The reduction in differential deflection is larger than the previous two bridges, about 0.160 in. total, or 0.071 in. total if the first case is not considered. It is also worth noting that the adjacent span that was not loaded experienced a maximum differential deflection of 0.0851 in., about 24.4% of that in the loaded span. In this span, the girders deflect upward, with the girder on the hardened side of the construction joint deflecting upwards more than the adjacent girder on the other side of the construction joint.

Table 6.3 - B-70-177 differential deflections under various loading conditions

Concrete Curing Time (days)	Concrete Compressive Strength (ksi)	Concrete Modulus of Elasticity Strength (ksi)	Differential Deflection - Both Lanes (in)	Differential Deflection - Far Lane (in)	Differential Deflection - Near Lane (in)
0	0.00	1	0.348	0.110	0.238
0 (w/ reinf.)	0.00	1	0.259	0.107	0.152
0.5	0.45	1223	0.203	0.094	0.108
1	0.82	1652	0.199	0.092	0.107
3	1.83	2459	0.194	0.089	0.105
7	2.80	3046	0.191	0.087	0.104
28	4.00	3640	0.188	0.085	0.103

Because this bridge had two traffic lanes open during staged construction, the effect of lane closures could also be investigated. Table 6.3 shows the magnitudes of differential deflections when just one of the traffic lanes is loaded. The “near” lane refers to the lane closest to the staged construction joint and the “far” lane is the lane furthest from the construction joint. In the most extreme case, the differential deflections reduced from 0.348 in. to 0.110 in. when the lane closest to curing deck was closed to traffic, a reduction of 68.4%. When the truck was only loading the

near lane, the differential deflection was reduced by 31.6%. This reduction becomes less pronounced as the Stage 2 deck hardens, gains stiffness, and distributes load more evenly between girders. Once the deck fully hardened, the differential deflections reduced from 0.188 in. to 0.085 in. when the lane closest to curing deck was closed to traffic, a smaller reduction of 54.8%.

6.5 Conclusions

The results from the numerical analysis of bridges B-16-136 and B-64-123 were consistent with the findings from the field monitoring task. Magnitudes of differential deflections predicted by the finite element models were very similar for both bridges. The reduction in deflection as the Stage 2 deck hardened was also nearly identical. Field monitoring of these bridges showed minimal differences between the differential deflection characteristics, and the results from the finite element models confirm this.

Maximum differential deflections predicted by the finite element models were generally slightly larger than those seen during field monitoring. The largest values, computed with a plastic concrete deck (curing time of zero days), were larger than those measured in the field. This is possibly because the instrumentation was not able to immediately be placed on the bridge and thus the actual stiffness was likely larger. Similarly, the finite element model did not account for stiffness of the formwork, which would help to reduce the measured differential displacements slightly. Furthermore, the truck loading that was applied was considered to be an upper bound loading. Because trucks producing this magnitude of deflection are not common, it is possible that no truck of this size was recorded during the field monitoring.

The numerical analysis of bridge B-70-177 showed that considerably larger deflections than those seen in the other two bridges are possible; the maximum differential deflection computed in this bridge was over five times larger. While the two lanes of truck loading definitely

contributed to this larger displacement, even when just the lane furthest from the staged construction joint was loaded, the differential deflections were still considerably larger. The much longer spans and steel plate girder configuration are possible factors in explaining why this is the case. Further modeling of staged construction bridges with different span lengths and configurations could possibly deliver conclusions on which parameter is more critical.

The results for bridge B-70-177 do show that closing traffic lanes closest to the staged construction joint is an effective way to reduce the magnitudes of differential deflections. If a lane closure can be afforded, this would likely be the preferred and most effective way of limiting the influence of traffic on the curing concrete deck. If a full lane closure is not possible, requiring heavier vehicles to move to the far lane would be the next best option.

Chapter 7: Experimental Study of Longitudinal Construction Joints

The final task of this research was to perform a laboratory investigation of how traffic-induced differential deflections during deck curing affect concrete-bar bond and integrity of the longitudinal joint region. Tests were also conducted on joint samples to evaluate the effect on joint leakage of treating the first-stage joint concrete with a concrete retarder.

Evaluation of the effect of traffic-induced vibrations on concrete-bar bond and integrity of the longitudinal joint region was conducted through the testing of two large-scale bridge deck specimens fabricated using a simulated staged construction process and subjected to differential displacements of varying magnitudes during curing of the concrete cast in the second stage. Once the concrete in the second stage had achieved its specified compressive strength, the specimens were subjected to a four-point bending ultimate test to evaluate the strength of the bar splice adjacent to the longitudinal joint. Instrumentation installed in the longitudinal construction joint region and on the spliced reinforcing bars were used to evaluate the integrity of the joint region and the quality of the bond in the spliced reinforcement.

Evaluation of the effect of applying a concrete retarder on joint leakage was conducted by subjecting four pairs of joint samples to a water head and measuring the drop in head over time. The joint surface for two pairs was treated with a concrete retarder, followed by water injection to remove surface paste and expose course aggregate. Joint surface in the other two pairs was left untreated. The effect of joint surface treatment on joint leakage was then evaluated by comparing the rate of drop in water head for the specimens with and without joint surface treatment.

7.1 Methodology (Simulated traffic-induced vibrations)

7.1.1 Experimental Overview

Two bridge deck specimens were constructed following a simulated staged construction procedure. The specimens replicated a transverse strip of concrete bridge deck supported on girders experiencing differential deflections. The construction and testing sequence for these specimens is outlined in Figure 7.1. Construction occurred in two stages; the first stage was cast normally without any disturbance, and the second stage was subjected to simulated traffic displacements during curing. Once the Stage 1 segment of the specimen had fully hardened, it was attached to a testing frame, with one end supported by a steel beam attached to the strong floor and the other supported by an actuator for future application of the simulated traffic differential displacements. Formwork for the Stage 2 segment, which was designed to be free to move, was attached to the loading frame and the Stage 1 segment. Steel reinforcement for the Stage 2 segment was placed and lap spliced with the bars protruding from the Stage 1 segment. The Stage 2 segment was then cast adjoining to the first stage, and subjected to the displacements from the actuator during curing. Once the Stage 2 concrete had reached the design strength, the formwork and supports were removed and the entire specimen was shifted over so a four-point bending test could be performed on the staged construction joint region.

The two specimens were subjected to different live traffic-induced deflection protocols during curing of the Stage 2 segment. The displacements applied to Specimen 1 were representative of those measured in the field, as well as those calculated in the finite element modeling task of this research. Specimen 2 was subjected to displacements with the same shape and frequency as those applied to Specimen 1, but scaled up by 2.5 times. Apart from the applied

displacements during curing, the design and construction procedures for the two specimens were identical.

The test specimens were designed to be as representative as possible of an actual bridge deck. The dimensions, reinforcement, formwork, and applied displacements were all chosen based on results and observations from actual staged bridge construction projects. Various instruments were used to quantitatively monitor the performance of the staged construction specimens. These included strain gauges, linear potentiometers, load cells, and an infrared-based position tracking system. Concrete test cylinders were fabricated and tested for all segments to monitor the strength gain at various key times. Tensile tests of the steel reinforcement were performed to determine the actual stress-strain response of the specimen reinforcement.

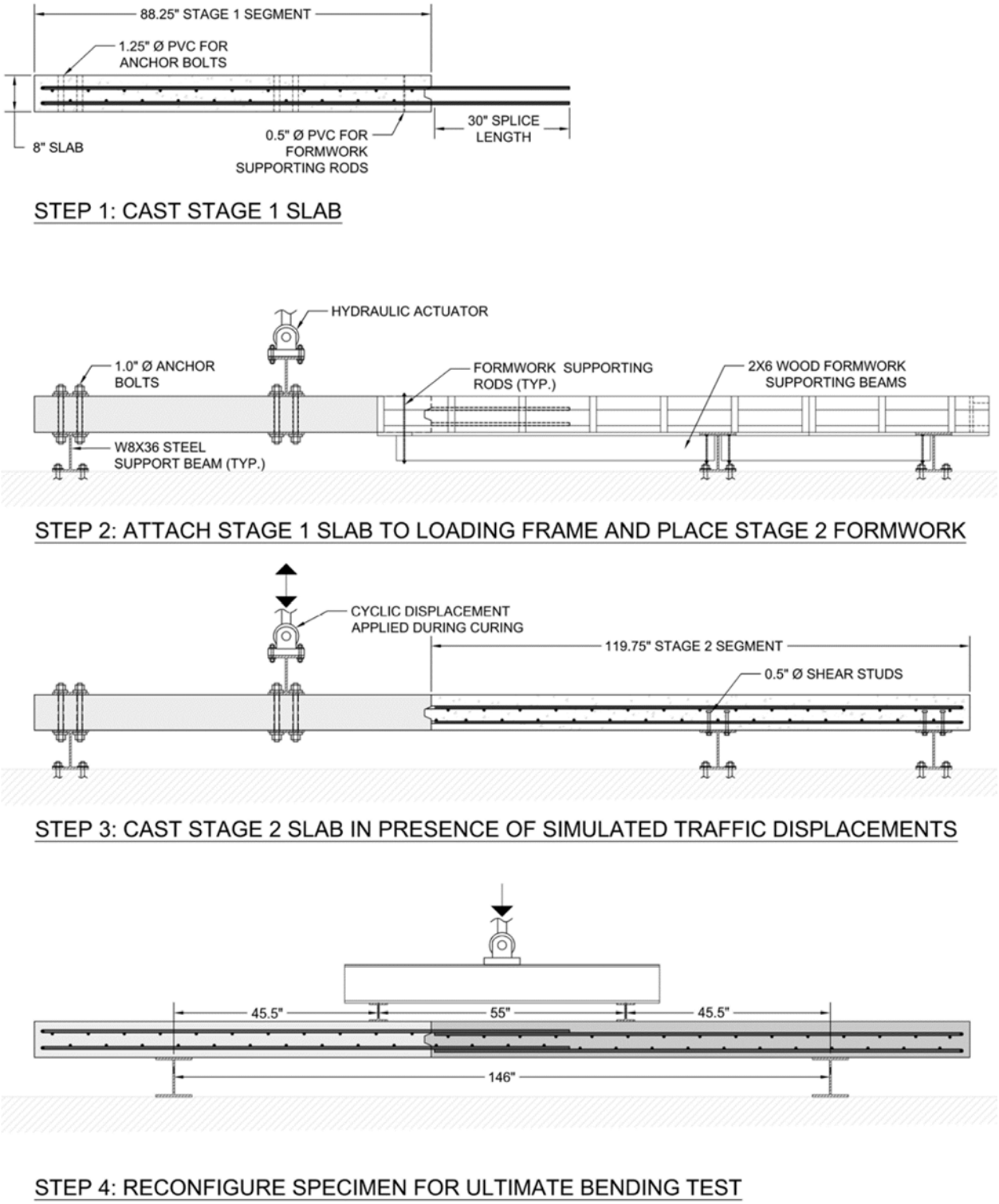

Figure 7.1 - Laboratory specimen construction and testing sequence

7.1.2 Test Frame

The test specimens were fabricated and tested underneath a steel loading frame. The frame consisted of two 13-in. deep built-up steel columns bolted to the laboratory strong floor and connected near the top by a W18X86 steel beam. A 55-kip hydraulic actuator was suspended from the middle of the beam. A photograph of a specimen underneath the loading frame can be seen in Figure 7.2.

Figure 7.2 - Specimen in place underneath loading frame prior to casting of Stage 2 portion.

Plan and side views of the specimen reinforcement details and support/loading configuration are shown in Figure 7.3. A cross section of the test specimens is shown in Figure 7.4. The specimens spanned between four steel supporting beams (one connected to the actuator, plus three bolted to the strong floor). The actuator support (Girder Line 2) represented the girder on the hardened side of the staged construction closest to the longitudinal joint. These four supporting beams were fabricated from 36-in. long steel W8X36 sections. There were three spans total, one main span and two half spans. The staged construction joint was located in the main, middle span. Eight feet separated the two supporting beams adjacent to the construction joint, representing a full-scale girder spacing. Space constraints in the laboratory did not allow for three full spans between girders, so two half spans were provided on either side of the main span to provide some continuity. The support beams at the ends of the specimen (Girder Lines 1 and 5) were assumed to be mid-span points.

7.1.3 Specimen Design

The concrete slab test specimens had total outside dimensions of 208-in. long, 36-in. wide, and 8-in. deep. Specimens were cast in two stages; the first stage involved casting an 88.25-in. segment isolated from any simulated traffic-induced displacements. After fully curing, the first segment was then moved to the loading frame where the second, 119.75-in. long segment, was cast. Given these dimensions, the specimen was symmetric about the center of the transverse reinforcement lap splice.

Many of the specimen design details were modeled after those from bridge B-16-136 discussed in previous sections of this report. These include girder spacing, deck thickness, and reinforcement details. The spacing between girders adjacent to the staged construction joint was 8.0 ft, which was the same as in bridge B-16-136. This spacing was also convenient because the

anchor bolt spacing for the laboratory strong floor is 4.0 ft. The slab thickness was 8.0 in., which was also the same as in the actual bridge.

Transverse reinforcement, which is perpendicular to the direction of traffic and typically in the short direction in an actual bridge, was placed in the long direction of the test specimen. Likewise, the longitudinal reinforcement, which is parallel to traffic and typically placed in the long direction of an actual bridge, was placed in the short direction of the test specimen. To avoid confusion, reinforcement will be referred to as transverse and longitudinal as it relates to an actual bridge. For both the test specimens and for actual bridges, the transverse reinforcement crosses the construction joint in the test specimen, while the longitudinal reinforcement runs parallel to the construction joint.

All reinforcing bars were Grade 60 steel and epoxy coated to represent typical practice. Transverse deck reinforcement for bridge B-16-136 and the test specimens consisted of #5 bars top and bottom at 6.5-in. spacing. In the experimental layout, these transverse bars spanned along the 208-in. length of the specimen. In the actual bridge deck, top and bottom transverse and longitudinal reinforcing bars were offset from each other. Because of the relatively small 36-in. width of the specimen, however, it was not possible to provide this offset to the transverse bars and still maintain the same number of bars in the top and bottom layers in the test specimens. Longitudinal reinforcement used in the test specimens consisted of #4 bars top and bottom at 8-in. spacing, and spanned along the 36-in. width of the slab specimen. Given the length of the specimens, these bars could be offset, as in bridge B-16-136. Clear cover was 1.5 in. and 2.5 in. for the bottom and top reinforcement, respectively.

At the staged construction joint, transverse reinforcing bars extended from the Stage 1 deck into the Stage 2 deck, and were lapped 30 in. (48 bar diameters) with the reinforcement from the

Stage 2 deck. This lap splice length was common in the inspected deck-on-girder bridges discussed in Chapter 4 of this report and it is what is recommended in AASHTO design standards (AASHTO 2012). A shear key was formed into the edge of the Stage 1 deck with a beveled 2x4, a detail that was also commonly used in the inspected bridges.

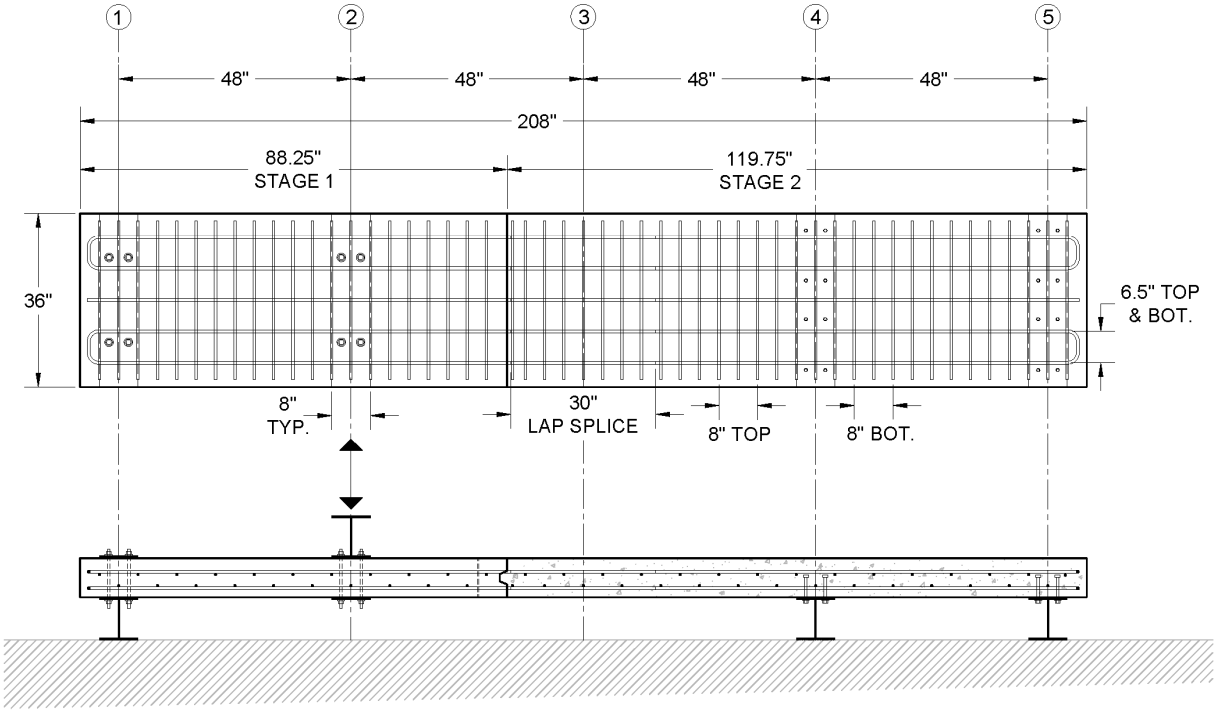

Figure 7.3 - Plan and side view of specimen reinforcement details

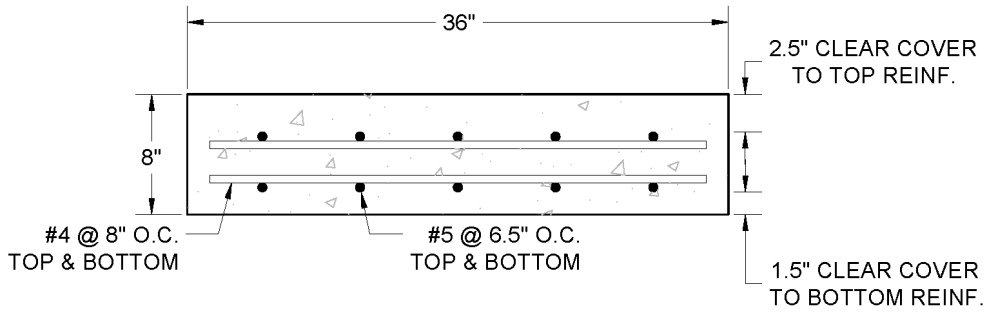

Figure 7.4 - Specimen cross section

Two different methods were used to connect the concrete specimen to the steel supporting beams, as shown in Figure 7.3. The Stage 1 segment was cast with eight 1.25-in. diameter PVC pipes embedded vertically in the deck, four at the end support (Girder Line 1) and four at the actuator support (Girder Line 2). 1-in. diameter steel threaded rods were then passed through the PVC pipes and used to bolt the hardened Stage1 segment to the flanges of the supporting beams. Before casting the Stage 2 portion, sixteen 0.5-in. diameter steel studs were bolted through holes in the other two steel supporting beams (eight in each beam at Girder Lines 4 & 5). The stud head protruded into the slab, serving the same function as headed shear studs in steel girder bridges. After the Stage 2 deck was cast and hardened, the nuts were removed from the steel studs and the deck could be lifted away from the supporting beams, allowing them to be reused.

All concrete used to cast the specimens was provided by a local ready-mix supplier. The concrete used was a WisDOT Grade A-FA mix, the typical mix specified by WisDOT for bridge decks. This mix has a design water-cement ratio of 0.40, maximum slump of 4 in., minimum 28-day compressive strength of 4,000 psi, and 6.0% ±1.5% air entrainment. All mixes were ordered with a maximum aggregate size of 0.75 in.

7.1.4 Instrumentation

Several different instruments were used to collect data during testing of the specimens. Among the most important of these instruments were strain gauges attached to the transverse steel reinforcement embedded in the concrete specimen. Strain gauges were installed on both the top and bottom layers of transverse steel in the splice region. Some gauges were also installed outside of the splice region in the Stage 1 segment. To install the gauges, first the surface of the rebar was ground down, sanded smooth and cleaned. The strain gauge was then adhered to the bare steel and

covered in several layers of watertight coatings to protect it against damage from being cast in concrete. The locations of the strain gauges can be seen in Figures 7.5 and 7.6.

The 55-kip hydraulic actuator was equipped with a load cell and an LVDT to measure the actuator displacement and load. During the application of the simulated traffic displacements, LVDTs and string potentiometers were placed underneath the specimen to measure absolute displacement of the specimen at two different locations, as shown in Figure 7.5. The actuator displacement and the absolute specimen displacement were compared to ensure that displacements commanded to the actuator were correctly applied to the specimen.

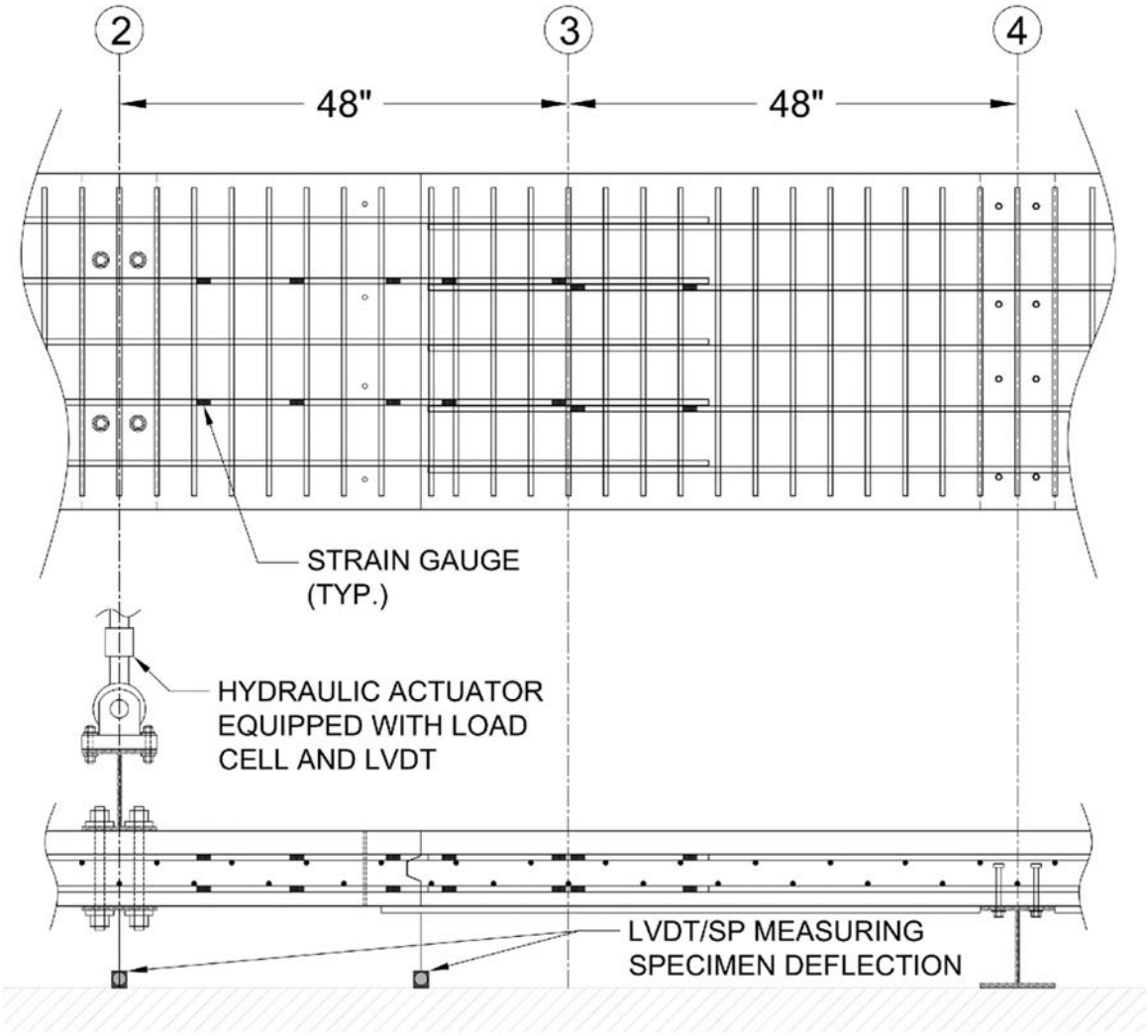

Figure 7.5 – Plan and profile view of instrumentation locations

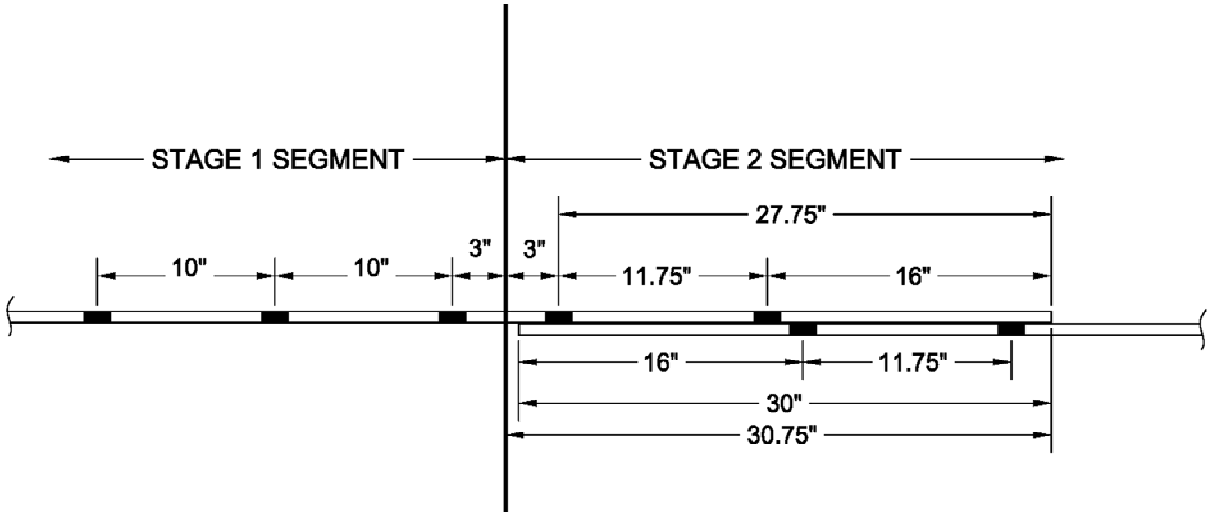

Figure 7.6 - Strain gauge locations within splice of longitudinal reinforcement

Another tool used throughout testing of the bridge deck specimens was an Optotrak Certus HD® tracking system. This optical camera can track position of special markers in three dimensions with excellent precision and accuracy. During the Stage 2 bridge pour, a grid of markers was attached to the specimen to track the displacement along the length of the specimen through time. A similar grid was also used during the ultimate test of the specimen to track the displacements and deflected shape of the specimen throughout the test. These marker grids for the Stage 2 deck pour and the ultimate test are shown in Figures 7.7 and 7.8, respectively.

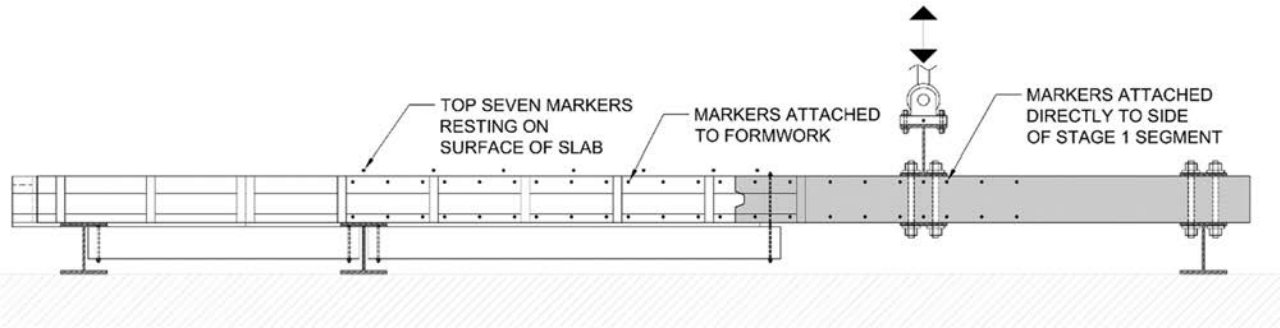

Figure 7.7 - Optotrak® marker layout for Stage 2 deck pour with simulated traffic loading

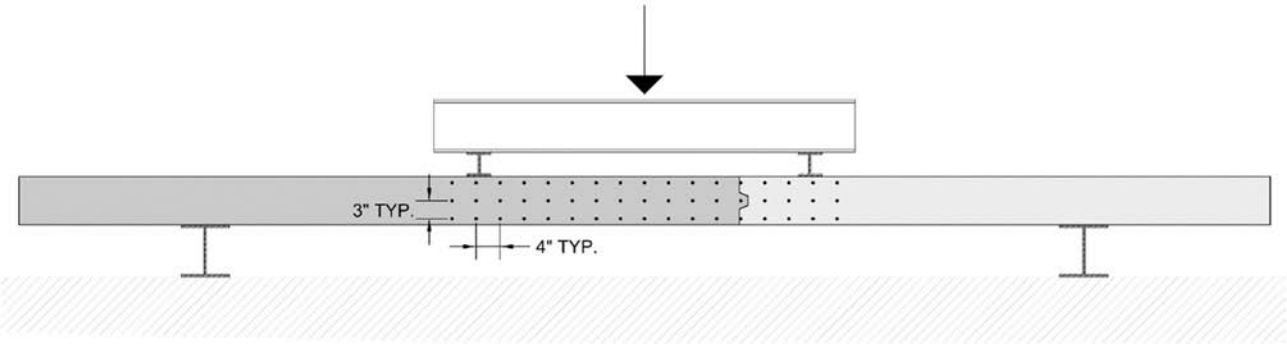

Figure 7.8 - Optotrak® marker layout for ultimate flexural strength test. Note that the outside 3 rows of markers on each side were only present in Specimen 2.

7.1.5 Formwork Design

Because the displacements were applied to the curing concrete specimen, special consideration was given to the design of the concrete formwork that experienced the same displacement. During field monitoring of staged construction bridges, notes were made of the formwork system. For the two deck-on-girder bridges discussed in Chapter 5, support for the Stage 2 slab as it cured was provided by plywood resting on wood beams supported by the girders or the hardened deck. In the case of bridge B-16-136, the wood beams were supported on both ends by the girders adjacent to the staged construction joint. In the case of bridge B-64-123, it was observed that the wood beams were supported by the girder on the Stage 2 side of the construction joint and by rods drilled through the Stage 1 hardened deck near the construction joint, as seen in Figure 7.9. The formwork for the laboratory specimens used a similar support system to bridge B-64-123.

Figure 7.9 - Formwork system as seen in staged construction of bridge B-64-123. Wood beams are supported by top flange of left girder and rods are drilled through Stage 1 hardened deck on right side.

Support for the curing concrete in the laboratory specimens was provided by 0.75-in. thick plywood resting on 2x6 wood beams. In the span containing the longitudinal joint, the beams were supported at one end by steel rods passing through the hardened Stage 1 slab, and at the other end by rods screwed into nuts that were welded to the underside of the top flange of the supporting steel beams. In the adjacent half span, the wood beams were supported on both ends by rods screwed into nuts welded to the steel support beams. With this formwork system, the weight of the curing concrete deck was supported completely by the supporting beams and the Stage 1 slab. The curing portion of the specimen was then free to deflect as it would in an actual bridge. Figure 7.10 shows a sketch of the formwork supporting system, and photographs are shown in Figure 7.11 and Figure 7.12.

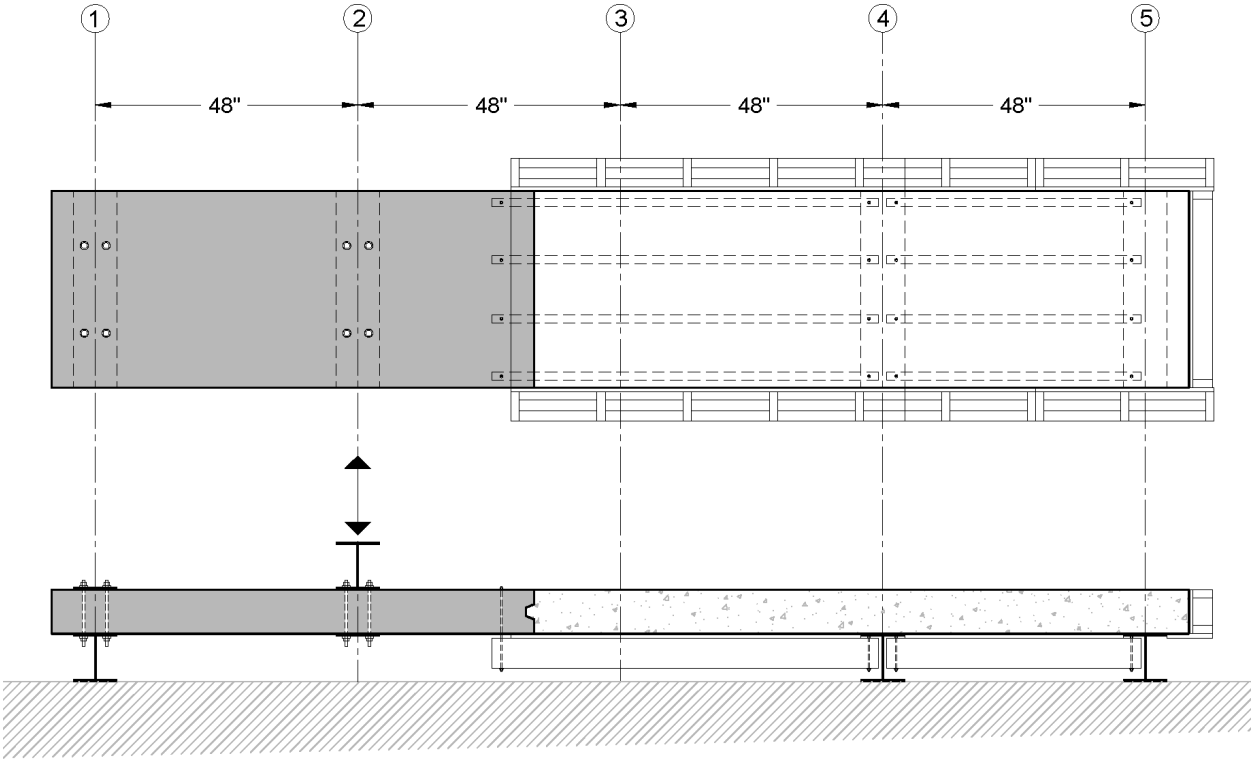

Figure 7.10 - Plan and profile view of formwork system supporting the Stage 2 segment.

Figure 7.11 - Wood supporting beams in place before plywood is placed on top.

Figure 7.12 - Formwork supporting system connections. Left: steel rod passing through hardened slab. Right: steel rod threaded into nut welded to steel supporting beam.

7.1.6 Stage 2 Bridge Deck Pour with Simulated Traffic Loading

Once the Stage 1 segment of the specimen was cast and attached to the loading frame, and the formwork and reinforcement for the Stage 2 segment was in place, the Stage 2 deck pour commenced. After the Stage 2 deck was poured, consolidated, and finished, the traffic displacement protocol described below was initiated. The specimen was covered with wet burlap during the curing period, observed as typical practice in the field. The burlap was used to moist cure the specimen for approximately 5 days.

While the displacement cycles were being applied, data were collected from the strain gauges, actuator load cell, actuator LVDT, specimen LVDTs, and the infrared-based position tracking system (Optotrak Certus HD®). The displacement cycles were started approximately 1 hr after the Stage 2 deck pour commenced and immediately after the pour was completed. The cycles were applied continuously for 12 hours before being ceased, corresponding to a time frame from 1 hr to 13 hrs after the start of the Stage 2 pour. The displacement cycles were restarted

approximately 24 hrs after casting and ran for 1 hr. It was assumed that any damage to the fresh concrete had already occurred by the end of the restarted cycling, and therefore loading was not continued as the Stage 2 deck gained sufficient strength past the reapplication of loading at 24 hours.

7.1.6.1 Traffic Displacement Protocol

The simulated traffic displacement protocol consisted of a series of displacement pulses applied to the Stage 1 portion of the specimen every 20 seconds. These pulses, which are equivalent to differential deflections between girders, included a larger magnitude pulse and a smaller magnitude pulse. The larger pulse had a magnitude 2.5 times that of the smaller pulse, and occurred once every 12 pulses. After the larger pulse, the smaller pulse was repeated 11 times, with a 20 second delay between the start of each. The delay time between pulses was chosen to result in a total number of cycles representing expected large-vehicle events on a moderately busy highway bridge with one lane open during staged construction. Refer to Figure 7.13 for a typical segment of the applied displacement history.

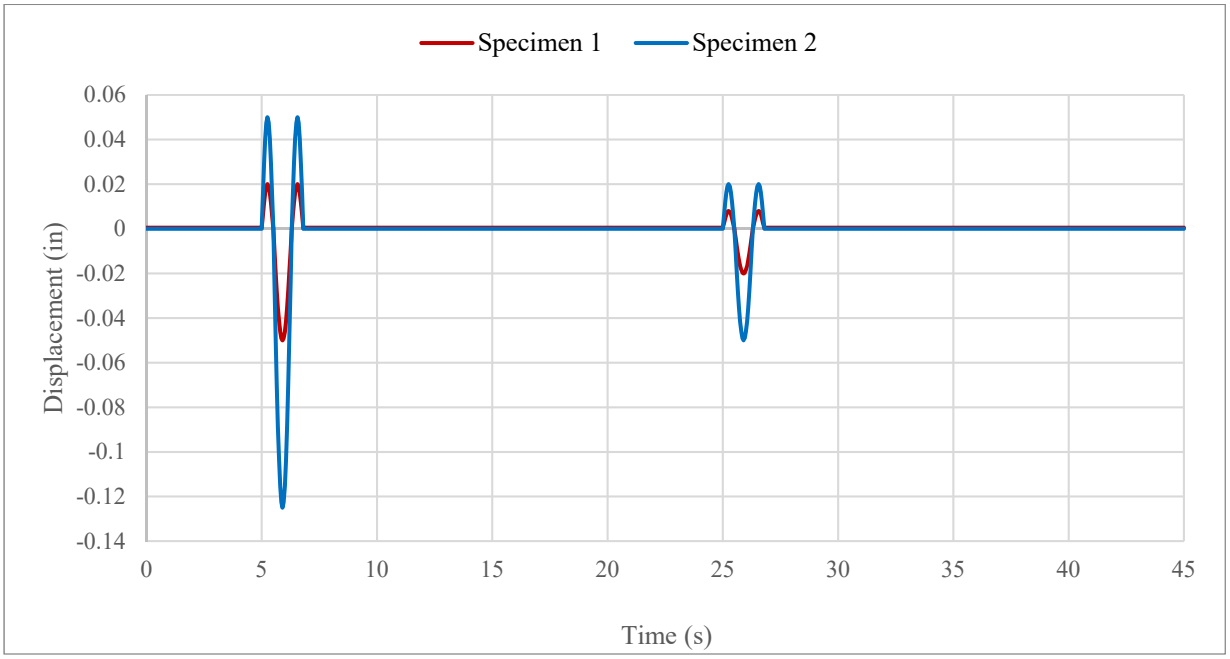

Figure 7.13 - A typical segment of the applied traffic displacements.

The shape of the pulses was similar to a sine wave, except that the magnitudes of the positive and negative displacements were not equal. Upward (positive) displacement would occur in a multi-span bridge from traffic traveling on adjacent spans. The magnitude of the positive displacement was selected to be 40% of the negative (downward) displacement based on results from the field monitoring and numerical analysis tasks. The cyclic displacements were applied at a frequency of 0.83 Hz. The duration of the pulse loading was calculated based on a vehicle traveling at 55 mph over a bridge with a typical main span length of 65 ft. Higher frequency vibrations caused by traffic were not used in the displacement protocol as no significant, especially detrimental, effect of traffic-induced high frequency vibrations was expected. Frequencies of up to 6 Hz were determined to be insignificant in causing damage to fresh concrete by previous researchers (Furr and Fouad, 1981; Swenty and Graybeal, 2012). Also, these vibration frequencies represent only a small percentage of the frequencies of most internal and rotary form concrete vibrators (between 100 and 200 Hz). Further, as discussed in Section 5.1.3 regarding the evaluation methodology for the field monitoring data, acceleration records were low-pass filtered at 30 Hz; other than removing high-frequency noise, the measured response was not significantly changed by this filtering, indicating that high frequencies may not play a significant role in longitudinal joint differential movement.

The magnitudes of the applied simulated traffic-induced displacements were the main difference between the two test specimens. The first specimen was subjected to a large pulse magnitude of +0.02/-0.05 in. and a small pulse magnitude of +0.008/-0.02 in. These magnitudes were selected considering results from the field monitoring and numerical analysis of bridges B-16-136 and B-64-123. The largest downward displacement of 0.05 in. was similar to that calculated for the finite element models and was considered to be an upper bound of a reasonable

displacement. The smaller downward displacement of 0.02 in. was similar to the average expected displacement calculated from the field monitoring of these two bridges. Thus, this loading scenario should be representative of the largest expected vehicle crossing the bridge every four minutes and an average heavy vehicle crossing the bridge every 20 seconds in between.

Specimen 2 was subjected to these same pulses scaled up by a factor of 2.5, with the large pulse magnitude being +0.05/-0.125 in. and the small pulse magnitude being +0.02/-0.05 in. While this magnitude of displacement was considered to be extreme, results from the finite element model of bridge B-70-177 and previous research (Furr and Fouad 1981) show that in certain situations it is possible to see differential deflections this large.

Consideration was given to how the deflected shape of the specimen during the Stage 2 deck pour simulation compared with the deflected shape of actual bridges subjected to traffic loads during staged construction. Ideally the deflected shape of the specimen during curing of the Stage 2 deck would be as realistic as possible. Figure 7.14 shows how the deflected shape of the laboratory specimens compares with that of an actual bridge during curing of the Stage 2 deck. Girders are depicted by solid vertical lines, and the longitudinal construction joint is depicted by the dashed vertical line. In this figure, position values greater than 112 in. correspond with the hardened Stage 1 deck, and values less than 112 in. correspond with the curing Stage 2 deck. The double-sided arrow shows where the hydraulic actuator applied displacements to the specimen.

Figure 7.14 – Comparison of deflected shapes for the laboratory specimens and bridge B-16-136 during curing of the Stage 2 deck.

Figure 7.14 shows that the deflected shapes of the Stage 2 decks are similar, but the specimens were subjected to larger rotations than the actual bridge. The specimen was also supported at the end of the Stage 1 segment (X = 192 in.), where the actual bridge displaced downwards due to the applied truck loading (not shown). Furthermore, the specimen experienced considerably higher rotation demands at the longitudinal construction joint during curing of the Stage 2 segment.

7.1.7 Ultimate Strength Test

After the specimen had been subjected to the simulated traffic-induced displacements during curing of the Stage 2 portion, an ultimate flexural strength test was performed to evaluate the concrete-bar bond in the splice region along the longitudinal joint. Once the concrete in the Stage 2 segment reached the specified compressive strength, the formwork and steel supporting beams were removed, and the whole specimen was shifted over to be centered with the loading frame. The specimen was positioned such that the centerline of the spliced transverse bars was directly underneath the actuator.

The specimen was tested in flexure through the four-point bending configuration seen in Figure 7.15. In this arrangement, the middle 55 in. of the specimen was subjected to constant moment and no shear forces (neglecting the effect of deck self-weight). This region encompasses the entire lap splice and thus allowed the stresses in the spliced reinforcement to be analyzed independent of moment.

The specimens were loaded until failure, which in both cases occurred through crushing of the concrete compression zone at the end of the spliced reinforcement. An error resulted in the two specimens being tested using different loading protocols. The first specimen was tested using load control and a loading rate of 2000 lbs per minute, and the second specimen was tested using displacement control at a rate of 0.10 in. per minute. This change did not affect the response of the specimen up to peak load, however; thus, direct comparison of the results from the two specimens could still be made up to this point.

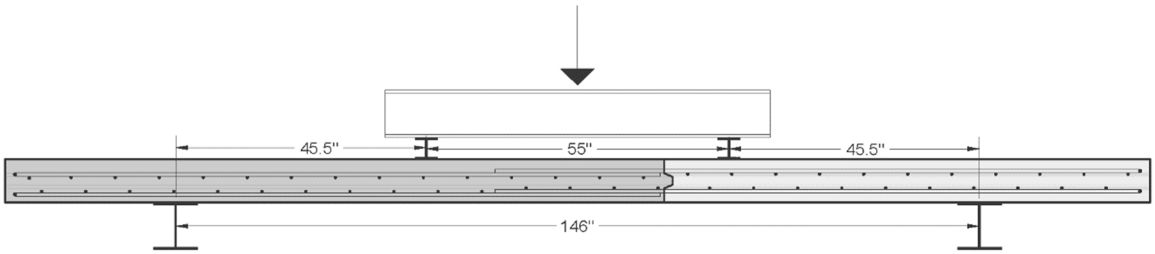

Figure 7.15 - Ultimate test four-point bending configuration.

7.1.8 Material Testing

7.1.8.1 Cylindrical Concrete Specimens

Cylindrical concrete test specimens were cast for all stages of both specimens to determine concrete compressive strengths. All compressive strength specimens were 6-in. by 12-in. cylinders cast in accordance with ASTM C31 – Standard Practice for Making and Curing Concrete Test

Specimens in the Field. All cylinders were cured in the same location and under the same temperature and humidity conditions as the test specimens. The concrete cylinders were not subjected to any vibrations or displacements during curing.

Nine compressive strength specimens were cast for the Stage 1 portions so the in-place compressive strength could be estimated at three different times: the 28-day strength, strength during the Stage 2 pour, and concrete strength during the ultimate strength test. The average strength of three cylinders was used to determine the cylinder compressive strength at each time. Twenty-four compressive strength specimens were cast for the Stage 2 portion. These specimens allowed for the estimation of the compressive strength after curing for 12 hours, 1 day, 3 days, 7 days, 14 days, 21 days, 28 days, and at the time of the ultimate strength test. Because the ultimate tests were intended to be performed when the Stage 2 portion of the specimen reached a certain strength, regular testing of early-age concrete cylinders was required to monitor the strength gain. The compressive strength at a particular time was taken to be the average strength of three concrete cylinders. If a single specimen had an unreasonably low maximum strength and there was reason to believe it may have been damaged during curing or improperly tested, that result was omitted from the average. Compressive strengths for all cylinders associated with Specimen 1 and Specimen 2 are presented in Table 7.1 and Table 7.2, respectively. Omitted results are shown as struck out.

The compressive strength of all cylindrical concrete specimens was determined in accordance with ASTM C39 – Standard Test Method for Compressive Strength of Cylindrical Concrete Specimens. Before compression testing, a sulfur mortar was used to cap the ends of all cylinders in accordance with ASTM C617 – Standard Practice for Capping Cylindrical Concrete Specimens.

Table 7.1 - Specimen 1 concrete cylinder compressive strengths.
Note: ~~Struck out~~ values are omitted from average.

Specimen	Stage	Age (days)	Corresponding Test	Slump (in)	Air Content (%)	Cylinder	Compressive Strength (psi)	Average Strength (psi)
1	1	28	--	2.25	6.0	1	7040	7370
						2	6860	
						3	8210	
		63	Stage 2 Pour			1	8190	8000
						2	8020	
						3	7790	
		71	Ultimate Strength			1	8740	8840
						2	8710	
						3	9060	
	2	0.5	Traffic Displacements Stopped	4.00	3.5	1	870	840
						2	870	
						3	770	
		1	--			1	2360	2480
						2	2530	
						3	2550	
		3	--			1	4010	4180
						2	4380	
						3	4160	
		7	--			1	5780	5660
						2	5540	
						3	~~3620~~	
		8	Ultimate Strength			1	5930	5860
						2	5840	
						3	5810	
		28	--			1	6550	6330
						2	5970	
						3	6460	

Table 7.2 - Specimen 2 concrete cylinder compressive strengths.
Note: ~~Struck out~~ values are omitted from average.

Specimen	Stage	Age (days)	Corresponding Test	Slump (in)	Air Content (%)	Cylinder	Compressive Strength (psi)	Average Strength (psi)
2	1	28	--	4.00	3.5	1	6550	6330
						2	5970	
						3	6460	
		91	Stage 2 Pour			1	6430	6540
						2	6400	
						3	6790	
		98	Ultimate Strength			1	5880	6130
						2	6730	
						3	5490	
						4	6010	
						5	6470	
						6	6210	
	2	0.5	Traffic Displacements Stopped	1.75	5.0	1	1060	1110
						2	1140	
						3	1140	
		1	--			1	2040	2030
						2	1910	
						3	2130	
		3	--			1	3970	4210
						2	4370	
						3	4290	
		7	Ultimate Strength			1	5320	5480
						2	5380	
						3	5730	
		14	--			1	6250	6240
						2	6490	
						3	5980	
		28	--			1	~~4350~~	6290
						2	6220	
						3	6360	
		28	--	0.25	5.0	1	8490	8460
						2	8420	
						3	~~4880~~	

7.1.8.2 Steel Reinforcement Test Bars

To correlate the data from the bar strain gauges with forces in the bars, tensile tests were performed on samples taken from the same mills. All steel reinforcement was ordered from the same supplier in two different batches. Each batch was accompanied with six 24-in. long tensile test bars of the same diameter and from the same steel mill as the reinforcement used in the test specimens. All tensile testing of deformed steel reinforcing bars was performed in accordance with ASTM A370 – Standard Test Methods and Definitions for Mechanical Testing of Steel Products. The Optotrak Certus HD® tracking system was used to measure displacements and calculate strains in the bars via four markers glued directly to the bar.

After analyzing the stress-strain response of the test reinforcement, a model was fit to the results that could then be used to calculate stress in the bars from the recorded strain data. This model divides the stress-strain response into four regions. The stress in the steel bar is defined by Equations 4-7 .

Region 1 – Linear Elastic Response: $\varepsilon_s \leq \varepsilon_y$

$$f_s = E_s * \varepsilon_s \quad (4)$$

Region 2 – Yield Plateau: $\varepsilon_y \leq \varepsilon_s \leq \varepsilon_{sh}$

$$f_s = f_y \quad (5)$$

Region 3 – Strain Hardening (Parabolic): $\varepsilon_{sh} \leq \varepsilon_s \leq \varepsilon_{sm}$

$$f_s = f_y + (f_{su} - f_y) * \left[2 * \frac{\varepsilon_s - \varepsilon_{sh}}{\varepsilon_{sm} - \varepsilon_{sh}} - \left(\frac{\varepsilon_s - \varepsilon_{sh}}{\varepsilon_{sm} - \varepsilon_{sh}}\right)^2\right] \quad (6)$$

Region 4 – Constant Stress until Fracture: $\varepsilon_{sm} \leq \varepsilon_s \leq \varepsilon_{su}$

$$f_s = f_{su} \quad (7)$$

where:

ε_s = strain in steel
ε_y = yield strain
ε_{sh} = strain at beginning of strain hardening
ε_{sm} = strain at end of strain hardening = $\varepsilon_{sh} + 2 * \left(\frac{f_{su} - f_y}{E_{sh}}\right)$
ε_{su} = ultimate (fracture) strain
f_s = stress in steel
f_y = yield stress
f_{su} = ultimate stress
E_s = elastic modulus
E_{sh} = tangent modulus at initiation of strain hardening

For each batch of steel reinforcement, the tensile stress-strain responses of six test bars was plotted and then the stress-strain model was fitted to the data by varying the previously defined parameters. Plots of the stress-strain responses for both batches of steel reinforcement and the fitted stress-strain model are given in Figure 7.16 and Figure 7.17.

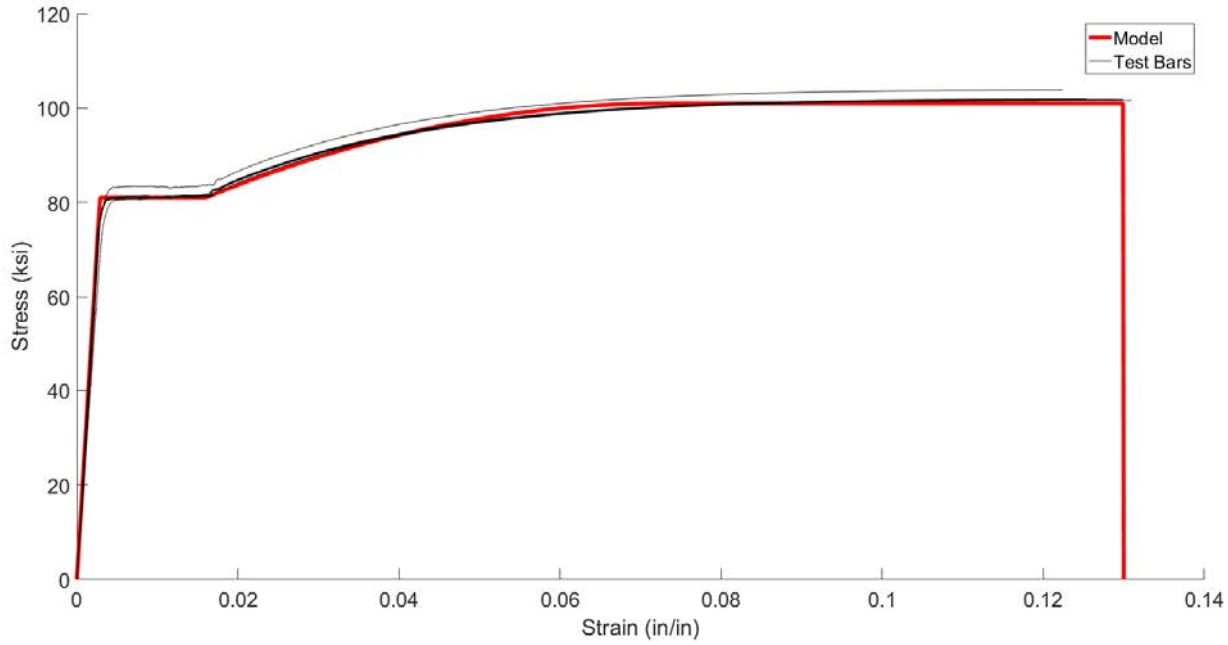

Figure 7.16 - Stress-strain response of Batch 1 #5 test bars.

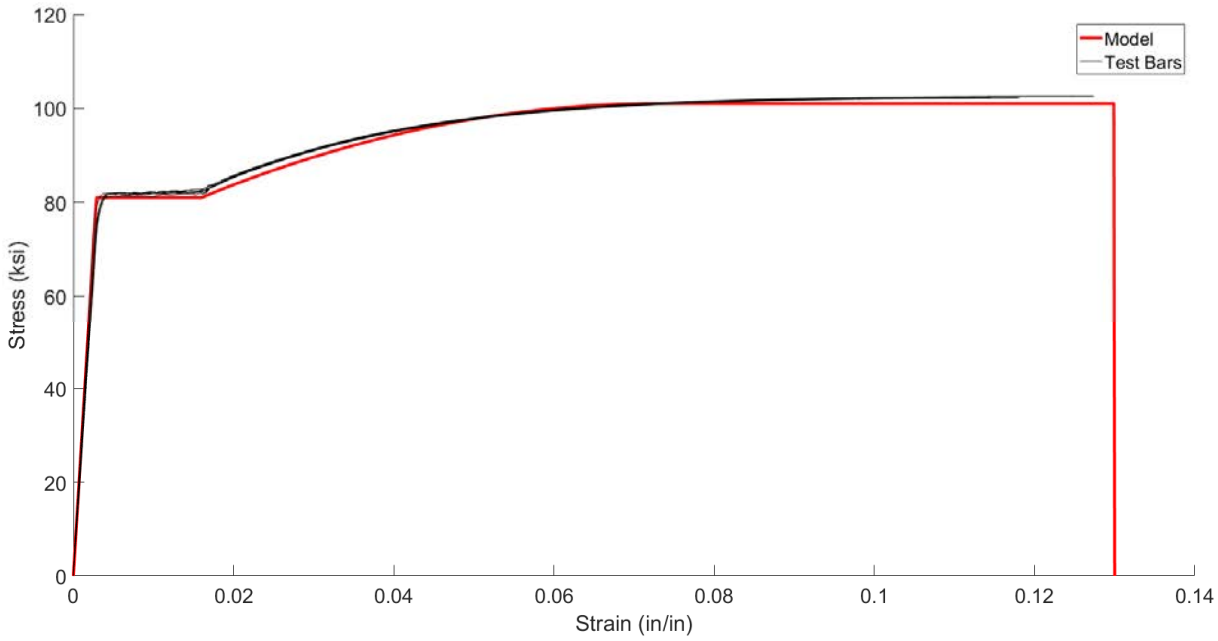

Figure 7.17 - Stress-strain response of Batch 2 #5 test bars.

The results from the reinforcement tension tests were very consistent among individual bars and between batches as well. Thus, the same fitted model was used for both batches. The parameters used in modeling the stress strain response are as follows:

$f_y = 81\ ksi$
$E_s = 28{,}200\ ksi$
$\varepsilon_y = \frac{f_y}{E_s} = 0.0029$
$\varepsilon_{sh} = 0.016$
$\varepsilon_{sm} = 0.073$
$E_{sh} = 700\ ksi$
$\varepsilon_{su} = 0.13$
$f_{su} = 101\ ksi$

7.2 Specimen 1 Test

7.2.1 Description

The main difference between the two tests was the amplitude of simulated traffic-induced displacements applied during the Stage 2 deck pour simulation. Specimen 1 utilized the first displacement protocol, with maximum downwards displacement of 0.05 in. applied every four

minutes and smaller downwards displacements of 0.02 in. applied intermittently every 20 seconds. These simulated traffic-induced displacements were run for 12 hours after casting of the specimen before being terminated. The displacement protocol was restarted approximately 24 hours after casting of the Stage 2 deck, and lasted for about one hour.

Eight days after the Stage 2 deck pour, the Stage 2 concrete had surpassed the specified strength of 4000 psi and the ultimate strength test was performed. For this test, the actuator was programmed to use load control with a loading rate of 2000 pounds of compression per minute. The specimen eventually experienced a compression failure of the concrete at the termination of the lap splice in the Stage 2 segment.

7.2.2 Results

Immediately after the casting of the Stage 2 segment and subsequent simulated traffic-induced displacements, there was little evidence to suggest that the integrity of the specimen had become considerably degraded due to the applied loading during curing. Visual inspection of the specimen after curing of Stage 2 revealed a single hairline crack in the top of the Stage 2 segment directly above steel support beam closest to the construction joint (Figure 7.3, Girder Line 4). The crack was parallel to the support beam and was determined to be a flexural crack due to the applied displacements during curing. A crack would be most likely to form at this location because the applied displacement induced maximum negative moment over this support. While the concrete was still fresh, it had practically no tensile strength. As it began to harden the tensile strength increased, but as soon as the concrete developed any amount of tensile strength, the applied displacement led to cracking at this location. No other damage was visible in the specimen after the Stage 2 pour.

Before performing the ultimate strength test, it was crucial to ensure that the concrete in the Stage 2 portion of the specimen had sufficient compressive strength. Throughout the laboratory experimentation, the concrete was observed to gain strength rapidly and had a 28-day compressive strength considerably larger than the specified design strength of 4000 psi. For example, the concrete used for the Stage 2 pour in Specimen 1 reached an average strength of 4180 psi after 3 days, and had a 28-day compressive strength of 6330 psi. Because concrete with this strength cannot always be expected in real bridge projects, the ultimate strength tests were performed earlier, when the concrete compressive strength was closer to 4000 psi. The ultimate test for Specimen 1 was performed 8 days after casting the Stage 2 portion, when the accompanying concrete cylinders had an average strength of 5860 psi.

The ultimate strength test allowed for the evaluation of the flexural strength in the construction joint region. If the simulated traffic-induced displacements cause degradation of the bar bond or the longitudinal joint to take place, then a flexural test would make this apparent. The ultimate test load-displacement response for Specimen 1 is shown in Figure 7.18. The peak load for this specimen was 41.3 kips, which corresponds to an ultimate moment capacity of 939 kip-in. (excluding the moment caused by the specimen self weight). The specimen eventually failed in compression, which in itself is a sign that the concrete-bar bond did not govern the strength of the specimen. Splitting cracks and subsequent crushing and spalling of the concrete occurred in the compression zone at a location directly above the termination of the bars extending from Stage 1 into the Stage 2 portion (see Figure 7.19). A failure was expected in either this location or at the other end of the lap splice right at the longitudinal joint given the fact that the termination of bars introduces a stress concentration and makes these two sections more susceptible to damage localization.

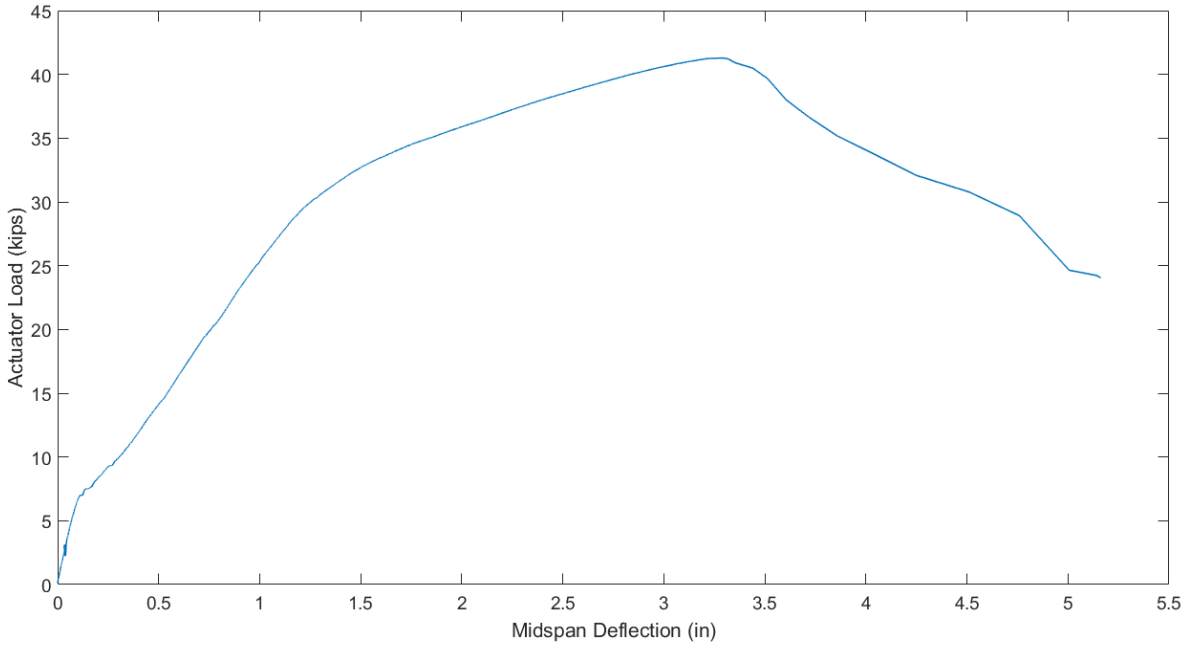

Figure 7.18 - Actuator load versus specimen mid-span displacement response for the ultimate test of Specimen 1.

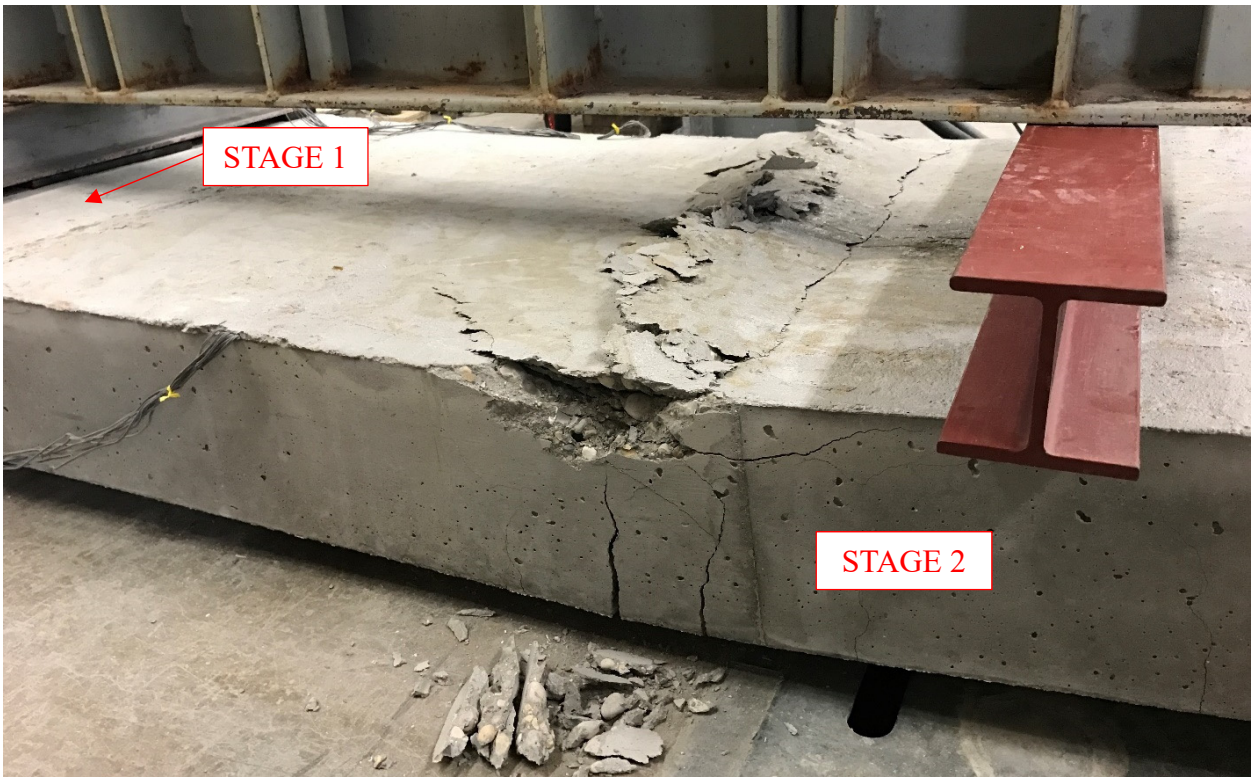

Figure 7.19 – Flexural-compression failure of Specimen 1 at the termination of the transverse reinforcement extending from Stage 1 into Stage 2.

Using the strain data collected during the ultimate test and the steel bar stress-strain model outlined in Section 7.1.8.2, stresses in the steel rebars were calculated at the strain gauge locations throughout the duration of the test. However, because of the presence of initial strains in the reinforcement prior to the tests, the yield point was determined from the applied load versus strain response of each instrumented bar and the stress-strain model adjusted accordingly. Average bond stress between location of strain gauges was calculated using Equation 8.

$$\mu_{avg} = \frac{\Delta f_s d_b}{4L} \quad (8)$$

where:

$\mu_{avg} =$ average bond stress
$\Delta f_s =$ change in stress over segment where average bond stress is being calculated
$d_b =$ bar diameter
$L =$ length of segment

This expression is equivalent to dividing the change in force along the segment where average bond stress is being calculated by the surface area of that bar segment. The stress in each spliced bar that was strain gauged is known at three points: The strain gauge at the continuous end of the splice, the strain gauge near the middle of the spliced bar, and at the end of the bar where the stress is known to be zero. The average bond stress in a spliced bar can be calculated over the three segments shown in Figure 7.20: Segment 1, which extends from the end of the bar to the middle of the splice; Segment 2, extending from the middle of the bar to the continuous end of the splice; and the Full Splice segment, which covers the entire splice from the continuous end of the splice to the end of the bar. This was done for all eight spliced bars that were instrumented (four spliced bars were instrumented in both the bottom and top layers of transverse reinforcement).

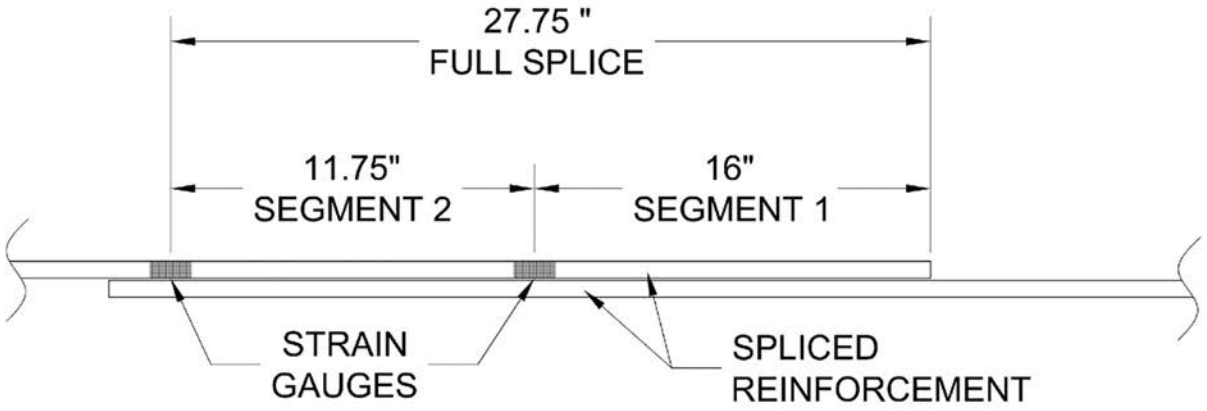

Figure 7.20 - Segments for which average bond stress is calculated

Average bond stress versus specimen mid-span displacement responses for the two spliced #5 bottom bars are shown in Figure 7.21 and Figure 7.22. The plotted deflection was calculated using the infrared markers at mid-span and is relative to the initial displacement after application of a small nominal load; therefore, the plotted zero deflection corresponds to a nonzero load and bond stress. The dashed lines depict the point at which the strain gauge at the continuous end of the splice was determined to reach the bar yield strain.

Prior to yielding, bond stresses in the bars extending from Stage 1 increased almost linearly with deflection and load, with a nearly uniform average bond stress over the splice length. The instrumented bars extending from Stage 2, however, showed lower bond stresses over Segment 2. It should be noted that strain gauge measurements are sensitive to the strain gauge location relative to the closest cracks, which is particularly important at early stages of the test. At the initiation of yielding, bond stress was evenly distributed throughout the length of the splice. After yielding, Segment 2 of the splice experienced a reduction in bond stress because of the decrease in the change in force over that segment. This was compensated by an increase of bond stress in Segment 1 as the bar force at mid-length of the splice increased. Yielding was observed

in all instrumented bars, indicating that the concrete-bar bond was sufficient to develop the yield strength of the reinforcing steel.

Average bond stress versus applied moment is plotted in Figure 7.23 and Figure 7.24 for the same two #5 bottom bars that were spliced together. Note that the applied moment is only that corresponding to the applied loading by the actuator and thus, it does not include the moment due to self-weight of the specimen. Again, the dashed lines depict the point at which the strain gauge at the continuous end of the splice was determined to reach the bar yield strain.

Yielding of the Stage 1 and Stage 2 spliced transverse bars occurred at moments of approximately 600 k-in. and 540 k-in., respectively. Once these bars began yielding and the strain was within the range of the yield plateau, the stress (and force) of these bars at the ends of the splice remained constant, while the applied moment continued to increase. These two observations indicate that the five transverse bars did not yield simultaneously. It is also likely that while some bars had already begun strain hardening, others were still strained within the yield plateau.

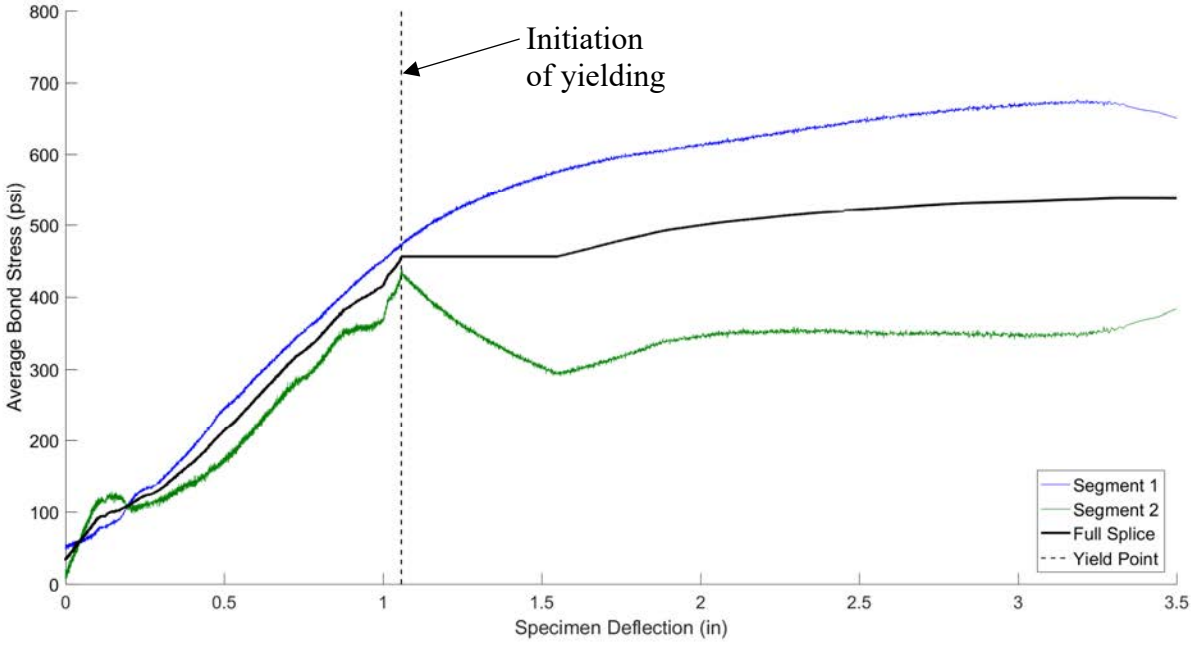

Figure 7.21 - Specimen 1 average bond stress versus specimen displacement for spliced Stage 1 bottom transverse reinforcement.

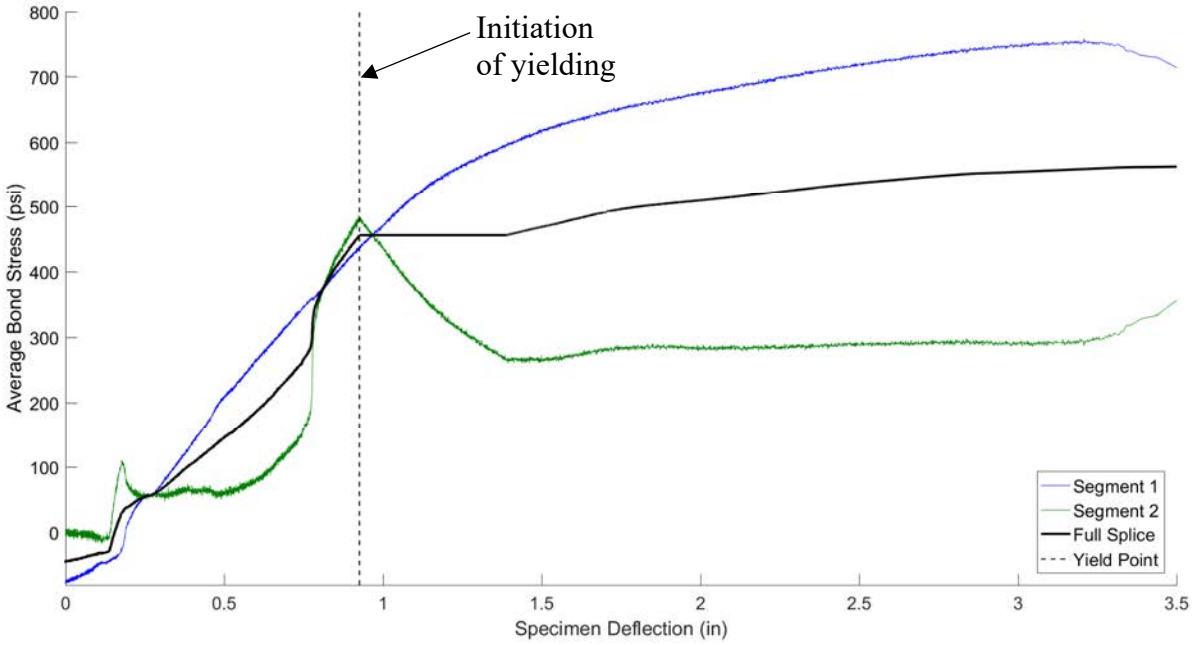

Figure 7.22 - Specimen 1 average bond stress versus displacement for spliced Stage 2 bottom transverse reinforcement.

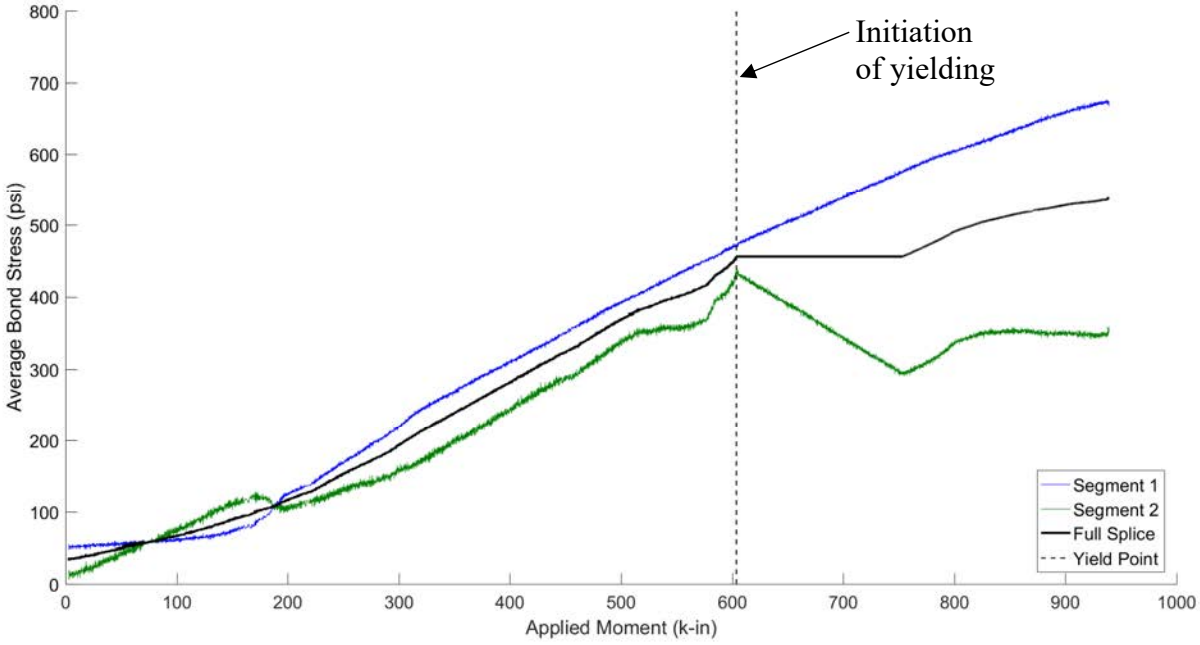

Figure 7.23 - Specimen 1 average bond stress versus applied moment for spliced Stage 1 bottom transverse reinforcement.

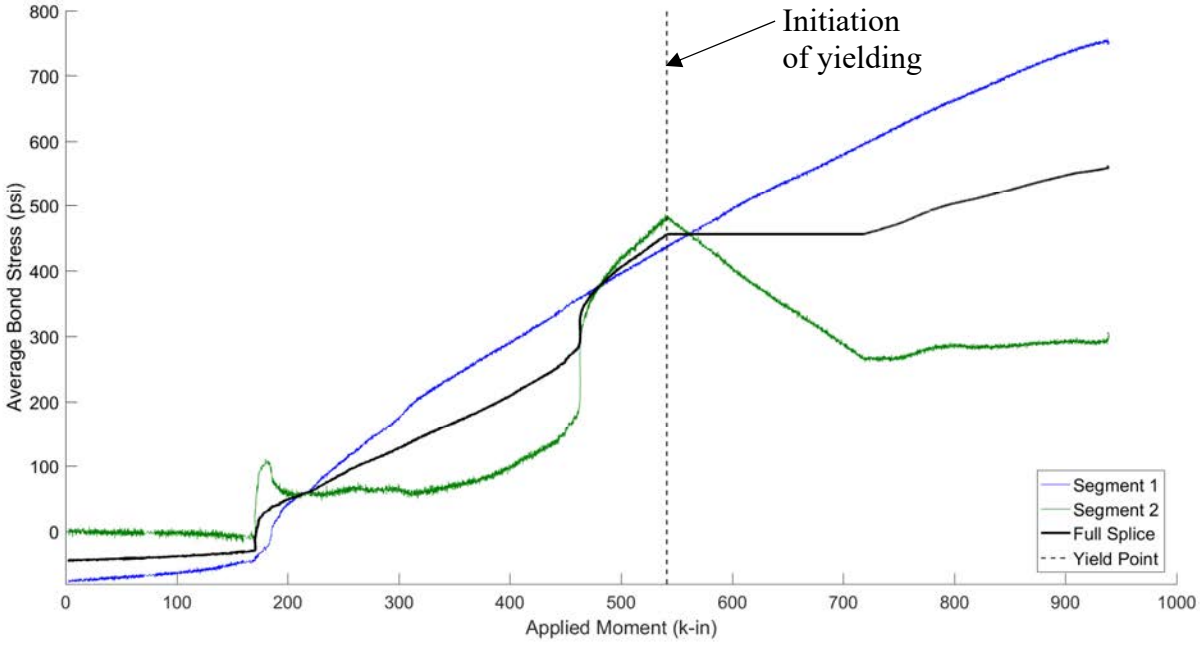

Figure 7.24 - Specimen 1 average bond stress versus applied moment for spliced Stage 2 bottom transverse reinforcement.

The maximum average bond stress during the ultimate test for the four instrumented transverse bars in the bottom layer of reinforcement is tabulated in Table 7.3. The values of maximum average bond stress for the different splice segments are reasonably consistent throughout all spliced bars. Note that the average bond stress that corresponds to developing a yield stress of 81 ksi over a length of 27.75 in. (the length from the gauge at the continuous end of the splice to the end of the bar) in a #5 bar is 456 psi. In all bars, the maximum bond stress over the full splice segment was greater than 456 psi, meaning that all spliced bars began strain hardening before the specimen ultimately failed in flexural compression.

Table 7.3 – Specimen 1 maximum average bond stress of spliced transverse bottom bars

	Stage 1 - Bar 1	Stage 2 - Bar 1	Stage 1 – Bar 2	Stage 2 – Bar 2
Segment 1	*	774 psi	630 psi	791 psi
Segment 2	*	468 psi	494 psi	427 psi
Full Splice	531 psi	544 psi	537 psi	560 psi

**Damaged gauge*

For single bars smaller than #11, Section 5.11.2.1 of the AASHTO LRFD code (AASHTO 2012) requires the tension development length to be calculated from Equation 9 below.

$$l_d = \frac{1.25 A_b f_y}{\sqrt{f_c'}} \geq 0.4 d_b f_y \qquad (9)$$

where:

$l_d =$ bar development length
$f_y =$ bar yield stress (ksi)
$A_b =$ area of bar
$d_b =$ diameter of bar
$f'c =$ concrete compressive strength (ksi)

For epoxy coated bars with cover less than three bar diameters, which was the case for the bottom layer of transverse reinforcement, the development length should be multiplied by 1.5. The development length for lap splices must be further multiplied by a factor depending on the

classification of the splice. All staged construction projects with spliced transverse bars encountered during this research required 100% of the transverse bars to be lapped at the staged construction joint, which means the splice is either Class B or Class C. If the ratio of area of steel provided to area of steel required is greater than two, the splice is Class B. If not, the splice is Class C. The development for a class B lap splice is multiplied by 1.3, and for a class C splice is multiplied by 1.7. It is therefore conservative to use Class C splices.

For a #5 bar, nominal bar yield strength of 60 ksi, and a concrete specified strength of 4000 psi, the required splice length is 29.6 in. for a Class C splice. A 30-in. long lap splice was provided in both specimens. The specimen ultimately failed in flexural compression and, as mentioned above, a stress difference greater than the yield strength of 81 ksi developed in all spliced bars. It was therefore concluded that a Class C lap splice (30-in. long, 48 bar diameters) was sufficient for the specimen to develop its flexural capacity, even when subjected to the first displacement protocol during curing.

Specimen displacements were recorded using data from the Optotrak® tracking system. The marker grid shown in Figure 7.8 allowed the deflected shape and curvatures of the specimen lap splice region to be calculated throughout the test. The deflected shape was plotted at increasing levels of moment throughout the ultimate strength test, as seen in Figure 7.25. At higher levels of moment, points of localized rotation become visible. The most pronounced point (at a marker position of approximately 36 in.) coincided with the location of the construction joint. Localized rotation was also seen, although to a lesser degree, at a marker position of 4 in., which corresponds to the location of the termination of the Stage 1 transverse reinforcement.

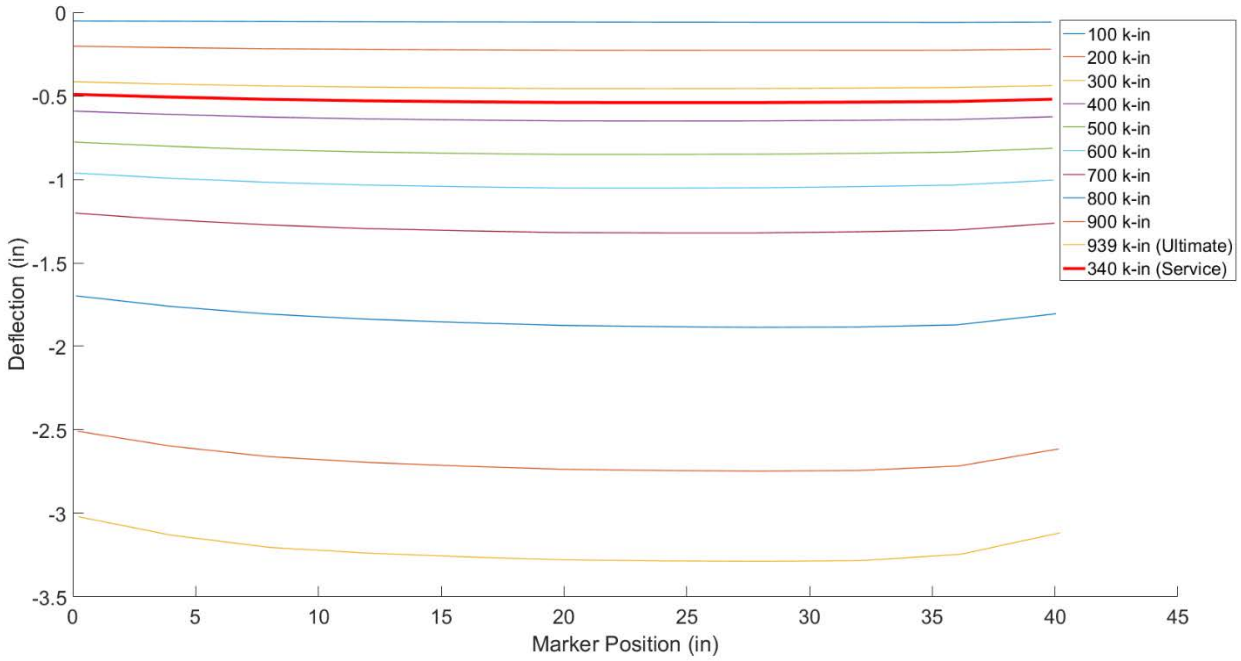

Figure 7.25 - Specimen 1 deflected shape plotted at different levels of moment throughout the ultimate test.

The Optotrak® markers were also used to calculate curvatures in the lap splice region. To calculate the curvatures, the top and bottom rows of markers were first used to calculate average strains near the top and bottom of the section. Then, the curvature was taken to be equal to the slope of the strain profile. Curvatures along the lap splice region are plotted at different levels of moment in Figure 7.26. Again, there are two distinct locations with localized curvatures. The largest average curvatures were concentrated at the construction joint, coinciding with the marker strip positioned at 34 in. The marker strip positioned at 6 in. encompassed the region where the Stage 1 transverse bars terminate. This distribution shows that the curvature in the lap splice region was almost completely localized at the two ends of the splice. The specimen appeared to develop hinges at the weakest sections (i.e. where the spliced reinforcement terminated). At larger moments, curvatures at the splice end near the construction joint were approximately 1.5 times that at the other end of the splice. Below 400 k-in the curvatures at the two ends were essentially equal.

To determine if these localized rotations could potentially result in localized damage over the life of the bridge deck, the deflected shape and curvature distribution in the lap splice region were analyzed under service conditions. It was assumed that a service load would correspond with a maximum stress in the steel reinforcement of $0.6f_y$, or 36 ksi based on the nominal yield strength of 60 ksi. During the ultimate test of Specimen 1, a stress of 36 ksi was reached at the continuous end of the spliced bars at a moment of approximately 340 k-in. The deflected shape and curvature distribution under this assumed service load is represented by the thick red line plotted in Figure 7.25 and Figure 7.26, respectively. These figures show that under a representative service load, the points of localized rotation and curvature are not well defined. Figure 7.26 shows that under service conditions, the curvature is nearly uniform in the lap splice region and localized curvatures at the ends of the splice are barely visible. Therefore, repeated cycles of deformation large enough to produce localized damage at the ends of the lap splice are unlikely to occur under normal service conditions.

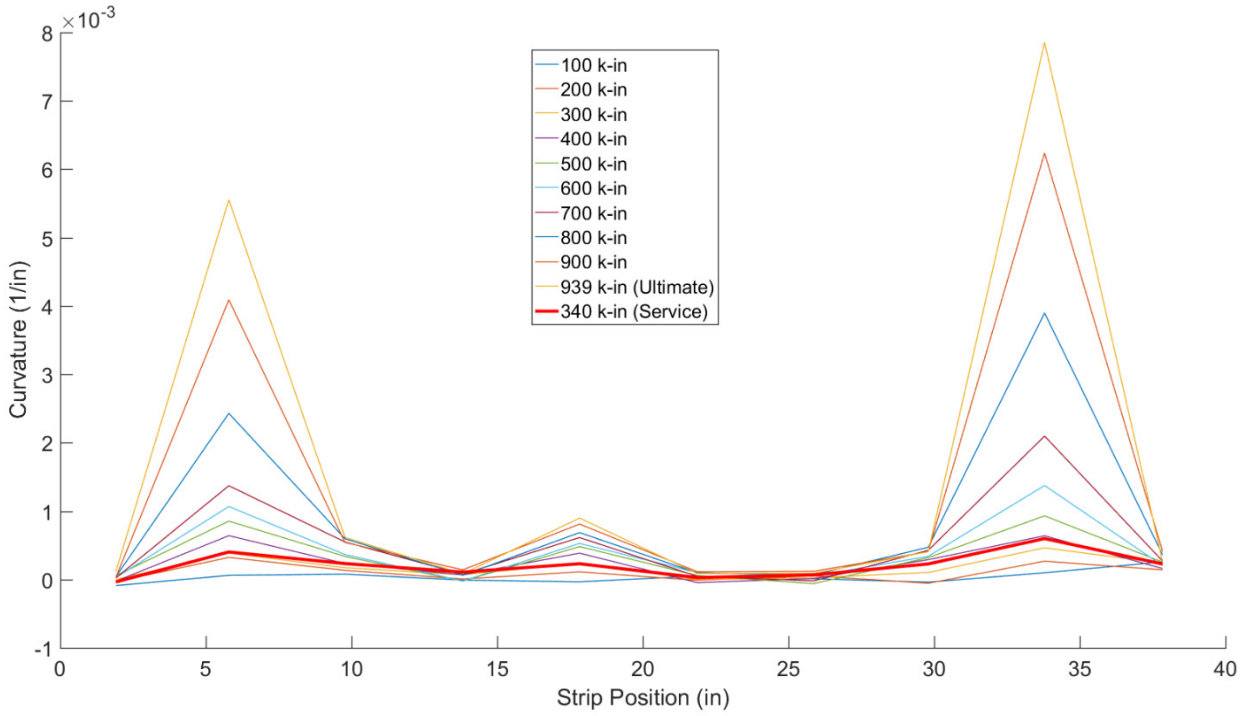

Figure 7.26 - Specimen 1 curvatures at different levels of moment throughout the ultimate test.

Cracks were mapped at the conclusion of the ultimate test showing where damage and cracks were localized in the specimen (Figure 7.27). The specimen ultimately failed in compression at the termination of the Stage 1 transverse bars. Two large cracks formed at this location. The other major crack occurred at the longitudinal construction joint. The joint opened up considerably and a diagonal crack extended from the shear key. Comparing the crack map to the specimen curvatures in Figure 7.26, the two points of localized curvature coincide with the largest cracks in the specimen, as expected. This increase in curvature at the ends of the splice becomes pronounced at loads that are much less than ultimate. It is possible that over time, repeated cycles of extremely heavy vehicles may produce sufficiently large rotations and curvatures to degrade the longitudinal construction joint region before the rest of the deck.

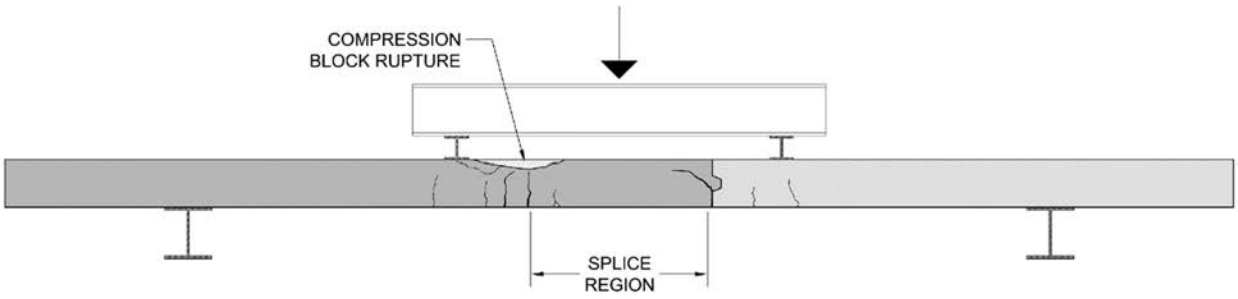

Figure 7.27 - Crack map for Specimen 1 ultimate flexural test.

In summary, because the specimen experienced a flexure-compression failure after substantial yielding of the reinforcement, the provided development length of 48 bar diameters was adequate, even though the measured yield stress of the reinforcement was 81 ksi. It may thus be concluded that the concrete-bar bond was not affected sufficiently (if at all) to reduce the flexural capacity of the section. Because results were not compared with those from an identical specimen constructed while isolated from displacements during concrete, it is impossible to say if the concrete-bar bond was completely unaffected. Localized rotations were observed at the ends of the spliced reinforcement, with the largest rotations occurring at the construction joint. Over time, it is possible that this could lead to degradation of the construction joint, although it is believed that such large deformation demands are unlikely during the life of the structure. The only defect that was definitively caused by displacements during curing was the hairline flexural crack above the steel support beam. Apart from this, the overall structural integrity of Specimen 1 was unaffected by the applied displacement protocol during curing of the Stage 2 deck.

7.3 Specimen 2 Test

7.3.1 Description

The second specimen incorporated all of the same details as the first specimen, and was constructed in exactly the same way. The main difference with Specimen 1 was the amplitude of simulated traffic-induced displacements applied during the Stage 2 deck pour simulation.

Specimen 2 utilized the second displacement protocol, with maximum downwards displacement of 0.125 in. applied every four minutes and smaller downwards displacements of 0.05 in. applied intermittently every 20 seconds. These displacements were run for 12 hours after casting of the specimen. The displacement protocol was restarted approximately 24 hours after casting of the Stage 2 deck, and lasted for about one hour.

Seven days after the Stage 2 deck pour, the concrete had surpassed the specified strength of 4000 psi and the ultimate strength test was performed. For this test, the actuator was programmed to use displacement control at a rate of 0.1 in. downward displacement per minute. Specimen 2 also eventually experienced a flexure-compression failure of the concrete, though the failure was located at the termination of the lap splice next to the staged construction joint, instead of at the end of the splice away from the construction joint.

While transferring the specimen from the Stage 2 casting position to the ultimate testing position, a laboratory mishap led to one of the steel bolt shear connectors (located at Girder Line 4 in Figure 7.3) being pulled out of the concrete, leaving a sizeable void in the bottom of the specimen. This defect was centered 35 in. away from the end of the lap splice region, far enough that it was assumed to have no impact on the concrete in the longitudinal joint region. To ensure that this did not compromise the overall strength of the specimen, the void was filled with high strength grout as seen in Figure 7.28. At the time of the ultimate test, the strength of the grout was 7910 psi, which was considerably larger than that of the surrounding concrete. After the ultimate test, the repair area was inspected for any damage. None was found, so it was believed that this repair did not affect the overall behavior of the specimen.

Figure 7.28 - High strength grout repair patch where a shear connector had accidentally been pulled from the underside of the specimen.

7.3.2 Results

Visual inspection of the specimen after curing revealed a single hairline crack at the top of the Stage 2 segment. This crack was in the exact same location as the one seen in Specimen 1, directly above the steel support beam closest to the construction joint (Figure 7.3, Girder Line 4). The crack, shown in Figure 7.29, was again determined to be a flexural crack from negative bending over this support during curing of the concrete. No other damage was visible in the specimen after the Stage 2 pour.

Figure 7.29 - Flexural crack resulting from deflections applied during curing of Stage 2 segment.

Specimen 2 also utilized concrete that had a 28-day compressive strength considerably larger than the specified strength of 4000 psi. The concrete used in the Stage 1 portion of this specimen was from the same batch as the concrete used in Stage 2 portion of Specimen 1, and had an average compressive strength of 6540 psi the day of the Stage 2 pour for Specimen 2. Concrete used for the Stage 2 pour in Specimen 2 reached an average strength of 4210 psi after 3 days, and had a 28-day compressive strength of 6290 psi. The strength gain of the concrete was monitored so that the ultimate test could be conducted when the compressive strength of the Stage 2 concrete was similar to that for Specimen 1. The ultimate test for Specimen 2 was performed seven days

after casting of the Stage 2 portion, when the accompanying concrete cylinders had an average strength of approximately 5480 psi.

The ultimate test load-displacement response for Specimen 2 is shown in Figure 7.30. The peak load for this specimen was 42.1 kips, which corresponds to an ultimate moment capacity of 958 kip-in. (excluding the moment due to the specimen self weight). This peak load was slightly larger than that of Specimen 1, even though the applied displacements during curing were more severe. The specimen eventually failed in flexure-compression after substantial flexural yielding, which again is a sign that the bar splices behaved adequately. The compressed concrete split apart at a location directly above the termination of the Stage 2 bars at the staged construction joint (see Figure 7.31).

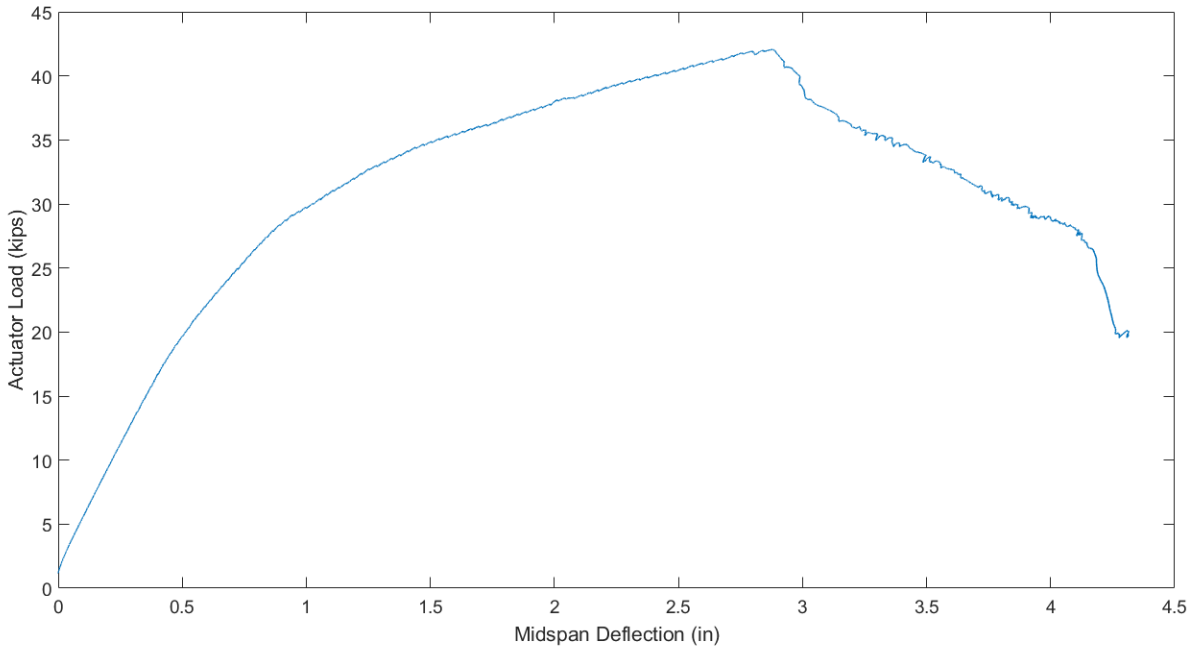

Figure 7.30 - Actuator load versus specimen mid-span deflection response for ultimate test of Specimen 2.

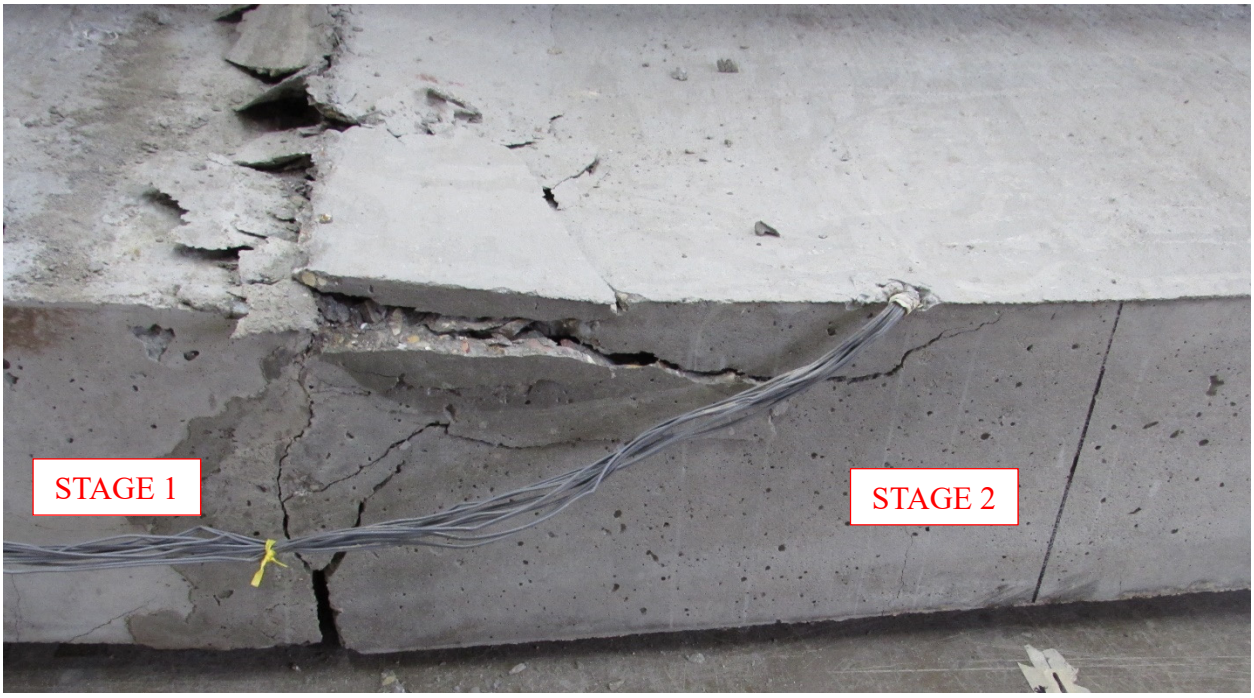

Figure 7.31 - Specimen 2 compression block failure at construction joint.

Using the strain data collected during the ultimate test and the steel bar stress-strain model outlined in Section 7.1.8.2, forces in the steel bars and average bond stresses were calculated as described previously for the first specimen.

Average bond stress versus specimen deflection is plotted in Figure 7.32 and Figure 7.33 for two bars that were spliced together. These were #5 bars in the bottom layer of transverse reinforcement. The dashed lines depict the point at which the strain gauge at the continuous end of the splice was determined to reach the yield strain of the bar. The plots of average bond stress for the two spliced bars show behavior similar to each other. Both bars in the splice had a relatively constant and uniform increase in bond stress along their length up to the yield point. After yield, the average bond stress in Segment 1 continued to increase while the average bond stress in Segment 2, where yielding had already occurred, decreased slightly.

Average bond stress versus applied moment is plotted in Figure 7.34 and Figure 7.35 for the same two #5 bottom bars that were spliced together. As for Specimen 1, the effect of self-

weight of the specimen is not considered. Again, the dashed lines depict the point at which the strain gauge at the continuous end of the splice was determined to reach the bar yield strain. Once yielding occurred, the applied moment continued to increase even though the instrumented bars were within the yield plateau. This was possibly due to all five transverse bars not yielding simultaneously, or some bars being strained within the strain range of the yield plateau while others had already begun strain hardening.

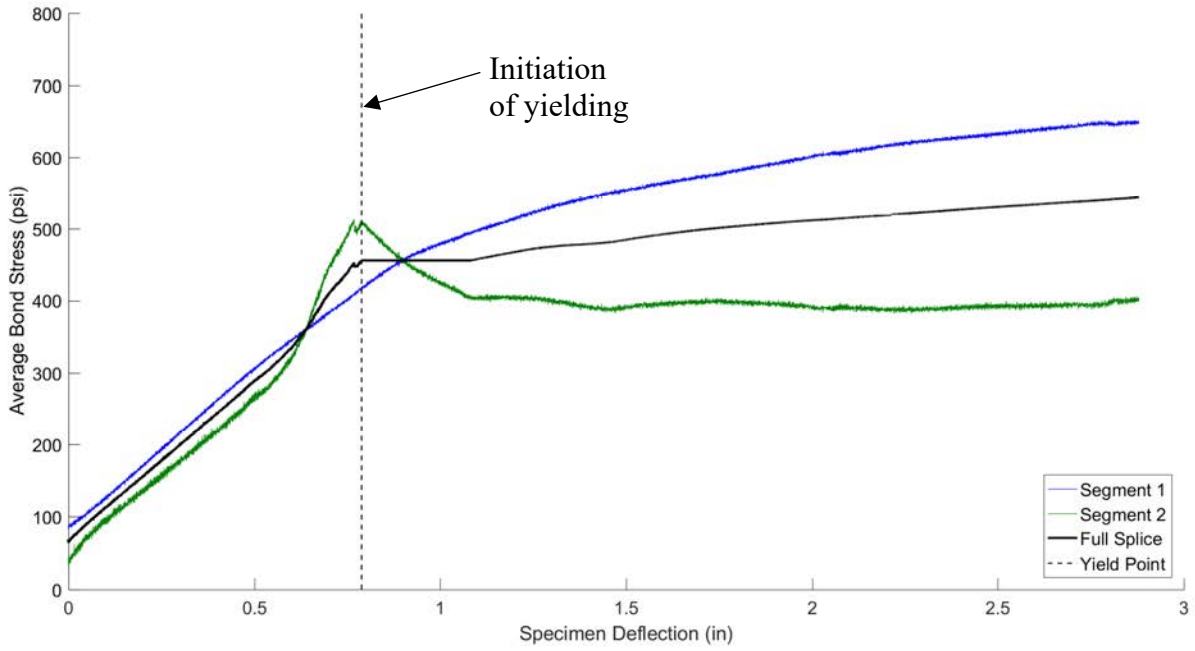

Figure 7.32 – Specimen 2 average bond stress versus specimen deflection for spliced Stage 1 bottom transverse bars.

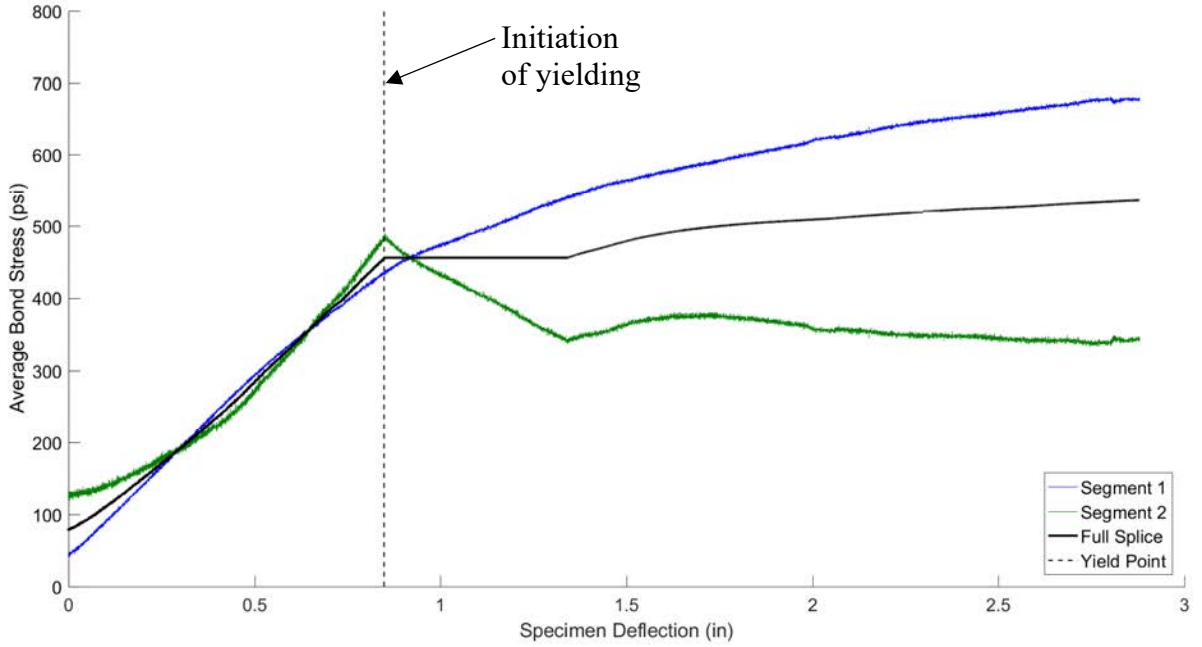

Figure 7.33 – Specimen 2 average bond stress versus specimen deflection for spliced Stage 2 bottom transverse bars.

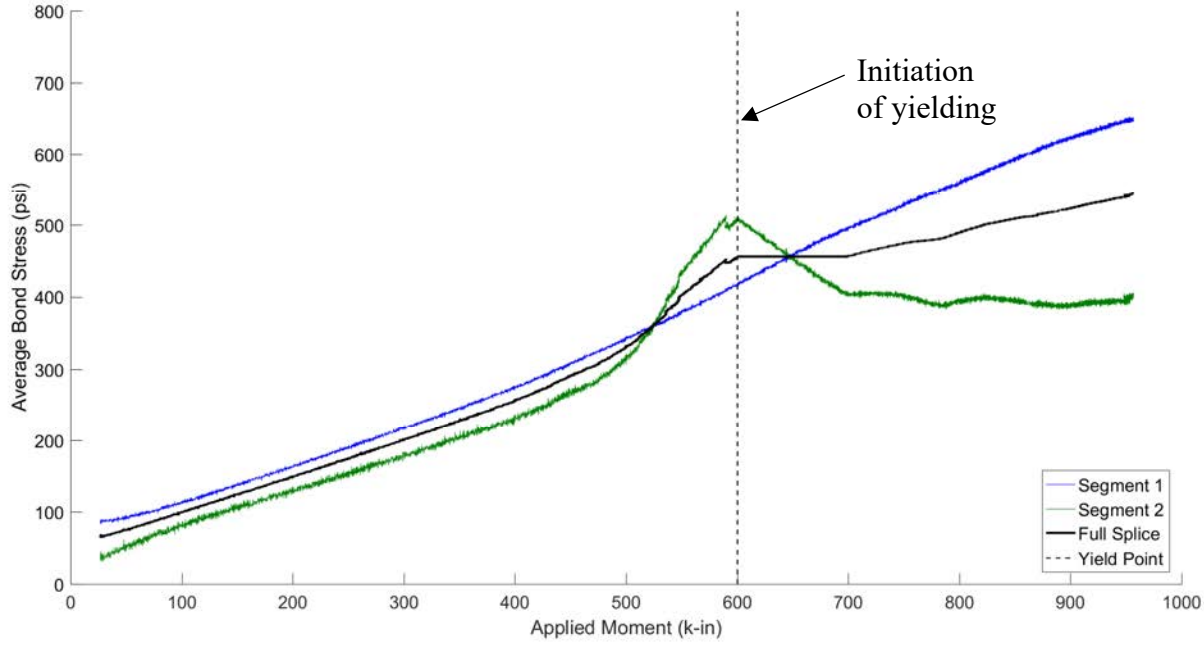

Figure 7.34 – Specimen 2 average bond stress versus applied moment for spliced Stage 1 bottom transverse bars.

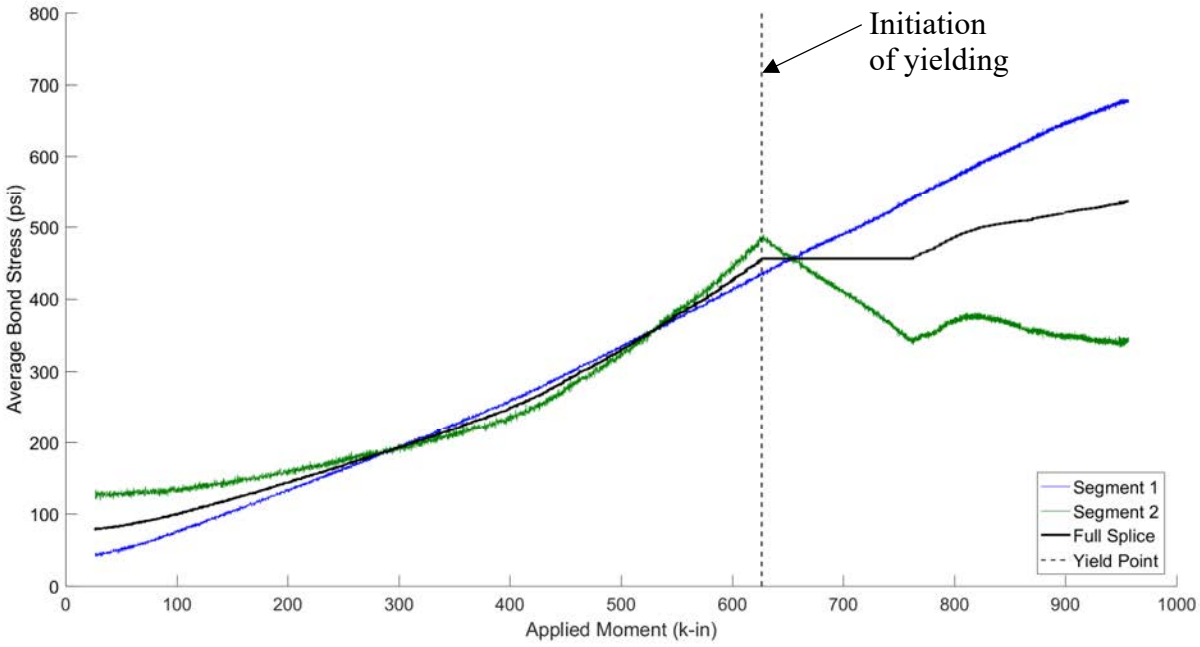

Figure 7.35 – Specimen 2 average bond stress versus applied moment for spliced Stage 2 bottom transverse bars.

The maximum average bond stress during the ultimate test for the four instrumented transverse bars in the bottom layer of reinforcement is tabulated in Table 7.4. Similar to the first specimen, the values of maximum average bond stress for the different splice segments are reasonably consistent throughout all spliced bars. Recall that to develop a yield stress of 81 ksi over a length of 27.75 in., an average bond stress of 456 psi is required. Again, in all bars, the maximum average bond stress over the full splice segment was greater than 456 psi, meaning that all spliced bars began strain hardening before the specimen ultimately failed in compression.

Table 7.4 – Specimen 2 average bond stress at first yielding of spliced transverse bottom bars

	Stage 1 - Bar 1	Stage 2 - Bar 1	Stage 1 – Bar 2	Stage 2 – Bar 2
Segment 1	645 psi	746 psi	670 psi	791 psi
Segment 2	523 psi	438 psi	443 psi	460 psi
Full Splice	544 psi	536 psi	560 psi	567 psi

As discussed in Section 7.2.2, the required splice length according to AASHTO (AASHTO 2012) is 29.6 in. for a Class C splice. Data from the strain gauges showed that the 30-in. Class C lap splice provided in this specimen was capable of developing a stress differential greater than the 81 ksi yield stress in all spliced bars. As discussed earlier, the specimen ultimately failed in flexural compression. It was therefore concluded that a Class C lap splice (30-in. long, 48 bar diameters) was sufficient for the specimen to develop its flexural capacity, even when subjected to the second, larger displacement protocol during curing.

Specimen displacements were recorded using data from the Optotrak® position tracking system. The marker grid shown in Figure 7.8 allowed the deflected shape and average curvatures of the specimen lap splice region to be calculated throughout the test. The deflected shape is plotted at increasing levels of moment throughout the ultimate strength test, as shown in Figure 7.31. Similar to the behavior of Specimen 1, at higher levels of moment, points of localized rotation became visible. Again, the most pronounced point (at a marker position of approximately 48 in.) coincided with the location of the construction joint. Localized rotation was also seen, although to a lesser degree, at a marker position of 20 in., which corresponded to the location of the termination of the Stage 1 transverse reinforcement.

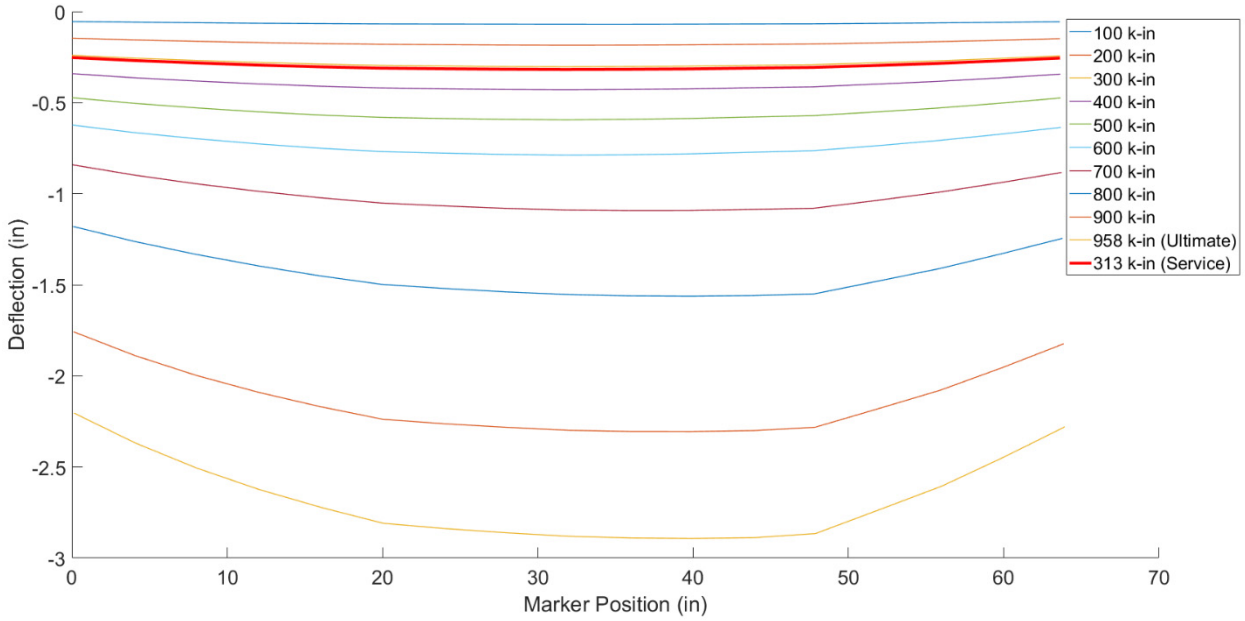

Figure 7.36 - Specimen 2 deflected shape plotted at different levels of moment throughout the ultimate test.

Specimen average curvatures in the lap splice region were calculated using the Optotrak® markers and the method described in Section 7.2.2. Curvatures along the lap splice region are plotted at different levels of moment in Figure 7.32. Again, there were two distinct locations with localized curvatures. The largest curvatures were concentrated at the construction joint, coinciding with the marker strip positioned at 50 in. The marker strip positioned at 18 in. encompassed the region where the Stage 1 transverse bars terminate. Similar to the response of Specimen 1, the curvatures were almost completely localized at the two ends of the splice. Throughout the test, the curvatures at the splice end near the construction joint were approximately 2.0 times that at the other end of the splice. The locations of localized curvature became clearly defined at moments larger than 400 k-in.

The deflected shape and curvature distribution in the lap splice region were again analyzed under assumed service conditions to determine if localized rotations and curvatures could potentially result in localized damage over the life of the bridge deck. As with Specimen 1, the

service load was assumed to correspond with a maximum stress in the steel reinforcement of $0.6f_y$, or 36 ksi based on a nominal yield strength of 60 ksi. During the ultimate test of Specimen 2, a stress of 36 ksi was reached at the continuous end of the spliced bars at a moment of approximately 310 k-in. As before, the deflected shape and curvature distribution under this assumed service load is represented by the thick red line plotted in Figure 7.36 and Figure 7.37, respectively. These figures show that under the assumed service load, the points of localized rotation and curvature are not well defined. The curvature distribution is nearly uniform in the lap splice region and localized curvatures at the ends of the splice are barely visible. Therefore, it appears that the magnitude of differential deflections applied in this test during curing of the Stage 2 deck has minimal influence on the integrity of the longitudinal joint region under service conditions. Additionally, repeated cycles of deformation large enough to produce localized damage at the ends of the lap splice are unlikely to occur under normal service conditions.

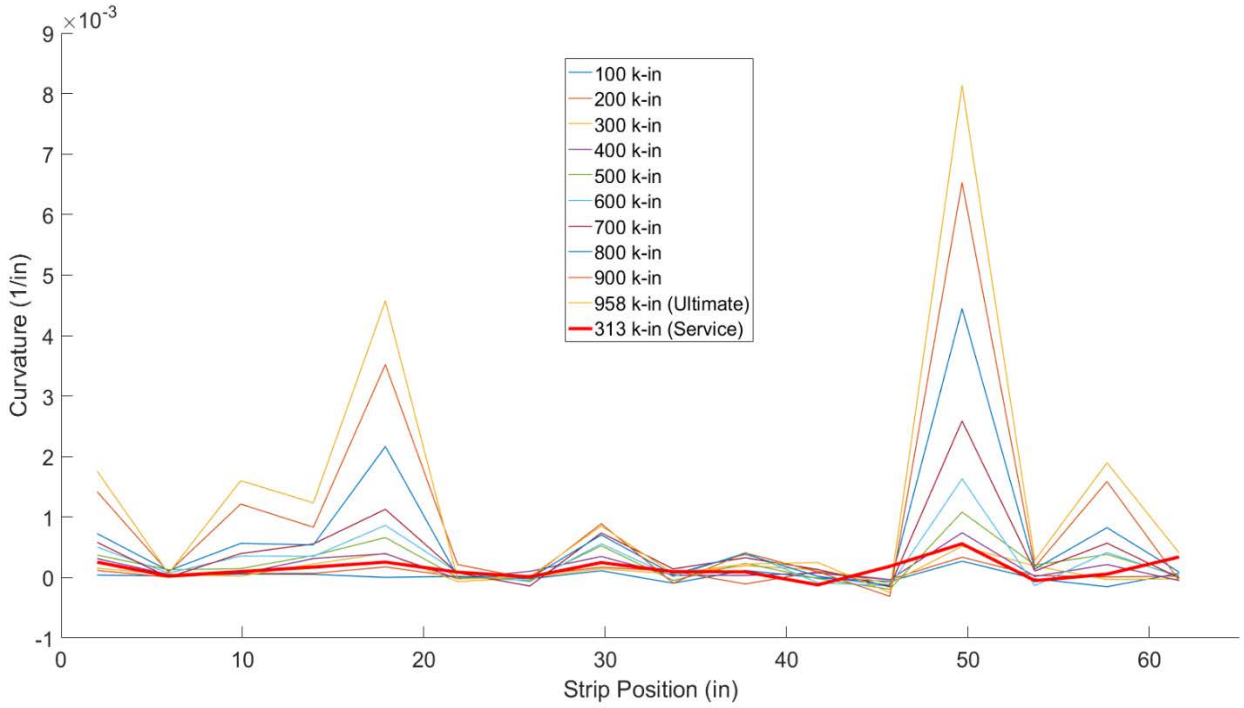

Figure 7.37 – Specimen 2 curvatures at different levels of moment throughout the ultimate test.

Cracks were mapped at the conclusion of the ultimate test showing where damage and cracks occurred in the specimen (Figure 7.38). The specimen ultimately failed in flexure-compression at the longitudinal construction joint. The largest crack occurred at this location with the construction joint opening considerably. The other major crack occurred at the termination of the Stage 1 transverse bars. Comparing the crack map to the specimen curvatures in Figure 7.37, the two points of localized curvature coincided with the largest cracks in the specimen. It is possible that some of the crack width at these locations may have been due to slippage of bars along the splice.

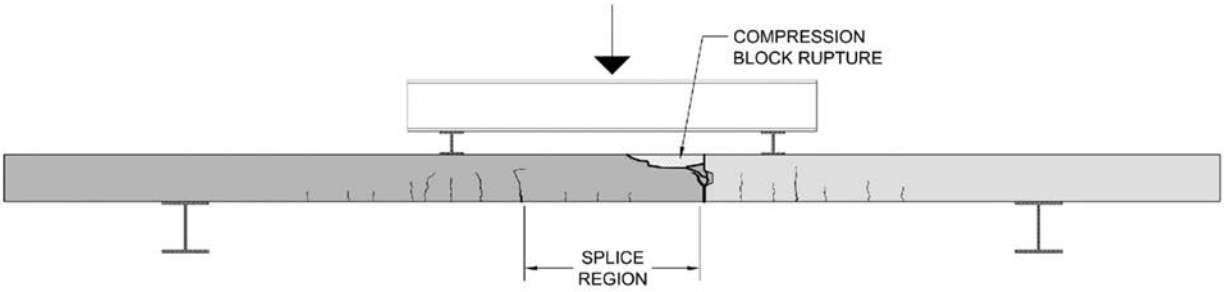

Figure 7.38 - Crack map for Specimen 2 ultimate flexural test.

After the conclusion of the ultimate test, the split compressed concrete allowed the cover concrete to the top spliced reinforcement to be easily removed, as shown in Figure 7.39. This allowed for the visual examination of the imprints left in the concrete by the reinforcing bars. It was noted that in all five splices the Stage 2 transverse reinforcement left a clearly defined, shiny imprint in the concrete, while the Stage 1 transverse bars left a slightly more disturbed and dull imprint, as seen in Figure 7.40. While there was no quantitative way to confirm this, the difference in bar imprints does suggest that the Stage 1 reinforcement experienced movement relative to the concrete during curing, causing this muddled bar imprint.

Similar to the first specimen, the reinforcement yielded in the spliced region. It is thus concluded that the concrete-bar bond was not affected enough to reduce the flexural capacity of

the section. When comparing results with those from the first specimen, there were almost no differences between the two. In both specimens, the only damage that was definitively caused by displacements during curing was the hairline flexural crack above the steel support beam.

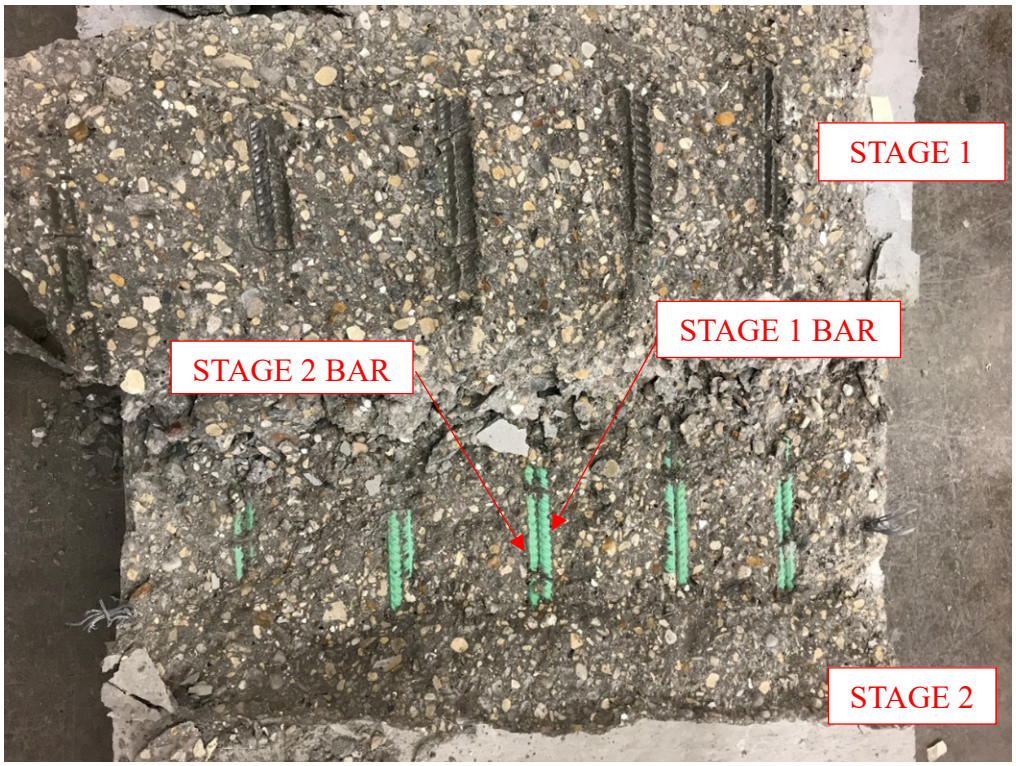

Figure 7.39 - Bar imprints were examined after removing the cover to the top spliced transverse reinforcement.

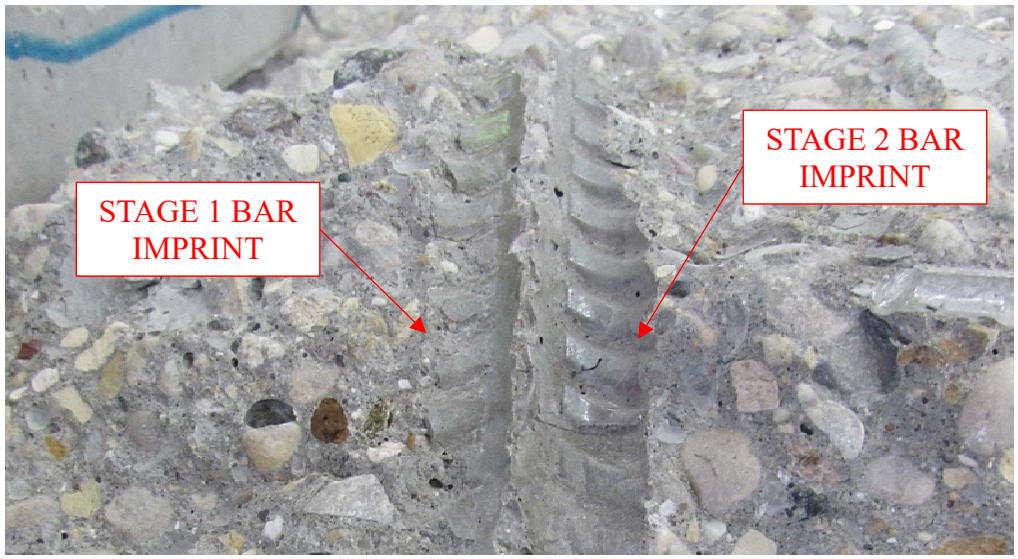

Figure 7.40 - Stage 1 spliced transverse bar imprint (left) is slightly muddled while the Stage 2 spliced transverse bar imprint (right) is clearly defined.

7.4 Leakage Tests

Leakage tests were also conducted to evaluate the effect of surface joint treatment on joint leakage. Four pair of specimens were tested. Each specimen consisted of a 24 in. x 12 in. x 4 in. concrete prism, representing a 12 in. wide joint strip. The specimens were constructed in two stages, simulating a bridge-deck staged construction, with a joint at mid-length of the specimens. A #3 reinforcing bar ran along the specimen length, located in the center of the specimen cross section, simulating dowel reinforcement used in real construction. A sketch of a joint specimen is shown in Figure 7.41.

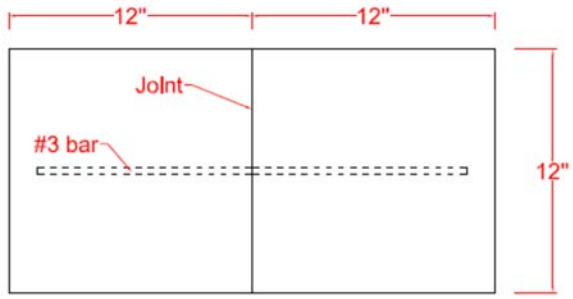

Plan view of joint specimen

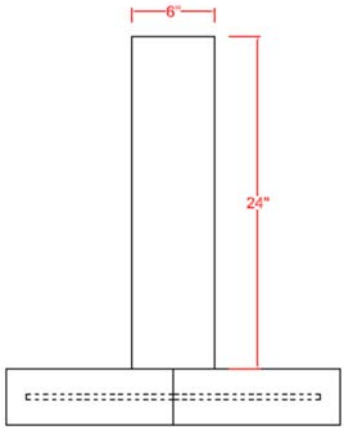

Side view of joint specimen, including PVC pipe

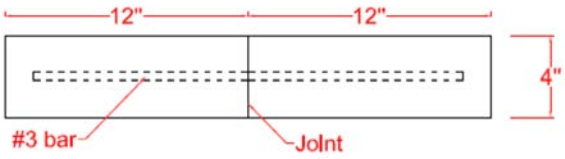

Side view of joint specimen

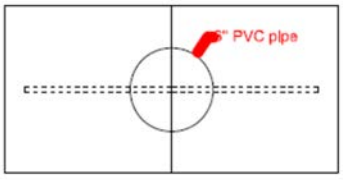

Plan view of joint specimen, including PVC pipe

Figure 7.41 - Joint specimens for leakage tests

For ease of construction, the specimens were cast in a vertical position. For the specimens with surface treatment, immediately after the first-stage concrete was cast, a concrete retarder for

exposed aggregate surface (Type S, manufactured by Euclid Chemical) was applied to the surface. It should be mentioned that the use of a surface retarder for preparation of bonded joints is referred to in Section 503.09(b) of the Illinois Department of Transportation *Standard Specifications for Road and Bridge Construction* (2016). Twelve hours after application of the concrete retarder, high-pressure water was injected to the treated surface to remove surface paste and expose the course aggregate. Figure 7.42 shows a comparison of an untreated versus a treated surface, while a closeup of a treated surface is shown in Figure 7.43.

The specimens were cast in two pairs, one with and one without surface treatment, and were constructed in two phases, the second phase 3 and 4 days after casting of the first phase for the first two pairs and last two pairs, respectively. Table 7.5 lists the cylinder compressive strength for each pair of specimens at the beginning of the leakage test.

Table 7.4 – Cylinder compressive strength at beginning of leakage tests

	Pair 1	**Pair 2**	**Pair 3**	**Page 4**
Phase 1	6400 psi	6400 psi	5300 psi	5300 psi
Phase 2	4400 psi	4400 psi	5000 psi	5000 psi

Figure 7.42 – Treated (left) versus untreated (right) joint surface

Figure 7.43 – Condition of treated joint surface

After the concrete used for both stages had gained sufficient compressive strength (at least 4000 psi), the top specimen surface, excluding the longitudinal joint, was sealed with epoxy to

ensure that water would only flow through the joint. Also, for Pairs 3 and 4, the top surface of the joint was ground over a depth of about 0.25 in. to ensure any concrete from the second phase covering the joint was removed and the joint was fully exposed (Figure 7.44). A 6-in. diameter, 24-in. long PVC pipe was then placed at the center of the specimen, with its base epoxy-glued to the concrete surface to prevent water leakage through the pipe-concrete interface (see Figure 7.45). Each specimen was then subjected to an 18-in. high water head, with the top surface of the pipe sealed to prevent water evaporation. Change in water head was then measured over time for comparison in leakage rate between untreated and treated joint specimens. It should be mentioned that change in water head over time is used to evaluate leakage in water containment structures (e.g., water tanks), as documented in the *Specification for Tightness Testing of Environmental Engineering Concrete Containment Structures (ACI 350.1-10 and Commentary).*

Figure 7.44 – Joint surface prior to (left) and after (right) grinding

Figure 7.45 – Joint leakage specimen prior to being subjected to a water head

For the first two pairs of specimens, one of the two specimens with an untreated joint was not capable of holding the water as it leaked through the glue joining the PVC pipe and the concrete surface. For the last two pairs of specimens, the pair without surface treatment could not hold the water. The same occurred for one of the two specimens with joint surface treatment. Thus, data are only available for four specimens (one without and three with treated joint surface). Drop water measurements for these specimens are shown in Table 7.5. As can be seen, drop in water head after 7 days was the same (1/8 in.) in three out of the four specimens that held the water (two with

joint treatment and one without). In the other specimen (with joint treatment), the drop in water head after 7 days was 3/8 in.

Given the limited data, a definite conclusion with regard to the ability of the joint surface treatment to reduce joint water leakage cannot be drawn. However, the fact that for the last two pairs of specimens, for which the joint was exposed through grinding, the two specimens without joint treatment were not capable of holding the water suggest that the applied surface treatment does have potential to reduce water leakage or, at least, it would not be detrimental to the performance of the joint.

Table 7.5 – Drop in water head for leakage test specimens

Specimen	3 days	7 days
Specimen 1, Pair 1 (without treatment)	-	1/8 in.
Specimen 1, Pair 2 (with treatment)	-	1/8 in.
Specimen 2, Pair 2 (with treatment)	-	3/8 in.
Specimen 1, Pair 4 (with treatment)	1/16 in.	1/8 in.

7.5 Conclusions

Laboratory testing of specimens constructed using a simulated staged construction process showed no evidence of an unacceptably degraded bond between the concrete and the spliced steel reinforcement in the construction joint region. While visual inspection of the bar imprints in the concrete showed that some relative movement did occur, its effect, if any, was negligible and both specimens ultimately experienced a flexural failure with crushing of the concrete compression zone after yielding of the tension reinforcement. Test results thus indicate that differential

deflections of up to 0.125 in. downward or 0.175 in. total movement do not significantly impact the integrity of the concrete-bar bond in spliced reinforcement. 48 bar diameter lap splices were used in both laboratory specimens and were proven to be sufficient in developing the full strength of the reinforcement even when subjected to traffic-induced displacements during concrete curing. For concrete bridge decks constructed in stages, it is therefore recommended to splice transverse reinforcement 50 bar diameters at the longitudinal construction joint.

An analysis of specimen deflections, curvatures and crack patterns in the lap splice region showed that when tested to ultimate, damage was localized at the two ends of the spliced reinforcement. Specimen 1 failed at the section where the Stage 1 transverse bars terminated and Specimen 2 failed at the section where the Stage 2 transverse bars terminated. It was determined that rotations tend to concentrate mostly at the longitudinal construction joint where a discontinuity exists. However, under service conditions (defined by a maximum tensile stress in the reinforcement of $0.6f_y$ = 36 ksi), localized rotations were practically nonexistent and would therefore be unlikely to cause damage in the construction joint region. While improbable, however, repeated loading from extremely heavy vehicles could result in deformations large enough to cause localized damage to occur in the lap splice region. Leakage, corrosion and spalling could result if the integrity and continuity of the construction joint becomes compromised.

The one defect that could be identified as having been caused by differential deflections was a hairline longitudinal crack directly over the Stage 2 support adjacent to the staged construction joint. The geometry and support conditions of the test setup used may have caused this cracking to occur at smaller displacements than would be required to cause the same type of cracking in a real bridge. Nonetheless, cracking in this location is a possible consequence of differential displacements during concrete curing.

Results from the water leakage tests proved inconclusive in terms of the ability of the applied joint surface treatment to reduce water leakage through the joint. However, the fact that for the last two pairs of specimens, for which the joint was exposed through grinding, the two specimens without joint treatment were not capable of holding the water suggest that the applied surface treatment does have potential to reduce water leakage or, at least, it would not be detrimental to the performance of the joint.

Chapter 8: Summary & Conclusions

8.1 Conclusions and Recommendations

Through a variety of methods, this research has sought to establish to what degree concrete bridge decks are compromised when a staged construction process is used and curing occurs in the presence of live traffic loads. A review of previous research, a survey of transportation officials, field inspections of bridge decks constructed in stages, field monitoring of deflections during staged construction, finite element modeling of existing structures, and laboratory testing of representative specimens has provided the basis for several conclusions and recommendations.

It was commonly stated in the reviewed literature and by the respondents of the survey that the most effective way to reduce the impact of differential deflections induced by traffic on curing concrete bridge decks is to minimize the impact of heavy vehicles. When heavy trucks cannot be restricted from using the bridge entirely, it is most effective to move them as far away from the curing deck as possible. This was confirmed in the finite element modeling of bridge B-70-177. Another important consideration in reducing the impact of traffic on curing concrete decks is the smoothness of the riding surface. This appears to be often overlooked, but previous research suggests providing a smooth surface is one of the most effective ways to reduce bridge differential deflections and vibrations during staged construction.

From field inspections of staged-constructed bridge decks, it was concluded that the majority of bridges show no adverse effects from live loading on the bridge during staged construction, through some deterioration may be caused by the staged construction process and presence of the longitudinal joint. Deck-on-girder bridges were for the most part in good condition. The one defect that was commonly found in staged construction bridges was underconsolidation of the concrete in the longitudinal construction joint region. Additional steel reinforcement and

shear keys often present in these regions make the moderate-slump concrete more difficult to consolidate properly. Where lap splices or shear keys exist, extra effort should be made to ensure that concrete is properly consolidated. Alternatively, using one-piece mechanical splicers will reduce congestion in these areas and make proper consolidation of the concrete easier.

The inspection of eight haunched slab bridges exhibited longitudinal construction joints that were in very poor condition. While it was impossible to determine the exact cause for their deterioration, the use of staged construction and the resulting presence of longitudinal construction joints are believed to be major factors in the deterioration of these bridges. It is reasonable to suggest that flat slab and haunched slab bridges are more susceptible to damage from differential deflections during staged construction if the necessary precautions are not taken. If shoring is not provided under the portion of the bridge that is open to traffic, all the vertical displacement will translate into differential deflections in the spliced reinforcement region in the curing concrete. It is therefore recommended to provide shoring under the entire bridge throughout construction of slab bridges, though this would likely necessitate other changes to the design of the shoring to support the live traffic loading. The researchers do not recommend the use of staged construction for slab or haunched slab bridges. Should staged construction become necessary, then heavy live traffic should be prevented during construction.

Differential deflections were measured in two prestressed concrete girder bridges during staged construction. Results from this field monitoring showed that the magnitudes of differential deflections in bridges of this type are very small. Finite element models of the same two bridges reinforced the conclusion that differential deflections in short-to-medium-span prestressed concrete girder bridges are extremely small and are highly unlikely to adversely affect the integrity of the deck.

Finite element modeling of a longer, steel plate-girder bridge showed that differential deflections can become considerably larger as the span length increases. This is especially true if more than one traffic lane is maintained during staged construction. If this is the case, it is recommended to close the lane(s) closest to the curing deck for at least 24 hours. At the very least, truck traffic should be restricted to the lane furthest from the curing deck for the same amount of time. Further analyses of long-span bridges should be performed to determine how much span-length and girder configuration influences the magnitude of differential deflections.

Two laboratory specimens were constructed using a simulated staged construction process and were subjected to different magnitudes of differential deflections during curing of the Stage 2 segment. After being subjected to an ultimate flexural strength test, it was concluded that the overall strength of both specimens was unaffected by differential displacements applied during Stage 2 curing. Differential deflections up to 0.125 in. downward or 0.175 in. total movement did not appreciably impact the integrity of the concrete-bar bond in spliced reinforcement. Forty eight-bar diameter lap splices were used in both laboratory specimens. This splice length was proven to be sufficient in developing the yield strength of the reinforcement when subjected to traffic-induced displacements during concrete curing. For concrete bridge decks constructed in stages, it is therefore recommended to splice transverse reinforcement at least 48 bar diameters at the longitudinal construction joint for #5 bars or smaller.

An analysis of deformations in the lap splice region showed localized rotations at the ends of the splice under bending. However, these localized deformations were practically nonexistent under assumed service loading conditions. It is therefore unlikely that damage in the construction joint region will result from normal service loading. However, exceptionally large vehicle loads could result in deformations large enough to cause localized damage to occur in the lap splice

region. Laboratory testing also showed that differential deflections during curing of concrete decks can cause longitudinal cracking of the curing deck over the girder closest to the staged construction joint.

The results from leakage tests were inconclusive with regard to the ability of joint surface treatment using a concrete retarder to reduce leakage through the joint. However, only one out of four specimens without joint treatment could hold the water head (i.e., water in other three specimens ran through the joint in a matter of seconds), while three out of four specimens with joint treatment held the water over time, suggesting that the applied surface treatment does have potential to reduce water leakage or, at least, it would not be detrimental to the performance of the joint.

8.2 Recommendations for Future Work

While this research has provided insight on several important aspects and consequences of staged bridge construction, it has also uncovered additional areas where further research may be required.

To effectively conclude if maintaining traffic during staged construction causes deterioration of bridge decks, inspections should be performed immediately and routinely after completion of construction. Defects directly resulting from the construction process should be present shortly after construction, so inspecting bridges immediately after construction would allow these potential defects to be differentiated from those occurring due to regular use of the bridge once it is in service.

The field monitoring of deflections during staged construction performed in this investigation did not allow the evaluation of reductions in differential displacement as the Stage 2

concrete gained stiffness. This was mainly due to the randomness of the traffic events during the field monitoring. To accurately measure the reduction in differential displacement as the Stage 2 deck hardens, deflections due to a control truck of known weight should be measured at specific times after the completion of concrete placement.

The most common defect noted in the field was underconsolidation of concrete at the longitudinal joint. This could be prevented through tighter control in bottom concrete cover during construction, or by increasing the minimum concrete cover. Future work could also focus on recommending details or procedures that aid in consolidation in this region.

The results from finite element analyses that were performed as part of this research suggested that differential deflections may vary considerably depending on span length, girder configuration, and position and number of traffic lanes. Additional modeling of prestressed concrete and steel girder staged construction bridges with varying span lengths and traffic patterns could provide insight on how these factors influence differential deflection magnitude. Additionally, finite element models of flat slab and haunched slab bridges could be helpful in estimating differential deflections in these types of bridges when unshored construction is used.

The laboratory tests performed as part of this research showed that bond strength of lap spliced reinforcement was adequate to develop the bars, even when subjected to differential displacements up to 0.125 in. during curing. It would be interesting to see how different reinforcement details such as different bar sizes, splice lengths, dowel bar splicers, bar couplers, and no shear keys affect the performance of the longitudinal joint. It would also be useful to establish at what level of differential displacement the bond between concrete and reinforcement begins to degrade considerably and compromise the strength of the section.

The use of closure strips was not investigated as part of the laboratory experiments. Testing similar specimens that utilize closure strips could provide insight into whether this practice improves or compromises the overall strength and/or durability of bridge decks.

While the laboratory experiment portion of this research focused mostly on short-term damage resulting from the construction process, the possibility of long-term degradation is equally important. Further investigation should be performed focusing on degradation of the longitudinal joint region due to long-term leakage and corrosion, and the possibility of increased permeability through the joint if live loads are present during construction. Further research may also investigate the efficacy of the surface retarder or other longitudinal construction joint details on long-term degradation of the joint.

References

AASHTO. (2012). *"AASHTO LRFD Bridge Design Specifications."* American Association of State Highway Transportation Officials, Washington, DC.

ACI Committee 209. (1992). *"ACI 209R-92 Prediction of Creep, Shrinkage, and Temperature Effects in Cocrete Structures."* American Concrete Institute, Detroit, MI.

ACI Committee 345. (2013). *"Guide for Widening Highway Bridges."* American Concrete Institute, Farmington Hills, MI.

Andrews, T. K. (2013). *"Effect of Differential Movement of Straight Reinforcing Bars During Early Age Curing on the Bond Strength."* M.S. Thesis, Clemson University.

Arnold, C. J. (1966). *"Deck Rippling on Various Michigan Bridges - Third Progress Report. Research Report No. R-608."* Michigan Department of State Highways, Lansing, MI.

Deaver, R. W. (1982). *"Bridge Widening Study."* Georgia Department of Transportation, Forest Park, GA.

Fu, C. C., Zhao, G., Ye, Y., and Zhang, F. (2015). *" Serviceability - Related Issues for Bridge Live Load Deflection and Construction Closure Pours."* University of Maryland, College Park, MD.

Furr, H. L., and Fouad, F. H. (1981). *"Bridge Slab Concrete Placed Adjacent to Moving Live Loads."* Report No. FHWA/TX-81/11+266-1F, The Texas A&M University System, Texas Transportation Institute, College Station, TX.

Harsh, S., and Darwin, D. (1984). *"Effects of Traffic Induced Vibrations on Bridge Deck Repairs."* M.S. Thesis, University of Kansas, Lawrence, KS.

Harsh, S., and Darwin, D. (1986). "Traffic-Induced Vibrations and Bridge Deck Repairs." *Concrete International,* May, 36-42.

Issa, M. A. (1999). "Investigation of Cracking in Concrete Bridge Decks at Early Ages." *Journal of Bridge Engineering*, May, 116-124.

Illinois Department of Transportation. (2016). *"Standard Specifications for Road and Bridge Construction."* Adopted April 01, 2016.

Manning, D. G. (1981). *"Effects of Traffic-Induced Vibrations on Bridge-Deck Repairs."* National Cooperative Highway Research Program, Washington, D.C.

Montero, A. C. (1980). *"Effect of Maintaining Traffic During Widening of Bridge Decks (A Case Study)."* The Ohio State University, Columbus, Ohio.

Ng, P., and Kwan, A. (2007a). "Effects of Traffic Vibration on Curing Concrete Stitch: Part I - Test Mothod and Control Program." *Engineering Structures,* 29, 2871-2880.

Ng, P., and Kwan, A. (2007b). "Effects of Traffic Vibration on Curing Concrete Stitch: Part II - Cracking, Debonding and Strength Reduction." *Engineering Structures,* 29, 2881-2892.

Oehler, L. T., and Cudney, G. R. (1966). *"Deck Rippling on the I 75 Rouge River Bridge - Second Progress Report. Research Report No. R-607."* Michigan Department of State Highways, Lansing, MI

Oliva, M. G., Bank, L. C., and Russell, J. S. (2007). *" Full Depth Precast Concrete Highway Bridge Decks."* University of Wisconsin, Structures and Materials Test Laboratory, Madison, WI.

Swenty, M. K., and Graybeal, B. A. (2012). *"Influence of Differenctial Deflection on Staged Construction Deck-Level Connections."* Report No. FHWA-HRT-12-057, Federal Highway Administration, Office of Infrastructure Research & Development, Mclean, VA.

Wisconsin Department of Transportation. (2007). *"SP4075: Maximum Weight Limitations Summary."* Retrieved from Wisconsin Department of Transportation: wisconsindot.gov/Documents/formdocs/sp4075.pdf

Wisconsin Department of Transportation. (2017). *"Bridge Manual Standard Drawings: 17.02 - Deck and Slab Details."* Retrieved from Wisconsin Department of Transportation: http://wisconsindot.gov/Pages/doing-bus/eng-consultants/cnslt-rsrces/strct/bridge-manual-standards.aspx

Appendix A – Survey of Staged Bridge Construction Practices

Participants:

- Wisconsin Department of Transportation
- Wisconsin Department of Transportation Bridge Maintenance Division
- Illinois Department of Transportation
- Missouri Department of Transportation
- Minnesota Department of Transportation
- Michigan Department of Transportation
- Ayres Associates, Inc. (Bridge Designer & Inspector)

Question 1a: Does your organization allow any vehicular traffic to continue using one or more lanes of a bridge while concrete is being placed and/or curing on the same structure?

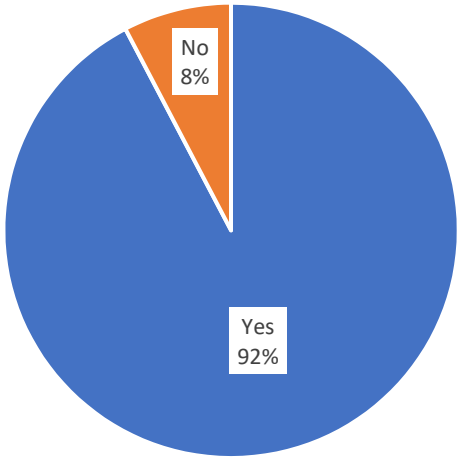

Yes	**12**	92.3%
No	**1**	7.7%

Question 1b: What are the reasons for allowing vehicular traffic during deck construction?

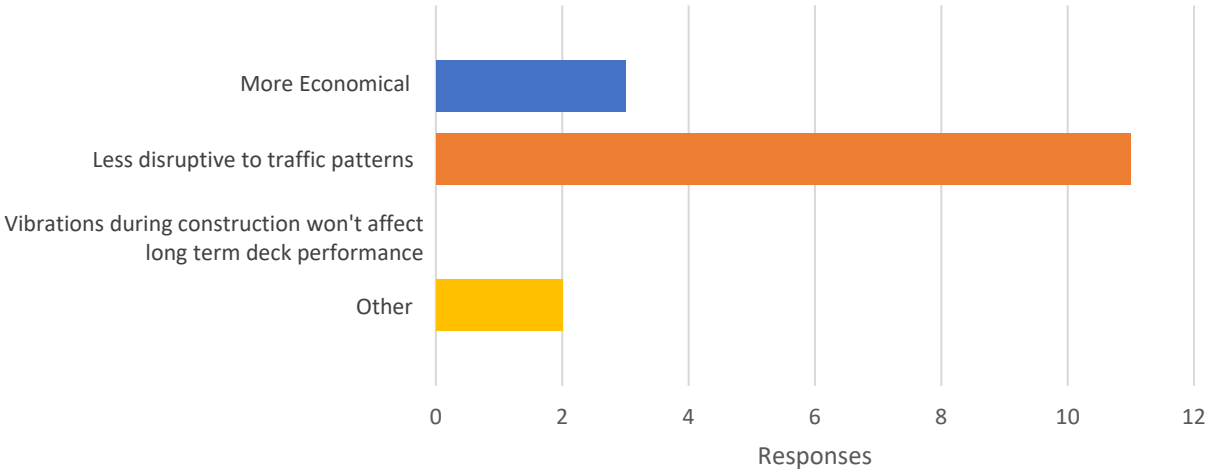

More economical	**3**	25.0%
Less disruptive to traffic patterns	**11**	91.7%
Vibrations during construction won't affect long term deck performance	**0**	0.0%
Other	**2**	16.7%

Other Responses:

- Traffic management
- Dead end road,
- No other way to businesses/homes

Question 1c: How do you justify these decisions?

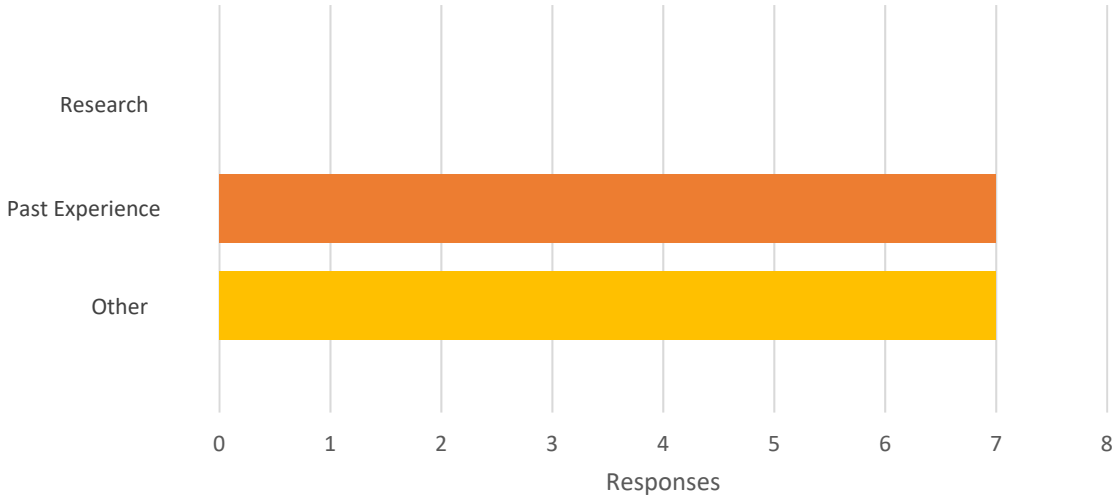

Research	**0**	0.0%
Past Experience	**7**	58.3%
Other	**7**	58.3%

Other Responses:

- Ongoing practice
- Research and past experience demonstrate that traffic vibrations do adversely affect the quality of the final bridge deck concrete, but traffic volumes and public demand cause our owners to request staged construction. Contractors would prefer that we not use staged construction and it requires more work for designers to prepare contract plans with staged construction as well. […] We always encourage owners to reroute traffic when possible or use closure pours rather than use staged construction.
- Contract requirements
- Stakeholder input
- Mobility restrictions through construction zones

Question 2a: Does your organization impose any restrictions on bridge traffic to reduce vibrations during concrete curing?

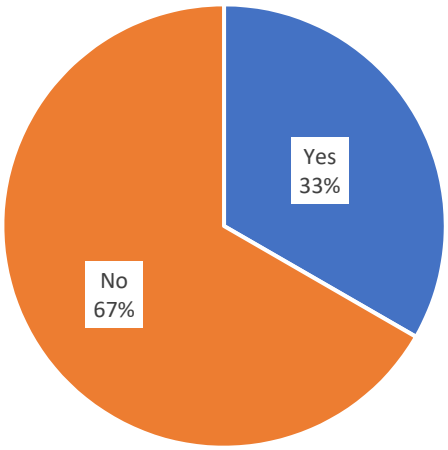

Yes	**4**	33.3%
No	**8**	66.7%

Question 2b: What restrictions do you impose on bridge traffic?

- Speed limit and lane closures when possible.
- Reduced speed limit, and provide additional couple feet behind temporary barrier curb or reduce lane and some cases reduce truck load.
- Move traffic as far away from the concrete pour as possible. Purposely narrow down the through lane so traffic slows down.
- Depending on cross section we will close the adjacent lane next to second deck pour to limit vibrations.

Question 3a: Does your organization impose any restrictions on construction operations to reduce vibrations during concrete curing?

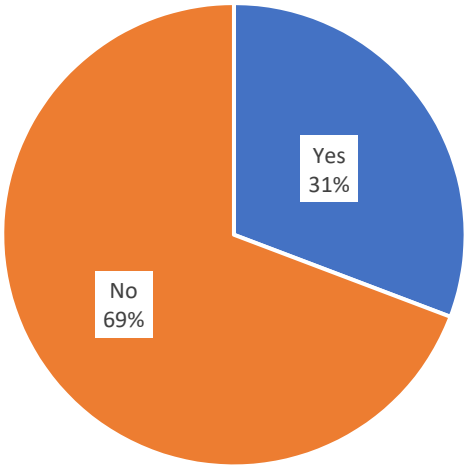

Yes	**4**	30.8%
No	**9**	69.2%

Question 3b: What restrictions do you impose on construction operations?

- […] we have improved requirements for bracing of the exterior beam and another study is due out soon which will further improve these requirements. We have fogging requirements based on the evaporation rate, temperature, humidity and wind speed. We encourage SureCure for curing our bridge decks. […]
- Timing, sequencing
- Load restrictions are in place until concrete reaches 3500 psi.
- No heavy equipment or vehicles on bridge deck until after 7 day wet curing period and the concrete has gained 100% design strength.

Question 4: What concrete properties (strength, slump, water-cement ratio, maximum aggregate size, etc.) are typically specified for closure pours and cast-in-place decks?

- f'c: 4000 psi
- Slump: - 2 - 4"; 1 – 4”
- Water/Cement Ratio: 0.32 - 0.44; 0.35 – 0.45; max 0.45
- Air Entrainment: 5% - 8%; 4.5% – 7.5%; 6.5%
- Maximum Aggregate Size: 1", 1.5”
- 30-40% fine aggregate,
- No chlorides
- Set retarders and water reducers are allowed
- Permeability: <2500 coulombs at 28 days, < 1500 coulombs at 56 days
- Shrinkage: < 0.04 at 28 days
- Durability: >90% at 300 cycles

Question 5a: Do you require/recommend any special reinforcement detailing in longitudinal joint regions?

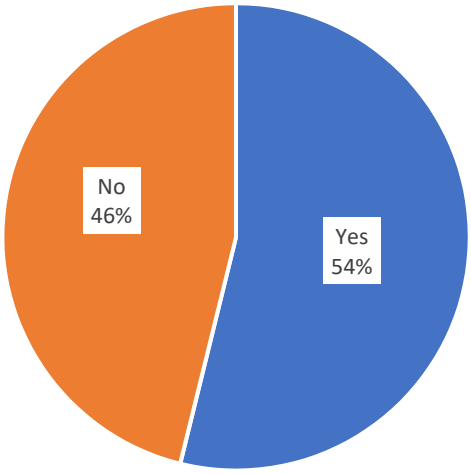

Yes	**7**	53.8%
No	**6**	46.2%

Question 5b: What reinforcement detailing do you require/recommend?

- When the deck width of a girder superstructure exceeds 90 feet or the width of a slab superstructure exceeds 52 feet, a longitudinal construction joint with reinforcement through the joint shall be detailed. […]
- For space and safety, we don't allow lap lengths along stage construction lines but require threaded bar splicers.
- We treat the first pour as an overhang. Therefore, we check the bar steel in the first pour to be sure that the steel is adequate to support the temporary overhang caused by the stage construction. Normally no extra steel is required.
- Provide required rebar splice if space is available. If not enough space available for rebar splice, then use mechanical connection for 8.5" deck and hook rebar or provide dowel for thicker slab.
- These can vary by plan (i.e. bridge thickness, load, etc.). One particular project requires a keyway, 2' 7" laps, and use of #5 top and bottom mat horizontal deck bars. The longitudinal joint is to be sealed at the end.

Question 6a: Do you limit longitudinal joints to a particular location?

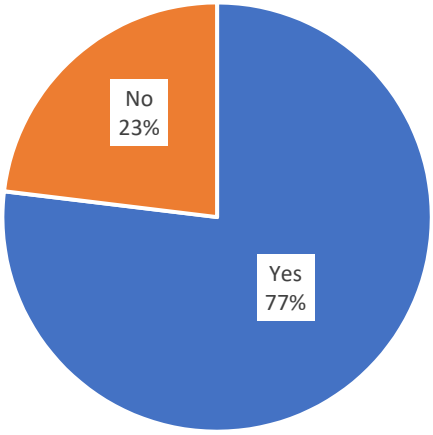

Yes	**10**	76.9%
No	**3**	23.1%

Question 6b: What limits do you impose on longitudinal joint locations?

- Longitudinal joints should not be located directly above girders and should be at least 6 inches from the edge of the top flange of the girder. Longitudinal joints are preferably located beneath the median or parapet. Otherwise, the joint should be located along the edge of the lane line or in the middle of the lane. Avoid under wheel line for safety of drivers
- It shall be located within the middle S/2 where S = beam spacing.
- Longitudinal joints over girders will create performance issues considering freeze/thaw and corrosion. A joint on top of a girder may never dry out, more likely to retain water.
- We try not to exceed the maximum overhang of 3'-7" for the location of the longitudinal joints. We also try to keep the joints outside of the final location of the wheel lines. (Either at the edge of lane or directly in the middle of the lane.) However, bridge width and traffic staging sometimes don't allow us to do this.
- Generally, try to provide longitudinal joint @ girder space/4.
- Over beams when geometry allows
- Strive to make longitudinal joint at lane line. Try to avoid longitudinal joint beneath wheel path. Do not locate longitudinal joint over beam flange.

Question 7: In your experience, have any of the following defects occurred prematurely in longitudinal joint regions as a result of traffic-induced vibrations and differential deflections during concrete placement and/or curing?

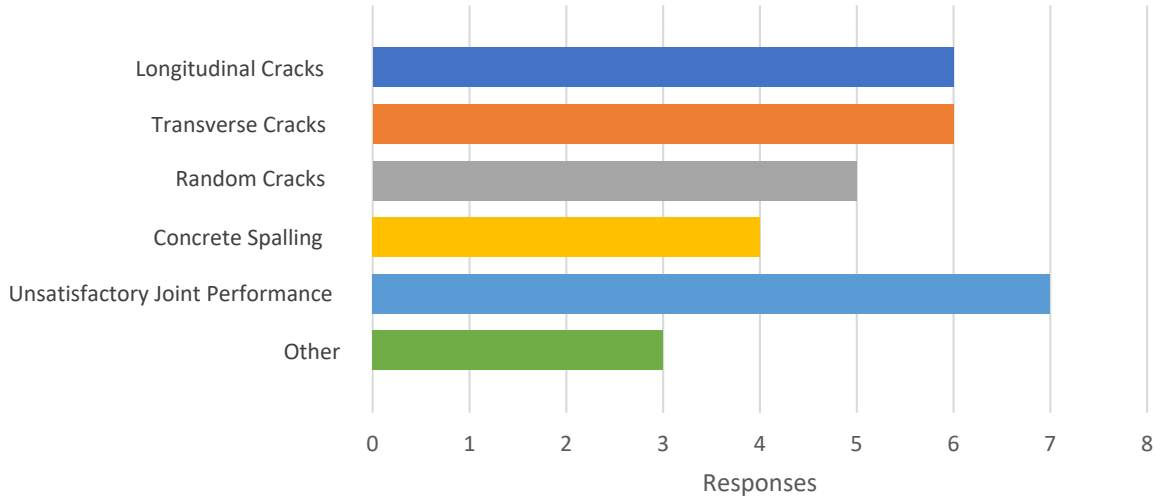

Longitudinal Cracks	**6**	50.0%
Transverse Cracks	**6**	50.0%
Random Cracks	**5**	41.7%
Concrete Spalling	**4**	33.3%
Unsatisfactory Joint Performance	**7**	58.3%

Other Responses:

- Leakage
- Reduction in bond and development of transverse steel in the vicinity of the joint as a result of vibration
- Poor ride at the joint

Question 8: Have you (or your organization) conducted any research in this field?

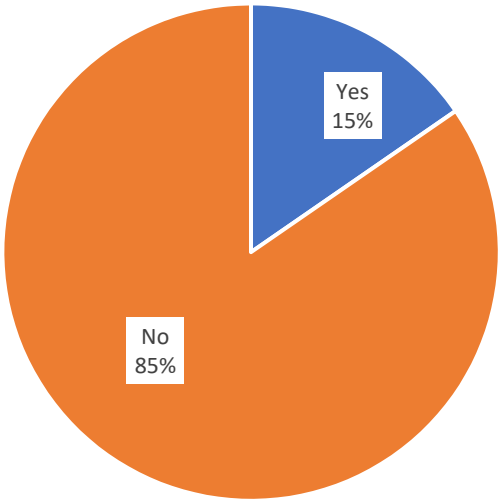

Yes	**2**	15.4%
No	**11**	84.6%

Please provide references or links to any conducted research.

- Please contact me at xxx-xxx-xxxx and we might be able to get links to some research. I know we have studied this specific issue but I would need to check with our Bureau of Materials and Physical Research to get possible links to these reports.
- Numerous bridge inspections and continuous involvement in the bridge inspection industry

Appendix B – Existing Staged Construction Bridge Inspection Details and Notes

Table B.1 - Existing staged bridge construction inspection log

Structure ID	On	Under	County	Average Daily Traffic	Built	# Spans	Span Lengths (ft)	Girder Configuration
B-13-176	IH 90 EB	Lake Drive Rd	Dane	22,700	1961 (New Deck & Widened 2011)	3	40, 50, 40	Cont. Steel
B-13-177	IH 90 WB	Lake Drive Rd	Dane	21,700	1961 (New Deck & Widened 2011)	3	37.5, 47, 37.5	Cont. Steel
B-20-059	CTH OO	IH 41	Fond Du Lac	7,300	1973 (New Deck 2009)	2	145, 146	Cont. Steel
B-40-363	USH 45 SB	STH 100 SB - Silver Spring	Milwaukee	46,900	1967 (Widened 2000)	2	78	Cont. Steel
B-40-364	USH 45 NB	STH 100 SB - Silver Spring	Milwaukee	49,400	1967 (New Deck & Widened 2001)	2	78	Cont. Steel
B-40-365	USH 45 SB	CNW RR	Milwaukee	52,600	1967 (Widened 2000)	3	46.5, 60.5, 46.5	Cont. Steel
B-40-366	USH 45 NB	CNW RR	Milwaukee	55,800	1967 (New Deck 2001)	3	46.5, 60.5, 46.5	Cont. Steel
B-53-007	USH 14	Blackhawk Creek	Rock	9,500	1951 (New Deck 1994)	3	40, 50, 40	Cont. Steel
B-53-081	IH 90 EB	Kennedy Rd & Bike Path	Rock	23,800	1962 (New Deck & Widened 2003)	4	67.5, 82, 82, 67.5	Cont. Steel
B-56-217	USH 12 - STH 78	Wisconsin River	Sauk	17,500	1965 (Widened w/ Concrete Overlay 2004)	7	108-136	Cont. Steel
B-67-109	IH 43 SB	Calhoun Rd	Waukesha	26,500	1969 (New Superstructure 1992)	3	33, 70, 41	Cont. Steel
B-67-110	IH 43 NB	Calhoun Rd	Waukesha	26,500	1969 (New Superstructure 1992)	3	33, 70, 42.5	Cont. Steel
B-67-123	IH 43 SB	Hilo Dr	Waukesha	15,650	1970 (New Deck 2012)	3	48, 73.5, 48	Cont. Steel
B-67-129	STH 83	IH 43	Waukesha	24,600	1971 (New Deck & Widened 2002)	2	124.5, 124.5	Cont. Steel
B-67-133	IH 43 SB	Edgewood Ave	Waukesha	17,320	1971 (New Deck & Widened 2012)	3	57.5, 95.5, 62	Cont. Steel
B-67-134	IH 43 NB	CTH I Beloit Rd)	Waukesha	36,600	1968 (New Deck 1992)	3	56, 110, 45	Cont. Steel

Table B.1 (cont.) - Existing staged bridge construction inspection log

Structure ID	Girder Spacing (ft)	Deck Thickness (in)	Location of Joint	Joint Details*	Deck Condition	Comments
B-13-176	8.8	8.5	B/w girders (3.04'/5.79' = S/2.9)	50 d_b lap splice w/ shear key	Minor cracking underneath (between all girders) with efflorescence. Localized areas of insufficient consolidation in the joint region. Diagonal cracking over piers in top surface of stage 2 deck.	
B-13-177	8.8	8.5	B/w girders (3.04'/5.79' = S/2.9)	50 d_b lap splice w/ shear key	Minor cracking underneath primarily in stage 2 deck (where the traffic lanes are) with efflorescence. Localized areas of insufficient consolidation in the joint region.	
B-20-059	10.6	9.5	Next to girder, 6" from edge of top flange (S/8.5)	51 d_b lap splice w/ shear key	No significant cracking or defects in joint region.	LCJ is partially under central median
B-40-363	9.4	9.0	Next to girder, 16.5" from edge of top flange (S/4.8)	52 d_b dowel bar splicer w/ shear key	No significant cracking or defects on bottom face of deck in joint region. Moderately sized cracks on top surface of deck in stage 2 side. Minor spalls in wearing surface along joint.	
B-40-364	9.4	9.0	B/w girders (3.96'/5.46' = S/2.4)	52 d_b dowel bar splicer w/ shear key	No significant cracking or defects on bottom face of deck in joint region. Moderately sized cracks on top surface of deck in stage 2 side.	
B-40-365	9.4	9.0	Next to girder, 18" from edge of top flange (S/4.8)	Bar couplers	Minor transverse cracking with light efflorescence on stage 2 side of joint (uniformly spaced)	
B-40-366	9.5	9.0	B/w girders (4'/5.5' = S/2.4)	Bar couplers	No significant cracking in longitudinal joint region. Moderate efflorescense coming through construction joint. One bar coupler exposed from insufficient concrete cover.	
B-53-007	5.5	8.0	B/w girders (1.52'/4.0' = S/3.6)	52 d_b dowel lap splice w/ shear key	No significant cracking in longitudinal joint region. Localized areas of insufficient consolidation in joint region.	
B-53-081	7.8	8.0	B/w girders (3.62'/4.27' = S/2.2)	52 d_b dowel bar splicer (both sides)	Minor cracking with light efflorescence and rust staining extending from joint into stage 2 deck. Moderately sized transverse cracks in wearing surface (also observed in adjacent bridge not constructed in stages).	
B-56-217	10.3	9.0	B/w girders (5.33''/5.0' = S/1.9)	51 d_b lap splice w/ shear key	Minor spalls underneath in stage 2 longitudinal joint region. One moderately sized crack in underside of stage 2 deck with efflorescence. Minor transverse cracking spaced regulrly in stage 2 wearing surface.	
B-67-109	4.7	8.0	Midspan b/w girders (2.33'/2.33' = S/2)	40 d_b lap splice w/ shear key	Transverse cracking with efflorescence throughout deck	
B-67-110	4.7	8.0	Midspan b/w girders (2.33'/2.33' = S/2)	40 d_b lap splice w/ shear key	Transverse cracking with efflorescence throughout deck	
B-67-123	12.9	10.5	B/w girders (4.55'/7.55' = S/2.4)	51 d_b lap splice w/ shear key	Minor patches and areas of underconsolidated concrete along LCJ	Adjacent bridge constructed without stages - no significant defects
B-67-129	9.2	9.0	B/w girders (7.13'/2.03' = S/1.3)	51 d_b lap splice	No significant cracking or defects in joint region.	
B-67-133	12.8	10.5	B/w girders (4.0'/8.83' = S/3.2)	52 d_b lap splice w/ shear key	Minor areas of undercolsolidated concrete	Adjacent bridge constructed without stages - no significant defects
B-67-134	12.0	9.5	B/w girders (4.5'/7.5' = S/2.7)	51 d_b lap splice w/ shear key	Random cracking throughout deck. Transverse cracking with efflorescence mostly concentrated to stage 2 side, leakage through LCJ.	

Table B.1 (cont.) - Existing staged bridge construction inspection log

Structure ID	On	Under	County	Average Daily Traffic	Built	# Spans	Span Lengths (ft)	Girder Configuration
B-67-135	IH 43 SB	CTH I Beloit Rd)	Waukesha	36,600	1968 (New Deck 1991)	3	68, 124, 48.5	Cont. Steel
B70176	IH 41 SB	STH 76	Winnebago	25,700	1995 (Widened 2011)	2	115.5	Cont. Steel
B70177	IH 41 NB	STH 76	Winnebago	10,043	1995 (New Deck & Widened 2010)	2	115.5	Cont. Steel
B-30-014	IH 41 SB - IH 94 EB	CTH KR	Kenosha	38,800	1959 (Widened 1970)	3	33, 43, 33	Haunched Slab
B-30-015	IH 41 NB - IH 94 WB	CTH KR	Kenosha	38,800	1959 (Widened 1970)	3	33, 43, 33	Haunched Slab
B-30-025	IH 41 SB - IH 94 EB	CTH E	Kenosha	34,410	1959 (Widened 1970)	3	33, 43, 33	Haunched Slab
B-30-026	IH 41 NB - IH 94 WB	CTH E	Kenosha	34,700	1959 (Widened 1970)	3	33, 43, 33	Haunched Slab
B-51-016	IH 41 SB - IH 94 EB	Braun Rd	Racine	38,800	1959 (Widened 1970)	3	33, 43, 33	Haunched Slab
B-51-017	IH 41 NB - IH 94 WB	Braun Rd	Racine	38,800	1959 (Widened 1970)	3	33, 43, 33	Haunched Slab
B-51-020	IH 41 SB - IH 94 EB	58th Rd	Racine	38,700	1959 (Widened 1970)	3	33, 43, 33	Haunched Slab
B-51-021	IH 41 NB - IH 94 WB	58th Rd	Racine	38,700	1959 (Widened 1970)	3	33, 43, 33	Haunched Slab
B-13-005	USH 14	Black Earth Creek	Dane	10,500	1935 (New Superstructure 1993)	1	62	SS PC
B-16-085	STH 35	Black River	Douglas	3,700	1997	1	85	SS PC
B-67-297	IH43 SB	CTH I Beloit Rd)	Waukesha	30,200	2007	1	134	SS PC

Table B.1 (cont.) - Existing staged bridge construction inspection log

Structure ID	Girder Spacing (ft)	Deck Thickness (in)	Location of Joint	Joint Details*	Deck Condition	Comments
B-67-135	12.3	9.5	B/w girders (4.83'/7.5' = S/2.6)	38 d_b lap splice w/ shear key	Random cracking throughout deck. Transverse cracking with efflorescence concentrated to stage 2 side, leakage through LCJ.	
B70176	10.5 - 12.0	10.0	B/w girders (4.0'/8.0' = S/3.0)	49 d_b lap splice	Significant patching underneath at longitudinal construction joint, possibly due to formwork or barrier anchors. Regularly spaced transverse cracks with leakage throughout span on widened portion, not throughout in original deck. Transverse cracking in wearing surface accross entire deck.	
B70177	10.5 - 12.0	10.0	B/w girders (8.0'/4.0' = S/1.5)	49 d_b lap splice	Regularly spaced transverse cracking with leakage throughout, both underneath and in wearing surface.	Modeled using Finite Elements
B-30-014	--	Varies 10.0 - 27.5	Two joints	24 d_b lap splice	Severe spalling at joint in main span with exposed corroded rebar. Extensive delaminations in approach spans. Large areas of previously patched concrete. Spalled concrete near waterstop joint with adjacent bridge - area has retained moisture	Concrete (1987) and bituminous (1998) overlays in place
B-30-015	--	Varies 10.0 - 27.5	Two joints	24 d_b lap splice	Extensive patching of concrete in longitudinal joint region. Large cracks extending through patches with severe eflorescense. Some areas of underconsolidated concrete. Opening of the crack at the LCJ is visable during truck passage (approx. 1/4"). Pulverized concrete gathering on embankment underneath LCJ	Concrete (1987) and bituminous (1998) overlays in place
B-30-025	--	Varies 10.0 - 27.5	Two joints	24 d_b lap splice	Extensive patching of spalled concrete in LCJ areas. Longitudinal cracks adjacent to LCJ with efflorescense. Minor delaminations in joint region	Concrete (1987) and bituminous (1998) overlays in place
B-30-026	--	Varies 10.0 - 27.5	Two joints	24 d_b lap splice	Extensive patching of spalled concrete in LCJ areas. Minor delaminations in joint region. Heavy efflorescense and corrosion near waterstop joint with adjacent bridge - area has retained moisture	Concrete (1987) and bituminous (1998) overlays in place
B-51-016	--	Varies 10.0 - 27.5	Two joints	24 d_b lap splice	Longitudinal cracking adjacent to LCJ with heavy efflorescense. Large delaminations adjacent to LCJ. Efflorescense and corrosion near waterstop joint with adjacent bridge - area has retained moisture	Concrete (1980) and bituminous (2001) overlays in place
B-51-017	--	Varies 10.0 - 27.5	Two joints	24 d_b lap splice	Large longitudinal cracks adjacent to LCJ in approach span with visable movement during passage of large trucks. Evidence of steel corrosion through cracks with efflorescense. Some patching of spalled concrete areas and exposed corroded rebars.	Concrete (1980) and bituminous (2001) overlays in place
B-51-020	--	Varies 10.0 - 27.5	Two joints	24 d_b lap splice	Longitudinal cracking adjacent to LCJ with heavy efflorescense. Delaminations adjacent to LCJ. Exposed corroded rebars. Closely spaced hairline transverse cracks. Efflorescense and corrosion near waterstop joint with adjacent bridge - area has retained moisture.	Concrete (1980) and bituminous (2001) overlays in place
B-51-021	--	Varies 10.0 - 27.5	Two joints	24 d_b lap splice	Longitudinal cracking adjacent to LCJ with heavy efflorescense and signs of corroded steel rebar within.	Concrete (1980) and bituminous (2001) overlays in place
B-13-005	6.5	8.0	Midspan b/w girders (3.25'/3.25' = S/2), bridge centerline	40 d_b lap splice w/ shear key	No significant cracking or defects in joint region, light efflorescense underneath at joint location.	
B-16-085	10.8	8.0	Midspan b/w girders (3.25'/3.25' = S/2), bridge centerline	40 d_b lap splice w/ shear key	Minor transverse cracking at regular spacing with light efflorescense in first bay over from joint (stage 2 side). Some minor cracking on top surface of deck mainly in stage 2 side.	Previous inspection noted cracking in newer portion of the deck
B-67-297	5.3	8.0	B/w girders (2.33'/2.33' = S/2.1)	44 d_b lap splice w/ shear key	Transverse cracking with efflorescence concentrated in stage 2 deck. Hairline longitudinal cracks adjacent to LCJ in Stage 1 deck	

Table B.1 (cont.) - Existing staged bridge construction inspection log

Structure ID	On	Under	County	Average Daily Traffic	Built	# Spans	Span Lengths (ft)	Girder Configuration
B-28-109	IH 94 EB	STH 26	Jefferson	13,400	2001	2	108.3, 108.3	SS PC - Cont. Deck
B-40-216	USH 45 SB	Menomonee River	Milwaukee	62,500	2000	2	122, 122	SS PC - Cont. Deck
B-40-217	USH 45 NB	Menomonee River	Milwaukee	62,500	2001	2	122, 122	SS PC - Cont. Deck
B-53-083	IH 90 EB	Wisconsin & Calumet RR	Rock	19,000	1961 (New Deck & Widened 2003)	3	43.6, 44.5, 43.6	SS PC - Cont. Deck
B-64-122	IH 43 NB	Elm Ridge Rd	Walworth	10,040	1975 (New Deck 2015)	3	43.5, 64, 36.5	SS PC - Cont. Deck
B-67-324	IH 43 NB	STH 164	Waukesha	21,000	2010	2	91, 91	SS PC - Cont. Deck
B-67-325	IH 43 SB	STH 164	Waukesha	21,000	2010	2	91, 91	SS PC - Cont. Deck
B-13-160	IH 39 SB	Door Creek	Dane	27,200	1961 (New Deck & Widened 2005)	1	83	SS Steel
B-13-161	IH 39 SB	Door Creek	Dane	27,200	1962 (New Deck & Widened 2005)	1	83	SS Steel
B-13-593	STH 19	Halfway Prairie Creek	Dane	2,000	1939 (New Deck 1989)	1	58.9	SS Steel
B-56-022	STH 60	Badger Valley Creek	Sauk	1,100	1957 (New Deck 1996)	1	30	SS Steel

Table B.1 (cont.) - Existing staged bridge construction inspection log

Structure ID	Girder Spacing (ft)	Deck Thickness (in)	Location of Joint	Joint Details*	Deck Condition	Comments
B-28-109	7..7	8.0	B/w girders (3.94'/3.77' = S/2.0)	Bar couplers w/ shear key	Minor transverse cracking (previously sealed). Longitudinal cracking approximately over both girders adjacent to LCJ (in stage 1 and stage 2 deck)	Partial overlay approx. 3 ft. wide placed over LCJ
B-40-216	8.3	8.0	Next to girder, 7" from edge of top flange (S/4.5)	52 d_b dowel bar splicer w/ shear key	Minor transverse cracking in joint region with light efflorescence. Small spots of corrosion at joint indication possible corrosion of embeded rebars.Two localized areas of insufficient consolidation and exposed rebar in joint region. Excessive spalling and bugholes on bottom flange of prestressed girder directly beneath joint.	
B-40-217	8.3	8.0	Next to girder, 7" from edge of top flange (S/4.5)	52 d_b dowel bar splicer w/ shear key	Minor transverse cracking (uniform spacing) with light efflorescence in longitudinal joint region (stage 2 side only). Small spots of corrosion at joint indicating possible corrosion of embedded rebars. Excessive spalling and bugholes on bottom flange of prestressed girder directly beneath joint.	
B-53-083	7.2	8.0	B/w girders (3.92'/3.25' = S/1.8)	51 d_b lap splice w/ shear key	No significant cracking or defects in longitudinal joint region. Signs of leakage through the joint. Minor longitudinal cracking over adjacent girder in stage 1 deck.	
B-64-122	12.3	10.0	B/w girders (4.13'/8.17' = S/3.0)	49 d_b lap splice w/ shear key	No significant cracking or defects in joint region.	Adjacent to Field Monitored B-64-123
B-67-324	11.3	9.5	B/w girders (3.75'/7.5' = S/3)	50 d_b lap splice	Hairline transverse cracking with efflorescense throughout deck. Leakage through LCJ	
B-67-325	11.3	9.5	B/w girders (3.75'/7.5' = S/3)	50 d_b lap splice	Hairline transverse cracking with efflorescense throughout deck. Leakage through LCJ	
B-13-160	8.8	8.5	Midspan b/w girders (4.42'/4.42' = S/2)	51 d_b lap splice w/ shear key	No significant cracking or defects in joint region.	
B-13-161	8.8	8.5	Midspan b/w girders (4.42'/4.42' = S/2)	51 d_b lap splice w/ shear key	No significant cracking or defects in joint region.	Precast deck panels, post tensioned both directions, prototype bridge in (Oliva, 2007)
B-13-593	4.5	7.0	Midspan b/w girders (2.23'/2.23' = S/2), bridge centerline	37 d_b lap splice w/ shear key	Extensive transverse cracking and delaminations underneath in joint region. Spalled concrete exposing corroded rebars in lap splice and across joint. Minor transverse cracking in top surface that had been sealed.	
B-56-022	5.1	7.0	Midspan b/w girders (2.56'/2.56' = S/2)	Bar couplers w/ shear key	Signs of leakage through joint with moderate rust staining. Spalled concrete exposing corroded rebar at longitudinal construction joint (stage 2 side). Some delamination of underside of deck in stage 2 joint region.	

Appendix C – Section 503.09 of Illinois Department of Transportation Standard Specifications for Road and Bridge Construction, April 2016

503.08 Depositing Concrete Underwater. Concrete shall not be exposed to the action of water before setting, or deposited in water, except with the approval of the Engineer and under his/her immediate supervision.

When concrete is deposited underwater, it shall be carefully placed in its final position by means of a tremie and shall not be disturbed after being deposited. Still water shall be maintained at the point of deposit and all form work designed to retain concrete underwater shall be watertight. The consistency of the concrete shall be carefully regulated and segregation of the materials shall be prevented. The method of depositing concrete shall produce approximately horizontal surfaces.

The tremie shall consist of a tube having a diameter of not less than 10 in. (250 mm) and constructed in sections having flanged couplings fitted with gaskets. The means of supporting the tremie shall permit the free movement of the discharge end over the entire top surface of the work and shall permit it to be rapidly lowered when necessary to choke off or retard the flow. The discharge end shall be entirely sealed at all times and the tremie tube kept full to the bottom of the hopper. When a batch is dumped into the hopper, the tremie shall be raised slightly to induce the flow of concrete but the lower end shall be kept below the top of the deposited concrete until the batch is discharged. The flow shall then be stopped by lowering the tremie.

At the Contractor's option, pumping equipment may be used in lieu of a tremie to deposit concrete underwater. The Engineer will approve the concrete pumping equipment and its piping before the work is started.

503.09 Construction Joints. Construction joints shall be made only at locations shown on the plans or approved by the Engineer, except in cases of breakdowns or other unforeseen and unavoidable delays.

All construction joints shall be bonded unless noted otherwise. When not shown on the plans, their location shall be confined, as far as possible, to regions of low shearing stress and to locations that will be hidden from view. When possible, the location of construction joints shall be planned in advance and the concrete placed continuously from joint to joint. The reinforcing steel shall extend through such joints. If a construction joint is necessary in the sloped portion of a wingwall or similar location where a featheredge would result, the joint shall be constructed so as to produce an edge thickness of not less than 6 in. (150 mm) in the succeeding layer. No construction joint shall be placed within 18 in. (450 mm) of the top of any wall or pier unless the details of the work provide for a coping having a thickness of less than 18 in. (450 mm), in which case, at the option of the Engineer, a construction joint may be made at the underside of the coping.

The face edges of all joints which are exposed to view shall be carefully finished true to line and elevation. Shear keys, formed into or out from the surface of the previously placed concrete or steel dowels, shall be used where required. Shear keys formed into the concrete shall be formed by the insertion and subsequent removal of beveled wood strips which shall be thoroughly saturated with water prior to insertion. Steel dowels may, at the discretion of the Engineer, be used in lieu of keys. The size and spacing of the keys and dowels will be as determined by the Engineer.

Between adjacent sections of retaining walls and abutment walls, a V-shaped groove shall be formed in the exposed face of the walls by the use of 1/2 in. (13 mm) triangular molding on each side of the joint.

Care shall be exercised not to injure the concrete or break the concrete-steel bond at any time. In constructing bridge decks and approach slabs where longitudinal joints are specified, a platform shall be constructed outside the longitudinal joints and supported on the lower form, and personnel will not be permitted to stand or walk on the projecting reinforcement bars until the concrete has hardened.

The Contractor, subject to approval of the Engineer, may pour a bridge deck full width with horizontal bonded construction joints between the deck and curbs, parapets, or sidewalks.

(a) Unbonded Construction Joints. Unbonded construction joints shall be made by forming or striking off the initial concrete placed to a true and even surface and allowing it to set. Loose material shall be removed. The new concrete shall be thoroughly consolidated against the existing concrete.

(b) Bonded Construction Joints. For bonding to hardened concrete, the existing cement paste shall be removed to create a prepared surface. The surface shall be prepared by washing with water under pressure or by sandblasting to expose clean, well bonded aggregate.

To facilitate the removal of the cement paste, the form in contact with the first pour or the exposed surface of the first pour, may be thoroughly covered with a surface retarder. When the surface retarder is applied directly to the fresh concrete surface, its application shall be completed within 30 minutes after concrete placement.

The surface retarder shall be a ready-to-use liquid compound that delays the set of a concrete surface, and shall be approved by the Engineer in advance of beginning the work. It shall produce results satisfactory to the Engineer and will be evaluated on the tests performed by the Engineer, and on the manufacturer's data recommendations.

The prepared surface of the existing concrete shall be wetted a minimum of one hour before application of the new concrete. The surface shall be maintained in a dampened condition during that period. Immediately before placing the new concrete, any excess water shall be removed.

503.10 Expansion Joints. Expansion joints shall be constructed to permit freedom of movement. After all other work is completed, all thin shells of mortar and projections of the concrete into and around the joint space that are likely to spall under movement or prevent the proper operation of the joint shall be carefully removed. Expansion joint devices shall be furnished and installed according to Section 520.

(a) Open Joints. Reinforcement shall not extend across or into an open joint. Open joints in railings or under projecting portions of rail posts shall be formed with square corners unless beveled corners are specified. When not